EVALUATION AND NUMERICAL MODELING OF DEFLECTIONS AND VERTICAL DISPLACEMENT OF RAIL SYSTEMS SUPPORTED BY EXPANDED POLYSTYRENE (EPS) GEOFOAM EMBANKMENTS

by

Shun Li

A thesis submitted to the faculty of
The University of Utah
in partial fulfillment of the requirements for the degree of

Master of Science

Department of Civil and Environmental Engineering

The University of Utah

December 2014

The University of Utah Graduate School

STATEMENT OF THESIS APPROVAL

The thesis of **Shun Li**

has been approved by the following supervisory committee members:

Steven Bartlett	, Chair	**May 9, 2014** Date Approved
Evert Lawton	, Member	**October 27, 2014** Date Approved
Luis Ibarra	, Member	**October 27, 2014** Date Approved

and by **Michael Barber** , Chair/Dean of

the Department/College/School of **Civil and Environmental Engineering**

and by David B. Kieda, Dean of The Graduate School.

ABSTRACT

This research seeks to develop a numerical method to evaluate the vertical rail deflection, sleeper (i.e., rail road tie), and embankment displacements for rail systems constructed atop Expanded Polystyrene (EPS) geofoam embankments. Such a model is needed for the design and safety evaluations of such systems. To achieve this purpose, laboratory testing of ballast material was performed in conjunction with the development and verification of two-dimensional (2D) and three-dimensional (3D) finite difference methods (FDM). These evaluations were done for multilayered rail systems undergoing deflections from typical locomotive and train car loadings.

The proposed FDM approach and models were verified using case studies of: (1) an earthen rail embankment and FEM modeling of that embankment as presented in the literature and (2) an EPS-supported multilayered railway embankment system and field deflection measurement from Norway for a commuter rail system.

The evaluation of these verification modeling examples show that the 3D FDM model can reasonably estimate the static vertical deflection associated with such systems subject to typical train loadings. However, more research is needed to measure the dynamic (i.e., rolling) train deflections and to develop evaluation methods for such systems constructed atop EPS-supported embankment.

TABLE OF CONTENTS

Appendices

ACKNOWLEDGEMENTS

I would also like to express my appreciation to my thesis committee. I thank all for your time, advice, and review of this research. I especially want to thank Dr. Steven F. Bartlett, chair of this committee, for his geotechnical expertise and needed guidance on my research and support and friendship in my daily life. I also thank Dr. Evert C. Lawton for greatly improving my knowledge about geotechnical engineering. I also thank Dr. Luis Ibarra for his review of this thesis. In addition, I am grateful to Drs. David Arellano (U. of Memphis) and Jan Vaslestad (Norwegian Public Roads Administration, NPRA) for their advice and input. In addition, Roald Aaboe from NPRA provided the information for the Norwegian rail case modeled herein. I also want to thank the National Center for Freight and Infrastructure Research and Education (CFIRE) located at the University of Memphis for the bulk of the funding of this research. Additional graduate assistantship and teaching assistantship support was also given by the Civil and Environmental Engineering Department of the University of Utah.

Finally, I am grateful for the unlimited support from my family and friends.

CHAPTER 1

INTRODUCTION AND LITERATURE REVIEW

1.1 The General Use of EPS Block for Embankment Systems

1.1.1 Construction History and Methods

Expanded polystyrene (EPS) geofoam has been used in embankment and roadway construction since 1972. The development initially began in Norway and nearby Scandinavian countries and soon spread to Japan and the U.S. The following is a brief history of EPS as pertaining to embankment applications.

1.1.1.1 Norway

The first attempt at building a nonsubsidence road with large EPS blocks instead of earth was successfully implemented in a marshland in Lillestrom, Norway in 1972 (Miki, 1996; Alfheim et al., 2011). The successful roadway repair and settlement mitigations was credited to Norwegian road construction engineers associated with what is now called the Norwegian Public Roads Administration (NPRA). This novel construction method was further improved and increasingly used in many construction sites in Norway and made its way steadily into Northern European countries and others.

1.1.1.2 Japan

The Expanded Poly-Styrol Construction Method Development Organization (EDO) was established in Japan in 1986 (EOD, 1993). This organization sought technical exchange with NPRA and committed itself to the development and practice of the EPS method; in Japan, EDO quickly embraced this technology. The Japanese engineers use the EPS method as an alternative to earth embankments in settlement-prone areas and areas with soft ground or slope stability concerns. For example, the EPS method is used in a soft ground application as a light fill method (Miki, 1996).

1.1.1.3 U.S.

Many states have used EPS geofoam in large and small highway projects since the mid-1990s. A few large and/or high-profile jobs are of particular note in the U.S.: (1) the Big Dig in Boston, Massachusetts (Riad et al., 2004), (2) the I-15 Reconstruction Project in Salt Lake City, Utah (Bartlett et al., 2012), (3) the Woodrow Wilson Bridge in Virginia (FHWA, 2013), and (4) the Utah Transit Authority (UTA) light rail system in Salt Lake City, Utah (Snow et al., 2010). EPS geofoam helped the projects maintain extremely tight construction schedules that did not have sufficient time for conventional embankment construction. These projects illustrated the ease and speed with which EPS geofoam can be constructed for embankments (FHWA, 2011).

In addition to these projects, engineers at the Minnesota Department of Transportation (DOT), the Maine DOT, and the Indiana DOT have realized significant time and cost savings for small and moderate-sized EPS roadway embankment projects constructed over deep, soft organic soil deposits prevalent in these state (FHWA, 2011).

EPS has also been used as light-weight embankment in slope stabilization projects. Projects have been completed in Colorado, New York, Alabama, and Arizona. After years of searching for permanent solutions to failing slope problems, the New York State DOT and the Alabama DOT turned to EPS geofoam. By replacing upper sections of the slide area, State engineers significantly reduced the driving forces that were causing the slide and successfully rehabilitated the roadway section (FHWA, 2011).

General guidance for slope stability projects have been developed by others found in the report "Guidelines for Geofoam Applications in Slope Stability Projects" (Arellano et al., 2011).

1.1.2 Long-Term Performance of EPS

1.1.2.1 Physical Properties

The compressive resistance of EPS is an important design property and is somewhat correlated with the density of the EPS material. One major indicator of possible deterioration of blocks with time would be a decrease in the material compressive resistance or strength (Aabøe and Frydenlund, 2011). Unconfined compressive strength tests performed on retrieved samples from embankments constructed in Norway that have been in the ground for up to 24 years are shown in Figure 1.1 as a function of dry unit density and compressive strength.

From Figure 1.1 and Figure 1.2, it may also be observed that the majority of tests show values of compressive strength in relation to unit density above that of a "normal" quality material (i.e., the expected compressive resistance for that particular density of EPS). The results indicate clearly that there are no signs of significant material

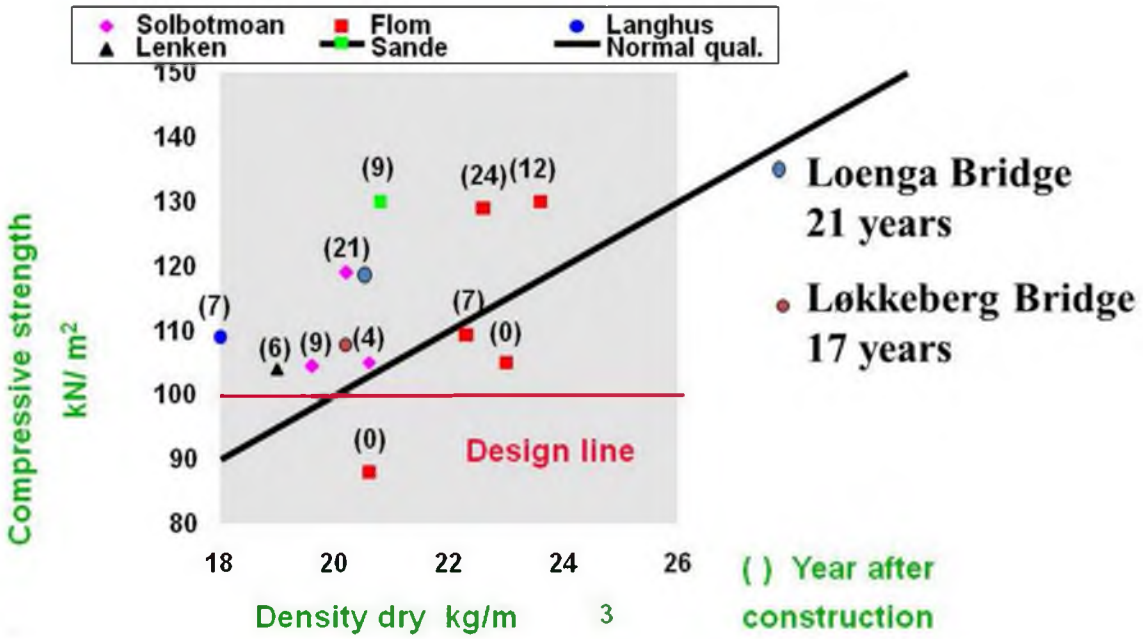

Figure 1.1 Compressive Strength on Retrieved Samples from EPS Embankments

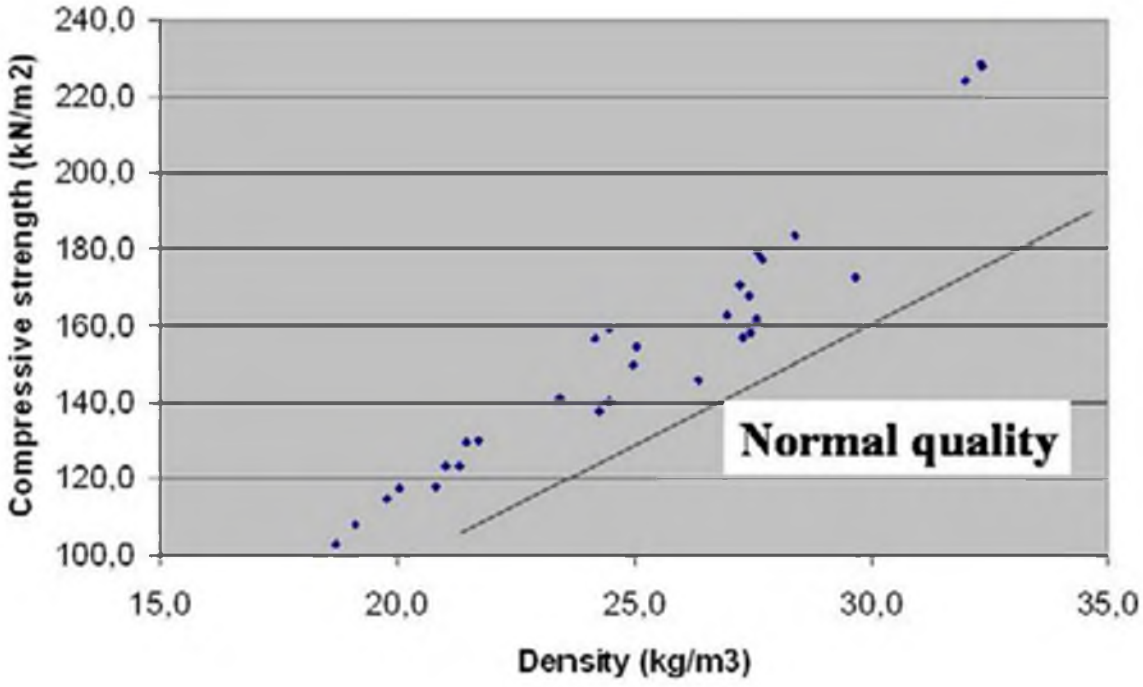

Figure 1.2 Loenga Bridge 1983 Compressive Strength after 21 Years of Burial

deterioration over the total time span of 24 years. Furthermore, there is no indication of significant variation in the material strength whether the retrieved specimens are tested wet or dry. This indicates that water pickup over years in the ground from groundwater does not appear to affect the material strength in a significant manner.

1.1.2.2 Creep

Creep strain can be significant in EPS geofoam, if it is overloaded beyond the elastic range. The design guidance for minimizing creep settlement can be found in the report "Guideline and Recommended Standard for Geofoam Applications in Highway Embankments" (Stark et al., 2004), and "Geofoam Applications in the Design and Construction of Highway Embankments" (Stark et al., 2004), for U.S. Projects and in the EPS Whitebook (2011) for Europe.

Laboratory and field creep measurements have been carried out to determine the allowable loading conditions in the EPS block to keep creep strain to tolerable limits. Some pertinent studies are summarized below.

To determine the EPS creep range under representative loadings, a series of tests were carried out by Duskov (1997). In the first series of tests, only EPS20 cylinders exposed to a single stress level were tested. In a second series, creep of both EPS15 and EPS20 samples was measured under two different stress levels. For both test series, only the EPS samples in dry conditions were used. The creep level of EPS20 caused by a static stress of 20 kPa was rather limited and seemed to be less than 0.2% after more than a year. Duskov concluded that creep seems to be semilinear log linear for both EPS15 and EPS20 when loaded statically in its elastic range. About half of the expected maximum

creep occurs already within the first day. Duskov concluded that all in all, the additional settlement of a pavement structure due to creep in the EPS sub-base will be rather limited, on the order of a few tenths of a percent. Therefore, this creep deformation was considered to be of minor practical importance for pavement performance.

The I-15 Reconstruction Project in Salt Lake City, Utah was designed so that the combination of the dead load and live load did not exceed the compressive resistance of EPS19 at 10% strain, which was the guidance given at that time in the draft European code (Bartlett et al., 2012). This is approximately equivalent to maintaining the combination of dead and live loads to a compressive resistance of about 1% axial strain. To monitor the performance of the EPS embankments for this project, instrumentation was installed at several locations to monitor the long-term creep and settlement performance of EPS embankments (Bartlett and Farnsworth, 2004). The most extensive array was installed at 100 South Street and the results obtained will be discussed below.

The I-15 reconstruction at 100 South Street in Salt Lake City, Utah required raising and widening of the existing embankment to the limits of the right-of-way. The geofoam fills in both the north and southbound directions were placed over a 406-mm high-pressure natural gas line and other buried utilities, as shown in Figures 1.3 and 1.4 (Negussey and Stuedlein, 2003). The southbound portion of this embankment employed approximately 3,400 m^3 of EPS20, and the height of the embankment decreased southward to conform to the roadway elevation. The embankment height (not including the pavement thickness) decreased from 8.1 to 6.9 meters, corresponding to 10 to 8.5 layers of geofoam blocks, respectively (Figure 1.3). The geofoam embankment

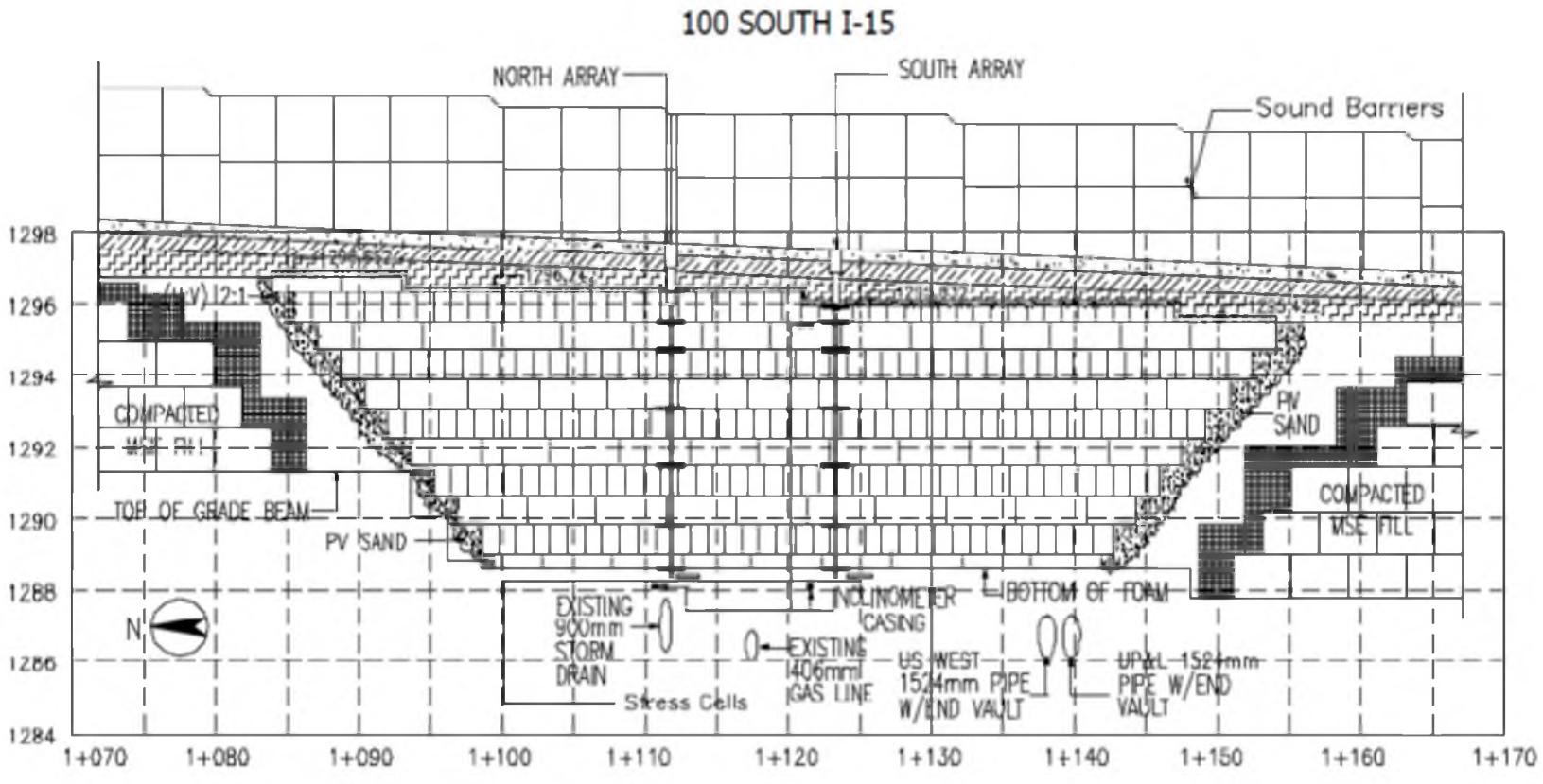

Figure 1.3 Profile View of the EPS Embankment and Instrumentation

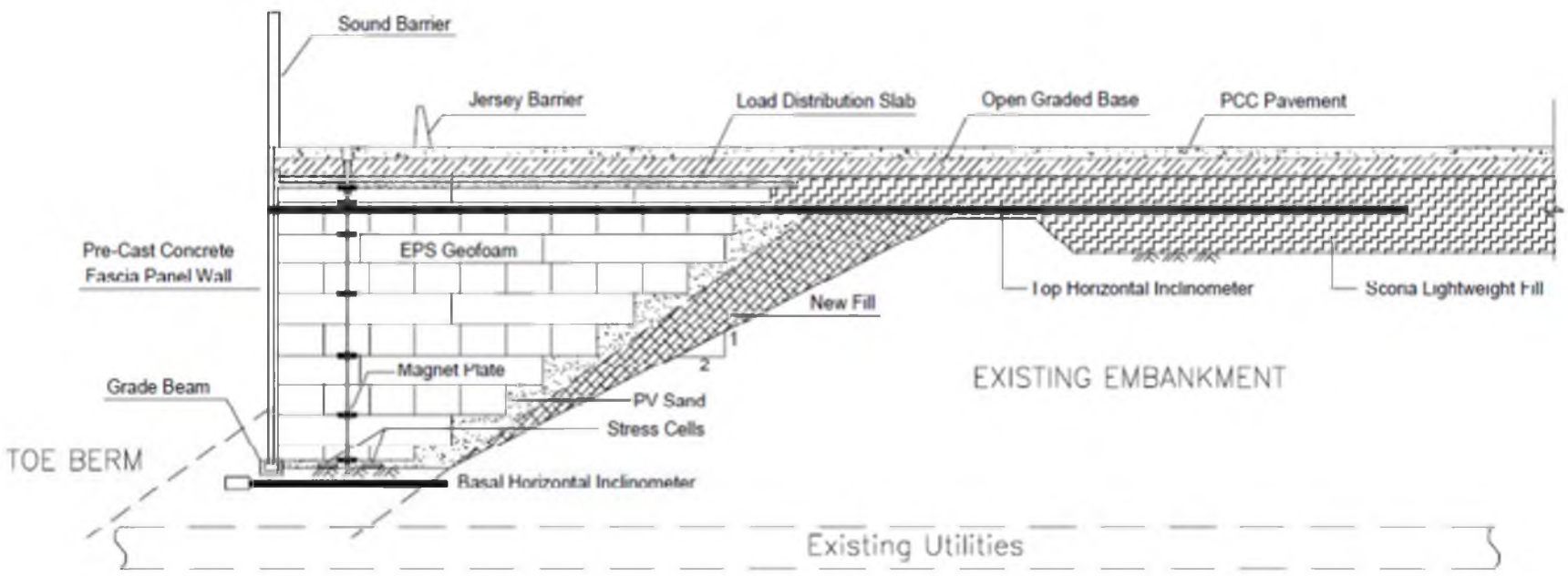

Figure 1.4 Cross-sectional View of the EPS Embankment and Instrumentation

transitions to two-stage MSE walls on both the north and south sides. In this area, the top part of the existing embankment was subexcavated and replaced with scoria fill to raise the roadway grade within the utility corridor without causing primary consolidation in the underlying, compressible, foundation soils.

The instrumentation installed at this location consisted of: (1) basal vibrating wire (VW) total earth pressure cells placed in sand underneath the EPS, (2) horizontal inclinometers (one placed near the base and one near the top of embankment), and (3) two magnet extensometers placed within the geofoam fill (Figures 1.3 and 1.4). The magnet plates for the extensometers were placed at EPS layers 0, 1.5, 3.5, 5.5, 7.5, 8.5, and 9.5 at the northern (i.e., left) location and at layers 0, 1.5, 3.5, 5.5, 7.5, 8.5, and 9 at the southern (i.e., right) location (Figure 1.3). All extensometer measurements were referenced to their respective base plate underlying the geofoam fill (and not the top of the riser pipe); hence, these data represent deformations of the geofoam fill with time and do not include any settlement of the foundation soils.

Figure 1.5 (Negussey and Stuedlein, 2003) shows the construction and postconstruction strain time history of the southern location as calculated from the magnet extensometer observations. The basal layers (0 to 1.5 m) underwent 1.8% vertical strain by end of construction at approximately 300 days. The total strain of the EPS embankment (0 to 9 m) was about 1% at end of construction at this same location (Figure 1.5). Figure 1.6 (Farnsworth et al., 2008) shows the construction and postconstruction strain of the entire embankment (0 to 9 m). The vertical strain at the southern location is about 1.5% after 10 years of monitoring and is projected to be about 1.7% creep strain after 50 years.

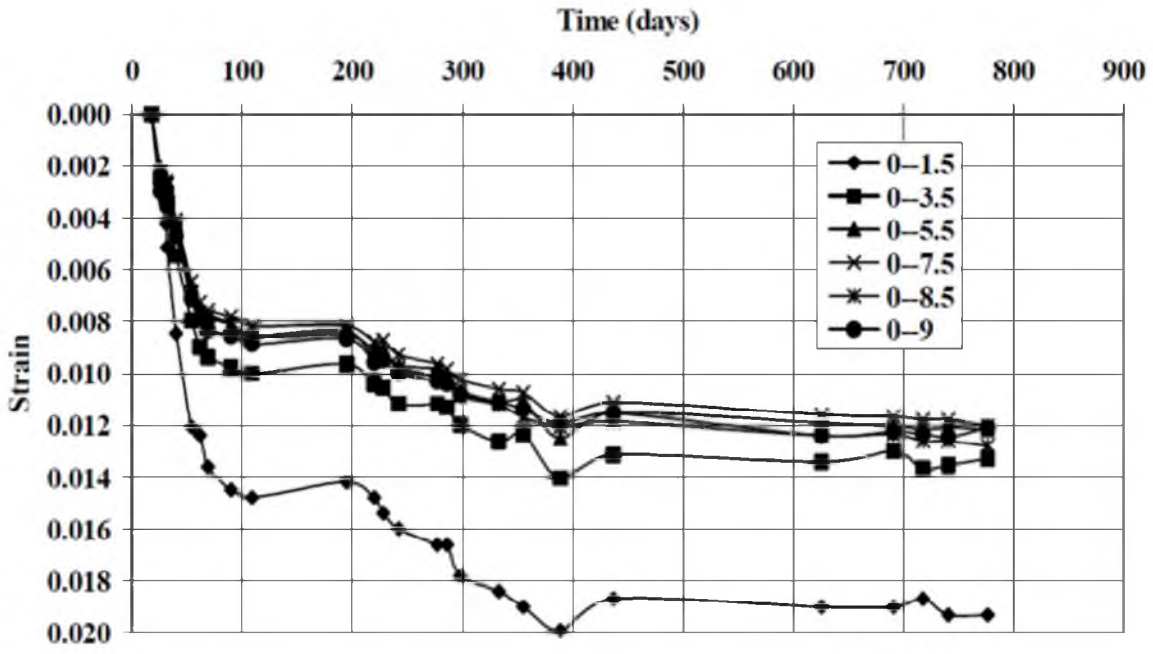

Figure 1.5 Construction and Postconstruction Strain in EPS

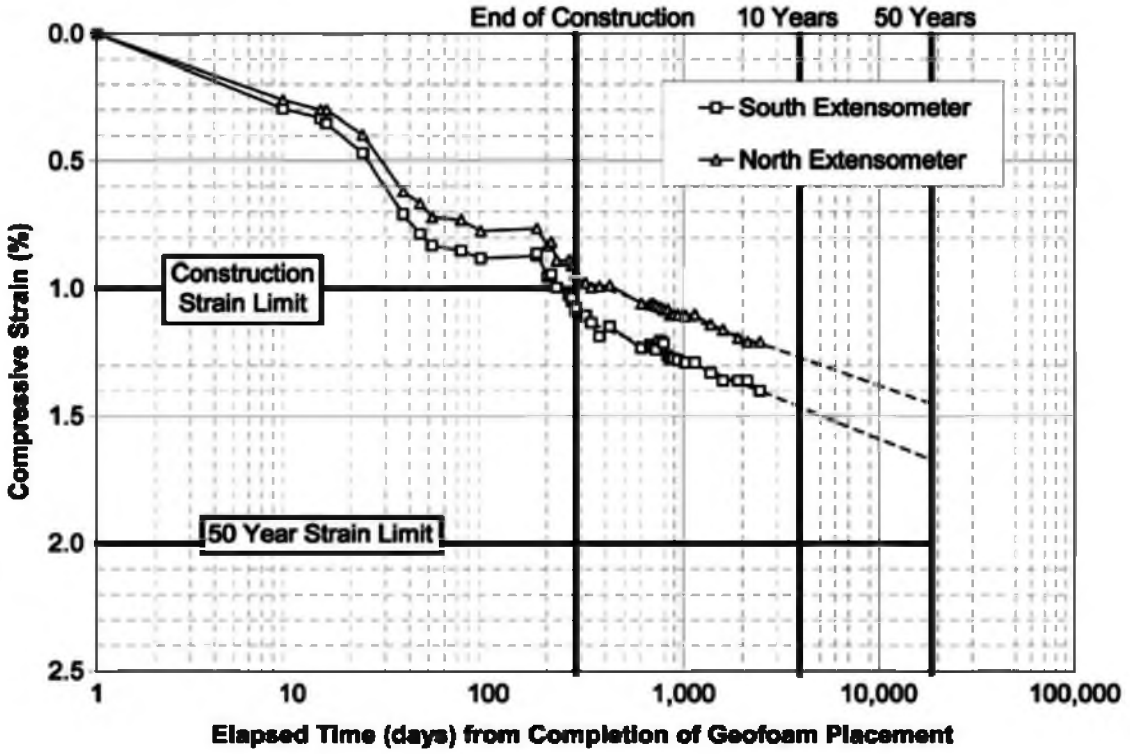

Figure 1.6 Construction and Postconstruction Global Strain of Entire EPS Embankment

The postconstruction settlement trend of Figure 1.6 is consistent with the limit 2% global strain in 50 years assumed in the I-15 design. Approximately 1% strain occurred during construction as materials were placed atop the EPS fill. The remaining strain is creep strain that has occurred postconstruction. Figure 1.5 shows that the lowest geofoam interval experienced more vertical strain when compared with the relatively uniform strain that occurred in the overlying layers. It should be noted that the foundation footing for the adjacent panel wall laterally restrains the lowest geofoam layer. As a result, the mean normal stress in the lower geofoam layers is probably somewhat higher than the corresponding states of stress in the overlying geofoam layers. This effect would produce more vertical strain and also suggests that the influence of confinement may need to be considered in future design evaluations, as appropriate.

1.2 The Use of EPS Block for Railway Embankment Systems

The primary focus of this thesis is on the use of EPS geofoam block for embankment support of rail systems. Unlike embankment support of roadway systems, this application is not widely used and is still in its development. The following section summarizes the known examples worldwide where EPS has been used for rail support.

1.2.1 Norwegian (NSB) Commuter Rail System

Plans to reconstruct national road 36 at Bole near the City of Skien in Telemark included building a new railway bridge at a road underpass (Frydenlund et al., 1987). In order to increase the free height at the underpass, the road level was lowered and the railway line elevated somewhat. The new bridge is constructed on footings in the sand

layer.

With the wider road and lowered road level, the upper clayey soil caused, however, stability problems, and the use of Expanded Polystyrene (EPS) as a superlight fill material against the northern bridge abutment was suggested and adopted. One problem to consider was that the loads from trains on the EPS material might create intolerable deflections close to the bridge, thus creating hammer effects on the bridge. In order to minimize such effects, it was decided to use EPS-blocks with unit density 30 kg/m^3. Furthermore, the total layer thickness of EPS was reduced somewhat towards the abutment. An approximate 1-m thick slab of Leca-concrete (Light Expanded Clay Aggregate) was cast on top of the EPS, being both fairly light and providing a platform for further load distribution. A 15-cm thick reinforced concrete slab is cast on top of the EPS- blocks. For fire safety, the outer blocks were specified as made of self-extinguishing EPS. The thickness of EPS-blocks used was 0.6 m.

After the new bridge was completed, load tests were carried out in order to measure deformations due to train live loads. Locations with various thicknesses of EPS along the railway track were selected and deformations measured with the 155 kN axle load at each location. Deflections were measured (1988-08-31) both on the sleepers and on bolts in the concrete slab above the EPS-blocks. The design adopted for the bridge is considered satisfactory, and trains are now passing the bridge daily. This case history will be modeled by this thesis, and details will be provided later in subsequent sections.

1.2.2 Utah Transit Authority (UTA)

Arellano and Bartlett (2012) reported that geofoam was recently incorporated in portions of the light and commuter rail systems in Salt Lake City, Utah by the Utah Transit Authority (UTA). Approximately, 60,350 m^3 (78,935 yd^3) of geofoam was used to construct approach embankments of four bridges along the 5.1 mile alignment of the West Valley TRAX light rail extension line. Also, approximately 68,810 m^3 (90,000 yd^3) of geofoam has been used for bridge embankments along the Salt Lake City Airport light rail extension. In addition to these light rail project, 10,988 m^3 (14,360 yd^3) of geofoam embankment has also been used along the UTA FrontRunner South commuter rail line that extends from Salt Lake City to Provo, Utah.

See Figure 1.7 and Figure 1.8 for examples of geofoam utilization by UTA.

The FrontRunner embankment shown in Figure 1.8 will also be modeled by this thesis and details regarding its construction are given later.

1.2.3 Netherlands

Esveld et al. (2001) reported that large areas of the densely-populated western and northern parts of The Netherlands consist of subsoil with geotechnical characteristics ranging from poor to very poor. Building of railway structures under these conditions would require a substantial improvement of the bearing capacity. The conventional approach consists of replacing a great deal of the poor soil by sand (subgrade improvement). Even if preloading of a subgrade layer is applied, relatively large settlements due to high weigh of a track structure are likely to occur during the initial phase of the structure's life. With the application of ultra-light materials, such as

Figure 1.7 Geofoam at UTA TRAX Light Rail

Figure 1.8 Geofoam at UTA FrontRunner Commuter Rail

EPS, a so-called "equilibrium" structure can be created, which would practically prevent the increase of grain stresses in the subgrade. In other words, the weight of the track structure plus lightweight material should approximately compensate the weight of the excavated material. In their research, an unconventional railway track, a so-called Embedded Rail Structure (ERS) is considered. Traditional ballast is replaced by a reinforced concrete slab in such a structure. To reduce the total weight of a structure and consequently stresses in the subgrade, an EPS layer is applied between the slab and subgrade. The static and dynamic properties of such a track are investigated to demonstrate the feasibility and advantages of EPS usage in railway track design.

Figure 1.9 shows the EPS geofoam bridge approaches constructed for the light rail system in Brederoweg, Schiedam, Netherlands. The picture was obtained in Google Earth.

1.3 Previous Modeling of Rail and Ballast Systems

This thesis seeks to develop a numerical method for modeling EPS embankments used to support rail systems. Important to its development is a brief summary of germane modeling studies performed by others.

1.3.1 Analytical Approaches

According to Zakeri and Sadeghi (2007), the most common analytical method of calculating sleeper deflection (deflection of the rail at the sleeper positions) is the Winkler equation. However, this model is of limited value in considering the behavior of the substructure beneath the rail. Since the EPS-supported embankment that is being

Figure 1.9 EPS Embankment in Netherlands

studied in this thesis is a multilayered system, this method cannot be used.

1.3.2 Numerical Approaches

Even though there are some numerical analysis on railway systems in the literature, they are generally not focusing on the vertical displacement of the system.

Most germane to this study is a modeling study performed by Powrie et al. (2007). These authors reported the results of finite element method (FEM) analyses carried out to investigate the ground surface displacement and stress changes due to train loading. This study will be discussed in more detail and used to develop and validate the proposed modeling approach presented herein.

1.3.2.1 Track System Geometry

The typical track structure shown was modeled in the FEA, but without geotextile. Depths of 300 mm of ballast, 200 mm of sub-ballast, and 500 mm of prepared subgrade were adopted in the analysis. The rail cross-section was modeled as a rectangle of 153 mm high × 78 mm wide. With a Young's modulus E = 210 GPa, the bending stiffness EI = 4889 kN·m^2 corresponds to a 56.4 kg/m steel rail. Sleepers were modeled as cuboids of 200 mm high, 242 mm wide, and 2420 mm long, with a spacing of 650 mm between centers. Rail pads were not modeled explicitly, as they would have no effect on the transmission of loads to the ground in a static analysis. More discussion will be provided in the modeling section in this thesis.

1.3.2.2 Loading Condition

The analyses were based on a typical modern freight car – an MBA box wagon as used by English Welsh & Scottish Railways (EWS) to convey heavy bulk materials such as coal, aggregates, and construction materials. These have an axle load of 25.4 tones (the maximum normally permitted on the UK rail network), corresponding to a static wheel load of 125 kN.

1.3.2.3 Adequacy of a Static Analysis

In reality, vertical loads exerted by a moving railway vehicle may be greater or less than the static value, depending on whether the vehicle is momentarily accelerating downward or upward. However, it is a common practice to carry out a static analysis, in which dynamic effects are taken into account by multiplying the static load by a dynamic

amplification factor (DAF). The DAF depends on the train speed, the track quality, and confidence intervals required and may normally range from 1.1 to 2.8 (Esveld, C., 2001). DAFs have not been used in this analysis, but with the geomaterials assumed to behave as linear elastic materials, the calculated stress changes will be directly proportional to the loads. Dynamic finite element analyses carried out by Grabe (2002) indicated that, for speeds up to 240 km/h, the impact of dynamic effects on the calculated maximum changes in stress in the ground below a railway line were small, whereas the ground response from moving train loads is essentially quasistatic for speeds up to 140 km/h (Kaynia et al., 2000). Thus, it was concluded that, for the purpose of determining representative ground surface displacement and stress changes, a static analysis would suffice.

1.3.2.4 Model properties

The geotechnical properties of all the materials were modeled by Powrie et al. (2007) as linear elastic.

CHAPTER 2

RESEARCH OBJECTIVES AND PLAN

2.1 Summary and Findings from Literature Review

The main purposes of the literature review were to: (1) explore potential methods to model EPS embankments and the deformations associated with train loadings, and (2) review models and embankment performance cases that could be potentially used in the development and validation of the propose modeling approach.

The methods of modeling deflections of rail systems supported by earthen embankment are summarized in Chapter 1. However, studies on deflections of rail systems supported by EPS embankment are rare, and thus, the approach to evaluate the deflections from train loading is still in development.

2.2 Research Objectives

This research seeks to develop a numerical method to evaluate the rail deflections for systems constructed atop EPS embankments. The objectives of this study are: (1) develop the numerical method, (2) validate the model through a series of modeling exercises, and (3) verify and calibrate the numerical approach for real rail systems using deflection measurements obtained from Norway, and from the UTA Frontrunner project in Draper, Utah. To accomplish these objectives, the following tasks/activities are

required: (1) literature review of current methods, (2) laboratory testing of material properties, (3) model development, (4) model validation, (5) model calibration, and (6) comparison with measurements obtained for real systems.

2.2.1 Development of Numerical Approach for Deflection Estimation

According to AREMA Manual for Railway Engineering, this type of analysis is conducted by considering the rail to be supported on an elastic foundation. Because the deformation caused by rail loads is very small compared to the size of the embankment system, the deformation can be assumed to be within the elastic range of the materials; hence, elastic propertied model can be used in the constitutive model. Therefore, the modeling done is this thesis will be elastic models using the finite difference method (FDM). Both two-dimensional (2D) finite difference models, i.e., FLAC2D v. 5 (Fast Lagrangian Analysis of Continua) (Itasca, 2005) and three-dimensional (3D) finite difference models, i.e., FLAC3D v. 3 (Itasca, 1993-2002) will be implemented. 2D models will be used as exploratory models to identify the appropriate mesh size and the associated level of discretization of 3D models.

2.2.2 Validation of Numerical Approach

For validation purposes, the FDM modeling approach developed in this thesis will be checked against existing closed-form solutions, other FEM models from the literature and with measurements obtained from case histories from real railway systems. It is hoped that the results obtain herein should reasonably match these modeling and case history examples in order to validate of the FDM modeling approach for potential use in

evaluating real systems.

To this end, the FDM model development will start from simple analytical cases and progress to modeling real rail systems supported on EPS embankment. The progressive modeling cases considered and compared will include: point load on homogeneous elastic half space using elastic theory (Appendix A), line load on homogeneous elastic half space using FEM (Helwany, 2007) (Appendix B), and circular load on layered soil system using FEM (Appendix C),

2.2.3 Verification and Calibration of the Numerical Approach

In order to model real rail systems, a large chamber test is developed to measure Young's modulus (resilient modulus) of the railway ballast and sub-ballast as a part of this thesis research as described in Chapter 3, which details the test set-up, process, and results. Other material properties, such as Poisson's ratio of the ballast and sub-ballast, the properties of other materials including EPS, rail, and sleeper etc. are obtained from the literature.

The deflections of rail systems supported by regular earth embankment due to train load have been analyzed using the FEM for a real system (Powrie et al., 2007). This case will be modeled in Chapter 4 using the FDM to further develop the modeling method. In addition, Chapter 4 will present the modeling of the measured deflections obtained from the Norwegian Railways (NSB) for a case history of EPS embankment in Central Norway. Finally, a major part of this thesis will focus on the development of a FDM model for the UTA Frontrunner EPS embankment in Corner Canyon, Draper Utah. This will be used to make a prior predictions of the deflections of this multilayered railway

system supported by EPS embankment. The results of the modeling will be later verified using survey field measurements. It is hoped that when validated, the FDM approach can be used in future projects for the design and evaluation of EPS-supported rail systems.

CHAPTER 3

LABORATORY TEST ON BALLAST

3.1 Introduction

The compression behavior of granular material is usually studied in the conventional one-dimensional compression equipment. However, the typical diameter of the ballast used for rail support is as large as approximately 2 to 3 inches. Thus, difficulties will be encountered and significant error will be introduced if conventional compression / compaction / consolidation apparatuses are used. Therefore, a large-scale "consolidometer" with a diameter of approximately 40 inches (Figure 3.1) was used to conduct a one-dimensional compression test on the ballast. The primary major purpose of this test is to determine the Young's modulus of the railway ballast to support the modeling of the embankment system.

3.2 Specimen Preparation

The ballast samples were supplied by Staker Rock Products, Inc., of Herriman, Utah. This pit was the same pit that supplied the ballast for the UTA commuter rail embankment in Corner Canyon, Draper, Utah. The diameter of the ballast ranges from 1 to 3 inches with a typical value of about 2 inches. To simulate the field condition of frequently used tracks, compacted (dense) ballast was prepared by impacting 75 blows

from a tamper, as shown in Figure 3.1, to each layer of ballast having a thickness of 6 inches. During the compaction process, the ballast was found to be very self-compacting. This compaction was adequate to produce densities close to the field compaction of the FrontRunner railway. All specimens were air-dried. Since the travel distance of the loading ram was limited, the sample was filled to within 6 inches of the top the chamber (Figure 3.2).

3.3 Test Set-up

The large-scale one-dimensional compression apparatus (Figure 3.3) consist of: the test chamber (inner diameter: 41.9 in., height: 36.0 in.); the axial loading system; the axial displacement and force monitoring system (Figure 3.4). The axial loading system consists of the loading ram and the load plate. The loading ram has a maximum capacity of 60 kips. The load plate is made of rigid steel so it can be reasonably assumed that the pressure can be applied uniformly on the surface of the ballast. The plate has a thickness of 1.5 in. and a diameter of 40 in.

3.4 Test Procedure

Three tests were conducted consecutively on the ballast. The first test was a cyclic strain (displacement) controlled test with an amplitude of 5 mm (0.1969 in.). The second test was a cyclic strain (displacement) controlled test with an amplitude of 30 mm (1.1811 in.). Both of the cyclic tests had a frequency of 0.5 Hz. Each test ran 1000 cycles. 20 data points were obtained for each cycle. There was no negative displacement throughout the tests because the tensile strength of ballast can be neglected. The third test

Figure 3.1 Compaction of Specimen

Figure 3.2 Amount of Specimen Used

Figure 3.3 Completed Test Set-up

Figure 3.4 Axial Displacement and Force Measurement System

was a stress (force) controlled test. During this test, the ballast was subjected to a monotonic loading at a force-increasing rate of 500 lb/min. This test lasted for 5257 seconds and the load increased up to 43.6 kips. After the last test was finished, the total weight of ballast was measured to be 2244 lbs. Volume of the ballast was also measured. Before the first test, the total volume was 23 ft^3; after the last test, the total volume decreased to 22 ft^3. Thus, the unit weight of ballast was calculated to be 98 pcf before the test and 103 pcf after test.

3.5 Test Data and Interpretation

The data from two cyclic tests are shown in Figure 3.5. Enlarged plots at different stages of the tests were also obtained.

They were the stress (σ)-strain (ε) behavior of the ballast near the beginning of the first cyclic test (Figure 3.6), near the middle of the first cyclic test (Figure 3.7), near the beginning of the second cyclic test (Figure 3.8), and near the end of the second test (Figure 3.9). Since negative stress was unlikely to exit for the ballast system, only the positive stress was considered. In other words, only the curves above the x axis will be used for calculation of the constrained modulus (M), which is proportional to the slope of the straight line represented in curves. Young's modulus (E) can subsequently calculated from M, based on the assumption that the Poisson's ratio (v) equals 0.3. The negative stress is due to the force generated by the loading system itself. Since this force is consistent and the calculation of the slope only involves the change of the stress, the results are not affected.

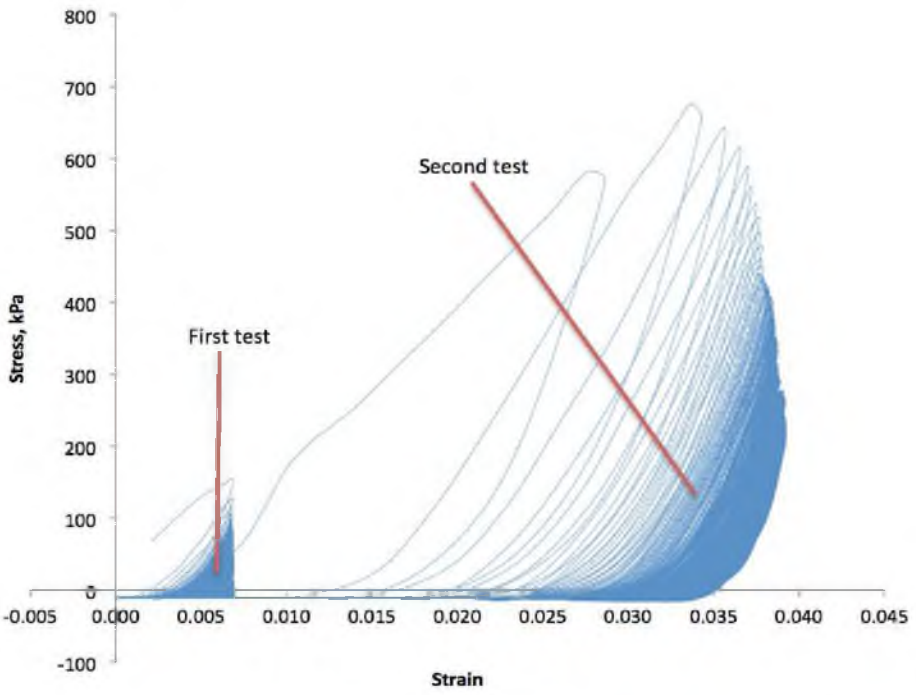

Figure 3.5 Stress-strain Behavior of Ballast under Cyclic Loading of Two Amplitudes

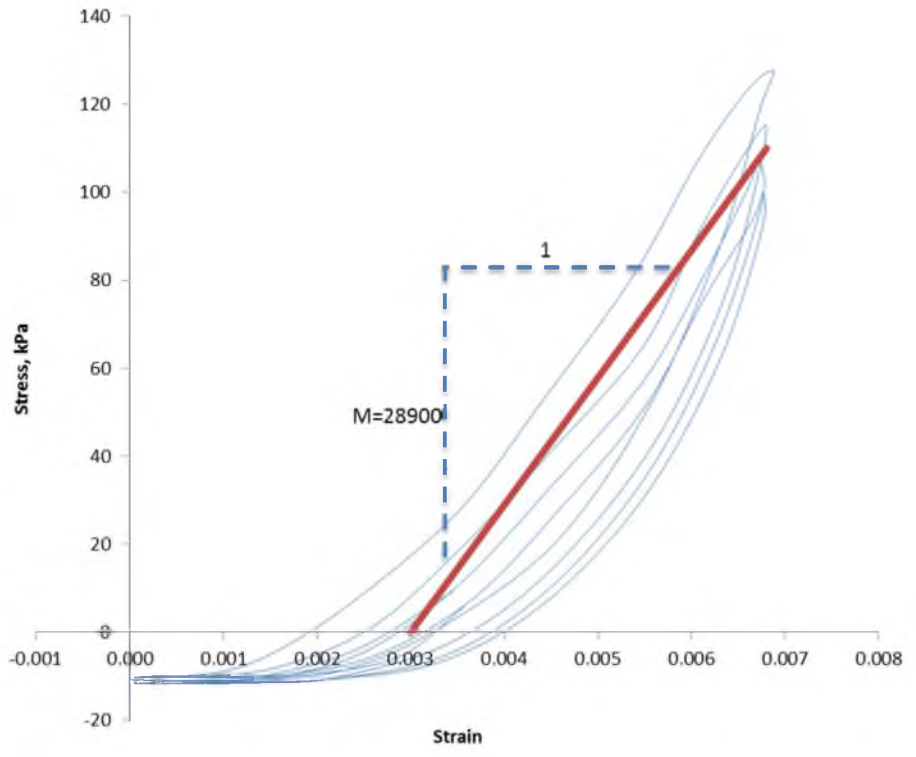

Figure 3.6 Stress-strain Behavior of Ballast near the Beginning of First Cyclic Test

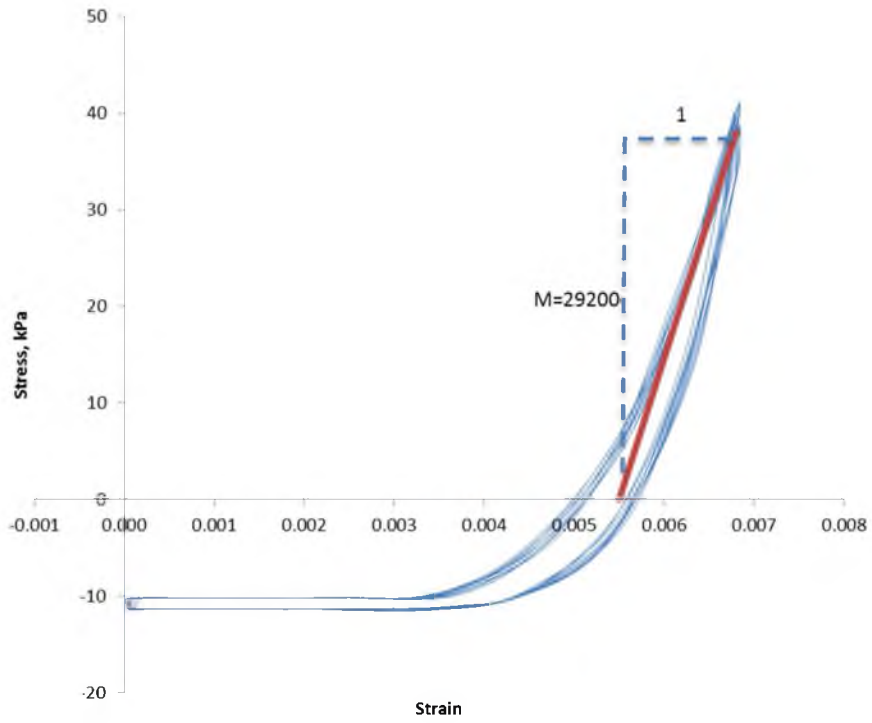

Figure 3.7 Stress-strain Behavior of Ballast near the Middle of First Cyclic Test

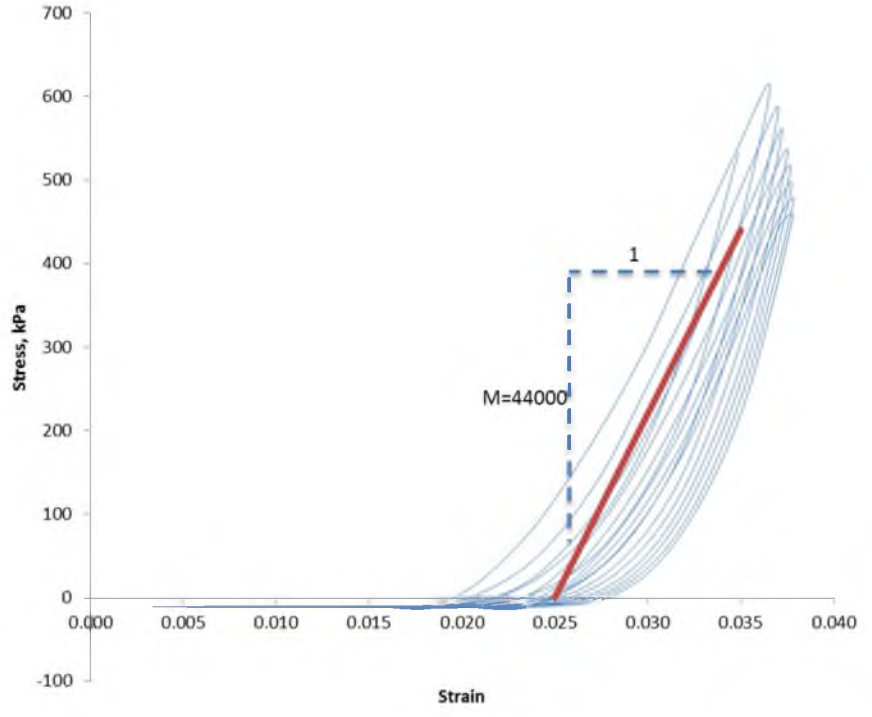

Figure 3.8 Stress-strain Behavior of Ballast near the beginning of Second Cyclic Test

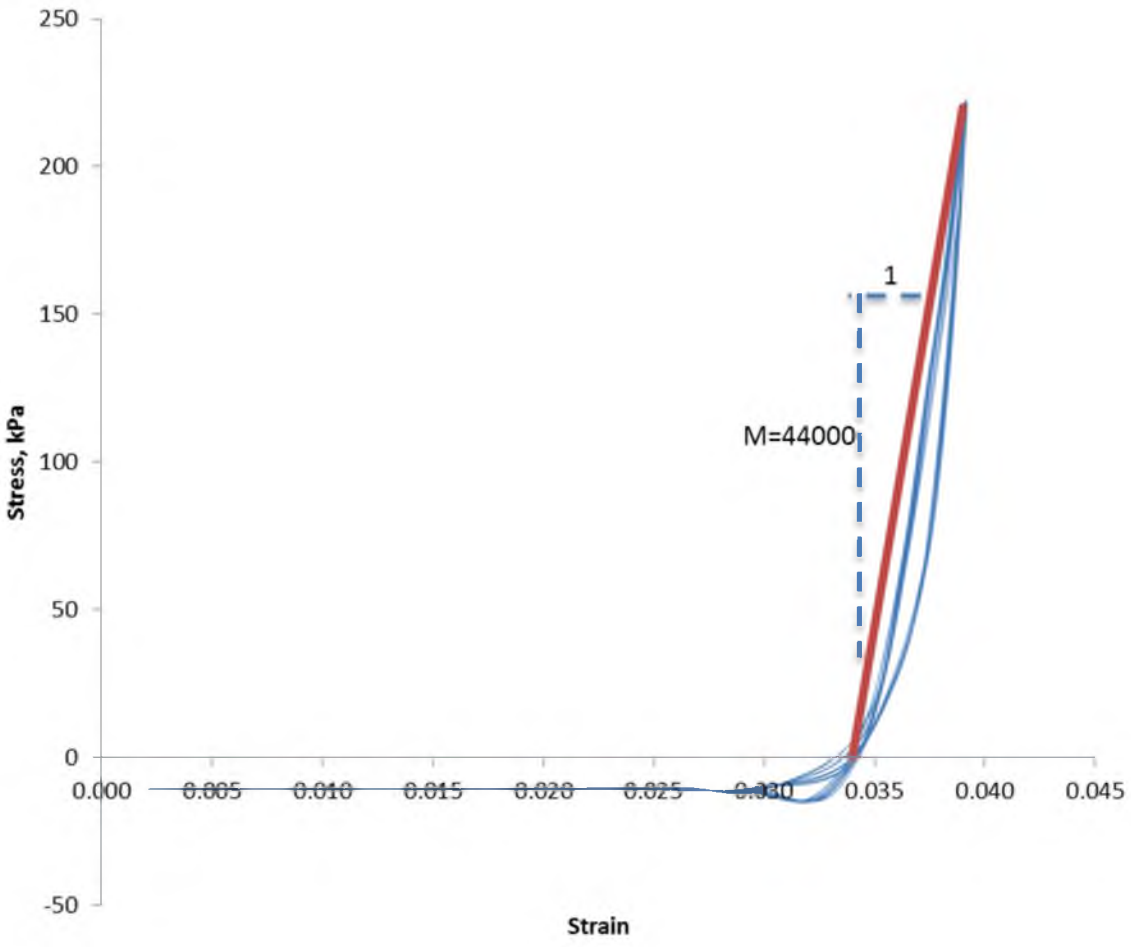

Figure 3.9 Stress-strain Behavior of Ballast near the End of Second Cyclic Test

Based on the plots above, the constrained modulus near the beginning and the end of the test is nearly the same for both tests. The results are summarized in Table 3.1.

Stress-strain behavior of ballast during monotonic loading is also shown in Figure 3.10. The monotonic loading starts from the strain level of the second cyclic test.

Since the ballast is used as the material for the pavement, the resilient modulus should be used in the numerical model for the UTA FrontRunner embankment. By definition, resilient modulus is Young's modulus while the material is subjected to low amplitude cyclic loading, which is a simulation of traffic loading. Thus, Young's modulus

Table 3.1 Summary of Cyclic Test Results

Amplitude (mm)	ε	M (kPa)	E (kPa)
5	0.00686	29089	21609
30	0.04118	44000	32686

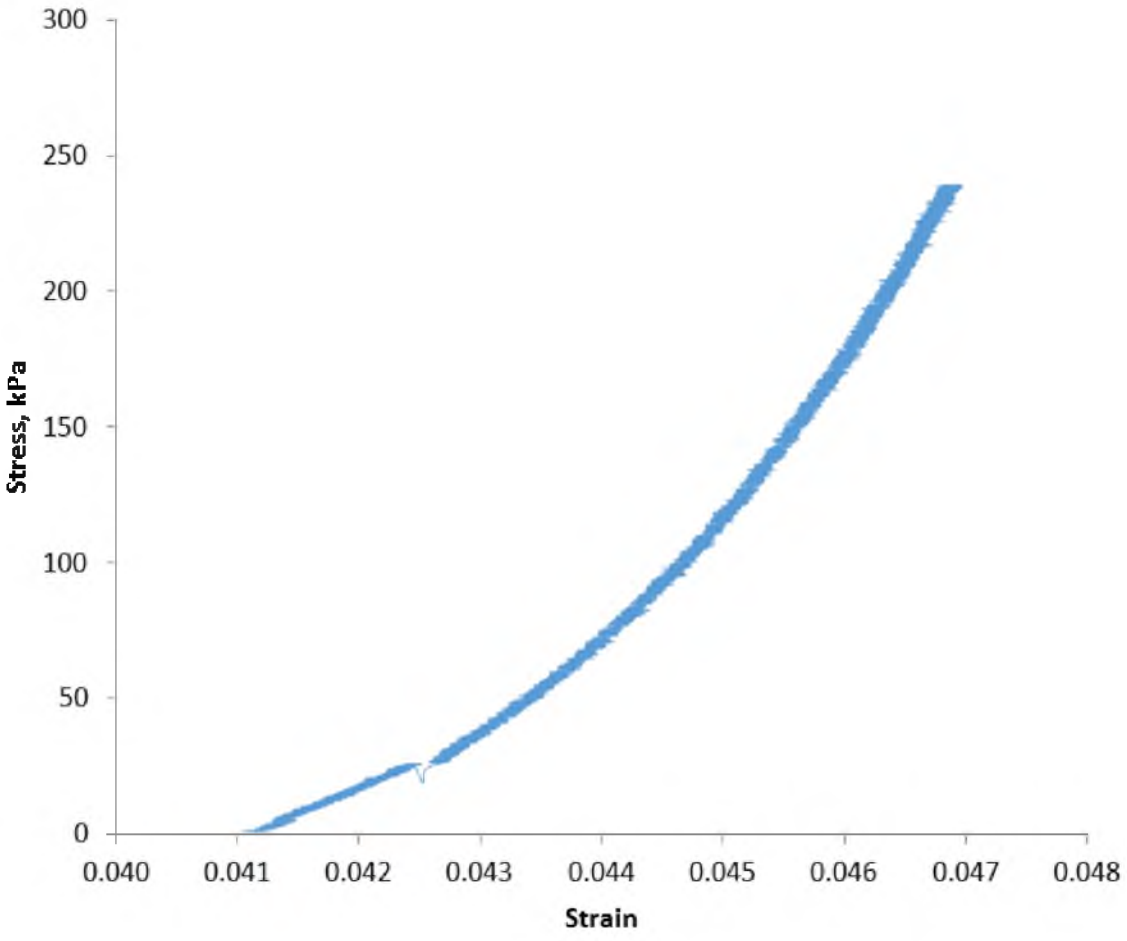

Figure 3.10 Stress-strain Behavior of Ballast during Monotonic Test

calculated from cyclic tests will be used, instead of the monotonic test. From the results in Table 3.1, Young's modulus is different at different strain levels. Interpolation or extrapolation methods will be used to obtain the Young's modulus for the strain level of the actual embankment.

CHAPTER 4

FDM MODELING

As a main part of this thesis, three FDM models were developed and evaluated: (1) a hypothetical earthen rail embankment where the results were compared and verified with FEM modeling of the same embankment as presented in the literature (Powrie et al., 2007), (2) an actual EPS-supported, multilayered, Norwegian, commuter railway embankment system where the results were compared and verified with field deflection measurement from Norway for that same system (Frydenlund et al., 1987), and (3) an actual EPS-supported embankment for the Utah Transit Authority (UTA) Commuter Rail System (i.e., Frontrunner) in Corner Canyon, Draper City, Utah where field measurements of the railway deflections are currently in progress by others.

This chapter contains problem statements for each case and the simplifications made for modeling purposes. In addition, the details of the FDM models including geometry, boundary and loading conditions, and model properties are also described. The results are presented and compared with the FEM modeling by others, or with actual field measurements of railway deflections, when available.

In order to calculate the vertical deflections induced in the rail systems, both 2D finite difference models, i.e., FLAC2D v. 5 (Fast Lagrangian Analysis of Continua) (Itasca, 2005) and 3D finite difference models, i.e., FLAC3D v. 3 (Itasca, 1993-2002) were

implemented. The 2D models are axisymmetrical or plane strain models that include structural elements. The 3D models are plane-symmetrical models.

4.1 Rail System Supported by Regular Earth Embankment

4.1.1 Problem Statement

Powrie et al. (2007) conducted a 2D FEM analysis on displacements caused by wheel load at the ground surface of a railway system supported by an embankment using the geometry shown in Figure 4.1 with a static wheel load of 125 kN. A similar 2D FDM analysis was conducted in this thesis for comparison and verification of the FDM modeling.

4.1.2 Assumption/Simplifications

To analyze the 3D railway system in a 2D model, Powrie et al. (2007) used the following simplification to convert the discrete sleeper spacing into an equivalent, continuous loading for the 2D plane strain model. Because in a 2D analysis the sleepers are inherently continuous, the Young's modulus (E) of the sleepers was scaled by the ratio of sleeper width (w, 242 mm) to spacing (a, 650 mm) to give the same value of lateral bending stiffness EI per meter length of the track as for the discrete sleepers.

4.1.3 Solution

4.1.3.1 FEM Solution

In order to determine the appropriate mesh spacing for the analyses, three mesh densities were investigated by Powrie et al. (2007): (1) an intermediate mesh (Figure 4.2)

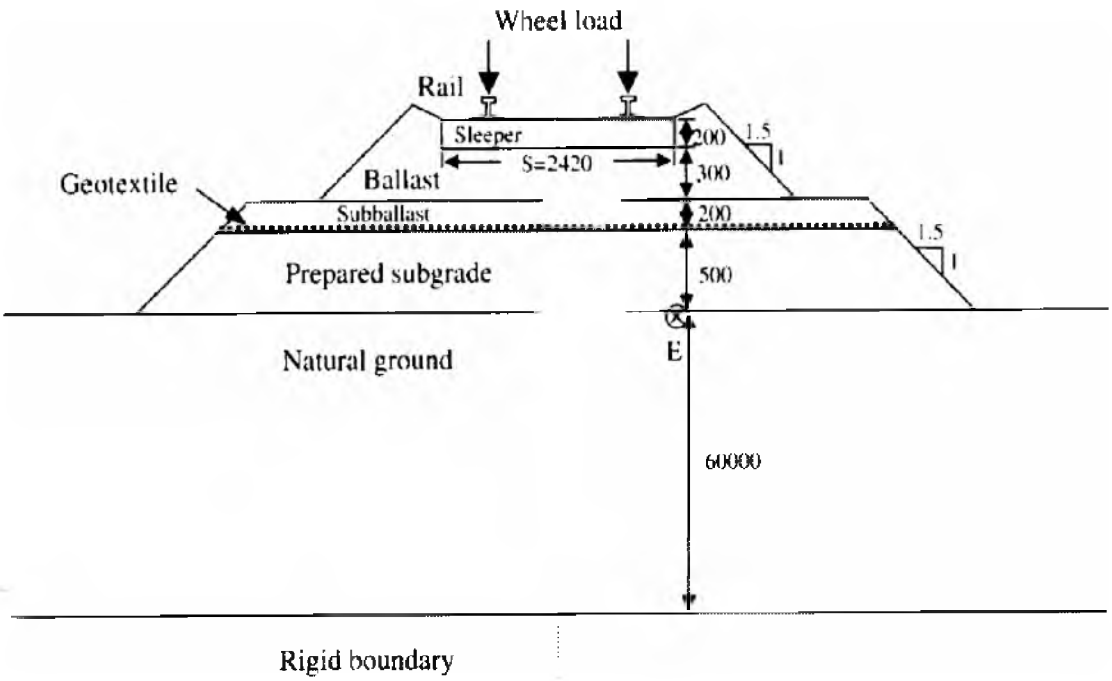

Figure 4.1 Schematic Cross-section of a Typical Track Structure (mm)

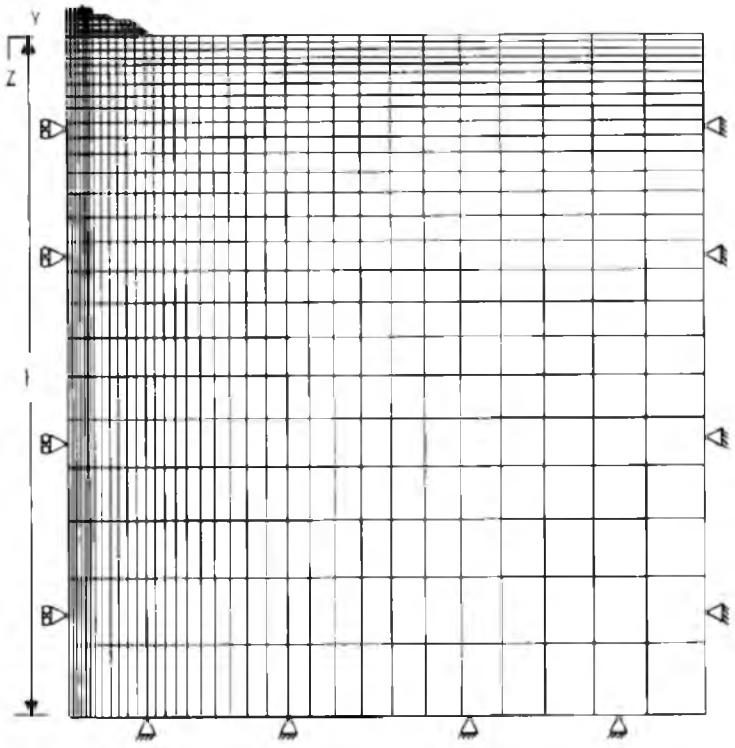

Figure 4.2 FEM Mesh

(2) a coarse mesh which had half the element density (i.e., approximately one-quarter of the number of elements), and (3) a fine mesh which had twice the element density (i.e., about four times the number of elements). In all cases, the bottom and right-hand boundaries were restrained in both the horizontal and vertical directions. The left-hand boundary was prevented from moving in the horizontal direction, but allowed to move freely in the vertical direction, which is consistent for an axis of symmetry found along the left-hand margin of the model.

Powrie et al. (2007) found that all three meshes gave almost identical ground-surface displacement. However, differences in the stresses within the ballast layer were noted, particularly for the coarse mesh, so the intermediate mesh was used by Prowie et al. for the subsequent analyses. The intermediate density mesh had dimension 60 m × 60 m for the depth and width of natural ground (Figure 4.2). A ground displacement of 1.14 cm was obtained by Powrie et al. (2007) for the 125 kN wheel load.

4.1.3.2 2D FDM FLAC Solution

The 2D FEM solution of Powrie et al. (2007) was modeled in FLAC 2D as a check of the 2D FDM approach. Figure 4.1 shows the geometry of the multilayer rail system that was used in the verification. In the FEM and FDM models, only half of the system was included because the system is symmetrical (Figure 4.2). Figure 4.3 shows the FDM mesh that was developed to represent the system. The FDM used approximately the same intermediate density mesh of Powrie et al. (2007) with dimensions of 60 m × 60 m (depth and width of natural ground).

The bottom and right-hand boundaries were restrained in both the horizontal and

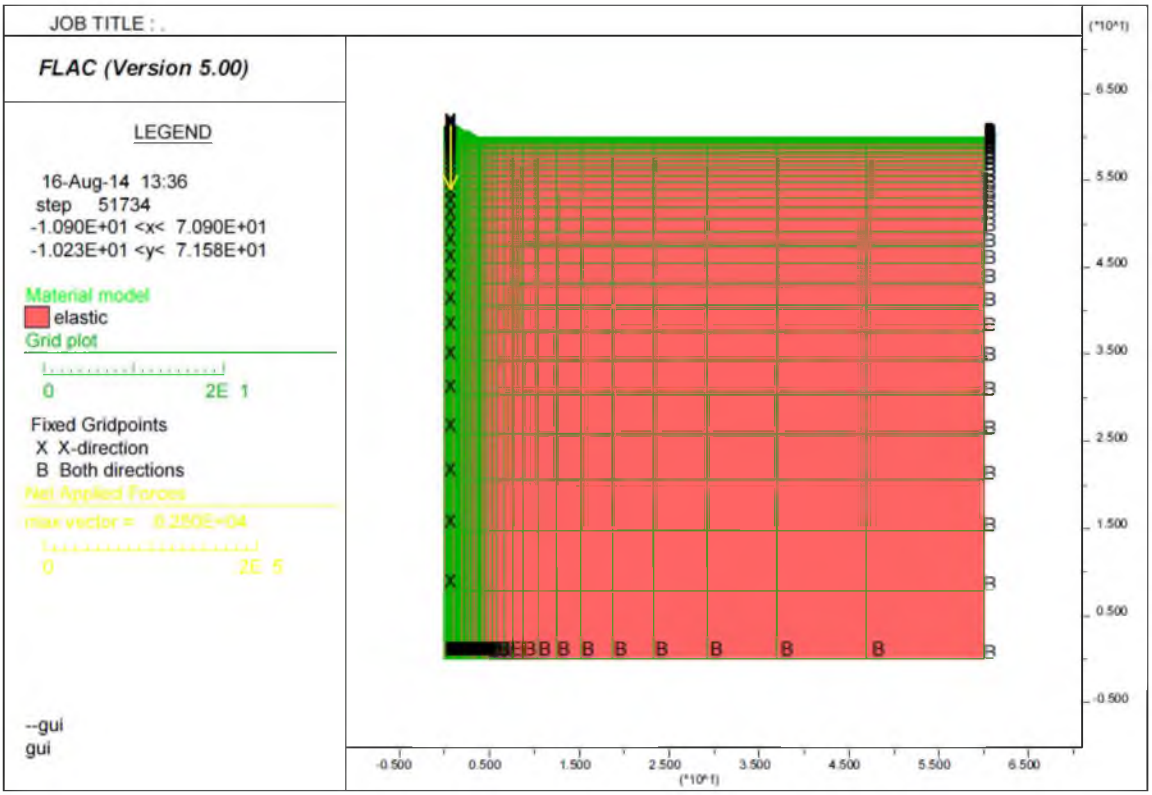

Figure 4.3 FDM Mesh (m)

vertical directions. The left-hand boundary was prevented from moving in the horizontal direction, but was free to move vertically. A wheel load of 125 kN was applied on each rail. (In the FLAC modeling, because there are two nodes assigned to a single rail, a vertical force of 62.5 kN was applied to each node.) The properties of each material are shown in Table 4.1. These were used for both the FEM and FDM modeling and were taken from Powrie et al. (2007). Values of the shear modulus (G) and bulk modulus (K) required for the FLAC modeling were calculated using elastic theory based on the values of Young's modulus (E) and Poisson's ratio (v) given in Table 4.1.

Table 4.1 Material Properties Used in FEM and FDM Analysis

Description	E (MPa)	v	Note
Rail	210000	0.3	78 mm wide, 153 mm deep
Sleeper (2D)	13000	0.3	242 mm wide, 200 mm deep
Ballast	310	0.3	
Sub-ballast	130	0.49	
Prepared subgrade	100	0.49	
Natural Ground	30	0.49	

4.1.4 Comparison, Conclusion and Discussion

The FDM, as implemented in the FLAC model, gave results that were very similar to those reported in Powrie et al. (2007) using the FEM. The vertical displacement contours for the FDM are shown in Figure 4.4. Directly under the rail, the FDM FLAC model estimates a total ground surface displacement of 11.7 mm from the 125 kN wheel load; the FEM analysis of Powrie et al. (2007) resulted in a total ground surface displacement of 11.4 mm. The difference in these modeling results is about 3%. The similarity in the results demonstrates that both methods are capable of producing consistent results when used to estimate ground surface displacement of railway system under static loading. The FLAC code used for this modeled case is found in Appendix D.

4.2 Rail System Supported by EPS Embankment in Norway

4.2.1 Problem Statement

The next step in the modeling progression was to see if the FDM is capable of estimating total ground displacement for a real system. This will be done using an example of an EPS embankment constructed in Norway that was subjected to a

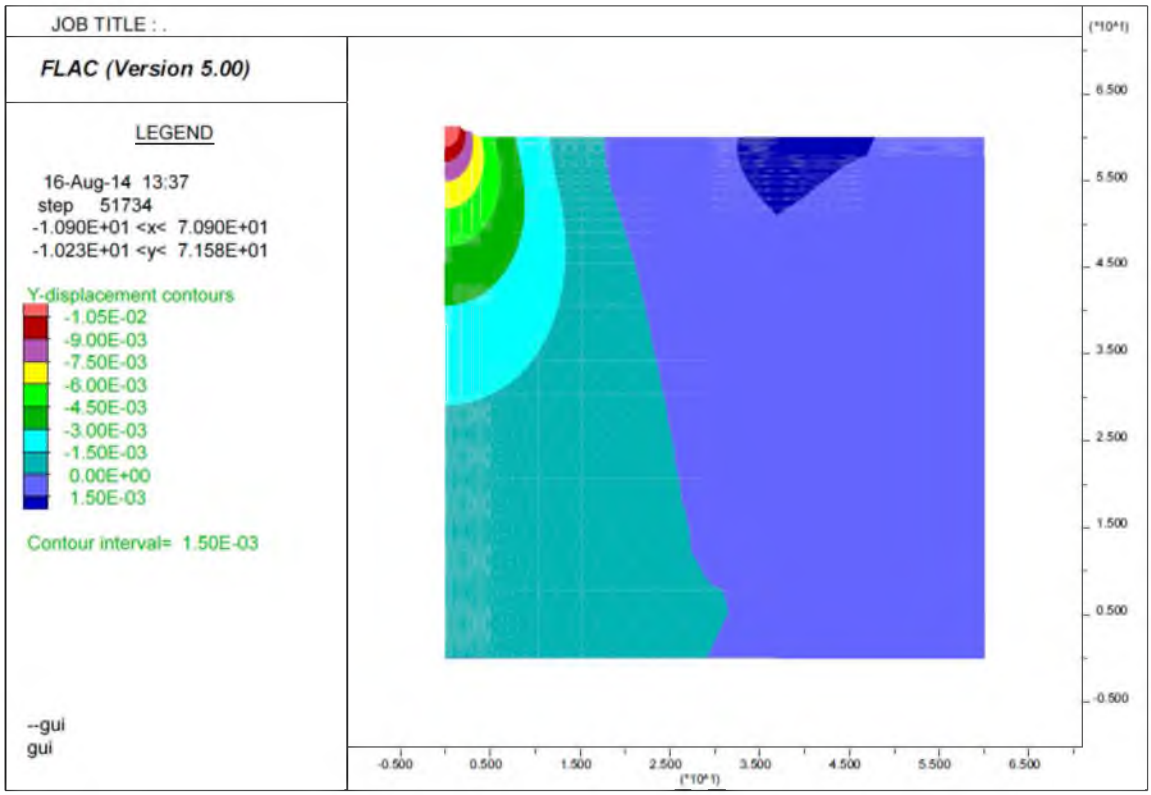

Figure 4.4 Vertical Displacement Contours (m)

commuter-rail loading. Survey measurements were made of the static rail deflections resulting from this loading and documented by the Norwegian Public Road Administration (Frydenlund et al., 1987).

Plans to reconstruct the National Road 36 at Bole near the City of Skien in Telemark, Norway included building a new railway overpass bridge at a road underpass (Frydenlund et al., 1987). In order to increase the headroom at the underpass for the highway, the road elevation was lowered and the railway line embankment was elevated somewhat. The new bridge was to be constructed on footings founded in a sand layer; however, associated with the wider road and lowered road level, the construction could potentially cause stability issues in the foundation soils which were soft and clayey in

nature. To address this issue, Expanded Polystyrene (EPS) geofoam block was selected as a superlight fill material against the northern bridge abutment.

EPS with a unit density of 30 kg/m^3 (i.e., EPS30) was used at this location. A 15-cm thick reinforced concrete slab was cast atop the EPS geofoam blocks (Figures. 4.5 and 4.6). The height of the EPS embankment was 4 blocks high (Figure 4.5), and the corresponding height of each individual block was 0.6 m, making the total EPS embankment height equal to 2.4 m. The length of the sleepers supporting the rail was estimated to be 2.42 m. The material properties used in the FDM modeling are given in Table 4.2. (Note that the EPS was modeled in the FLAC model using published properties from ASTM D6817 for EPS29 (density = 29 kg/m^3) instead of EPS30 (density = 30 kg/m^3) because material properties were not available from Frydenlund et al. (1987) for EPS30. Because EPS29 has nearly the same density as EPS30, only very minor differences in the material properties are expected, and these differences should not affect the modeling results in a significant manner.)

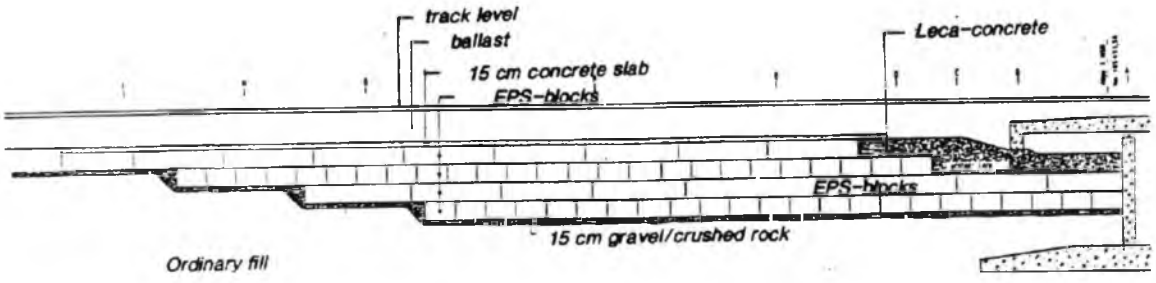

Figure 4.5 Longitudinal Section of the EPS Supported Embankment

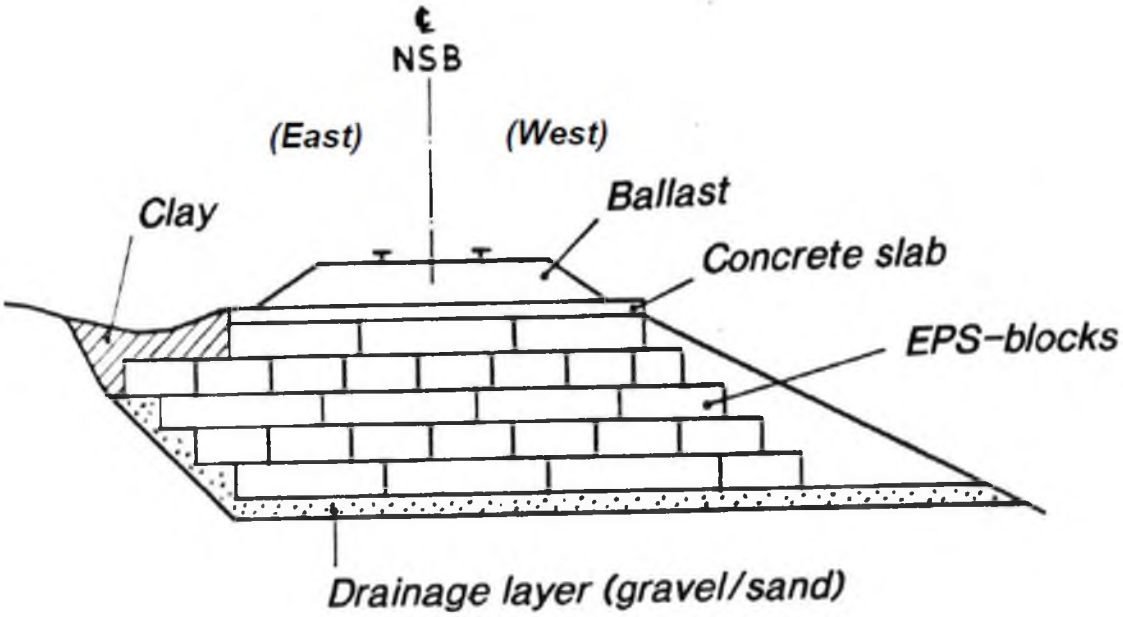

Figure 4.6 Cross-section of the EPS Supported Embankment

Table 4.2 Material Properties Used in FDM Analysis

Description	E / MPa	v	Note
Rail	210000	0.3	78 mm wide, 153 mm deep
Sleeper (3D/2D)	31000/13000	0.3	242 mm wide, 200 mm deep
Ballast	130	0.3	
Concrete Slab	40000	0.2	
EPS29	7.5	0.103	
Drainage Layer	300	0.3	
Fill	300	0.3	
Sand (Natural Ground)	100	0.3	

4.2.2 2D Model Preparatory Study

To model the Bole embankment rigorously, a 3D model is required; however, a 2D model was developed beforehand to identify the appropriate mesh size and the associated level of discretization required to reasonably estimate the total surface displacement from the train loading. This exploratory use of a 2D model was preferable because it required significantly less computational time and computer memory.

Similar to Powrie et al. (2007), three mesh densities were investigated: (1) an intermediate mesh (Figure 4.7, see also FLAC code in Appendix E), (2) a coarse mesh, and (3) a fine mesh. In all the cases, the bottom and right-hand boundaries were restrained in both the horizontal and vertical directions. The left-hand boundary was prevented from moving the horizontal direction, but free to move vertically. All three meshes produced nearly the same vertical displacement of the sleeper. Thus, within this range, the influence of mesh density was negligible on the prediction of vertical displacement, which was also found by Powrie et al. (2007) in their FEM. An intermediate or fine mesh was used in the subsequent 2D and 3D modeling.

Five mesh sizes were developed and investigated. For these, a line load of 155 kN/m was applied at the top of the rail in the FDM model. The vertical displacement of the sleeper as a function of mesh size is found in Figure 4.8.

These results suggest that the predicted vertical displacement of the sleeper converged rapidly, and a mesh size of 60 m × 60 m (width × depth) was sufficient to produce stable results. Thus, this spacing was used in the 3D modeling described in the next section.

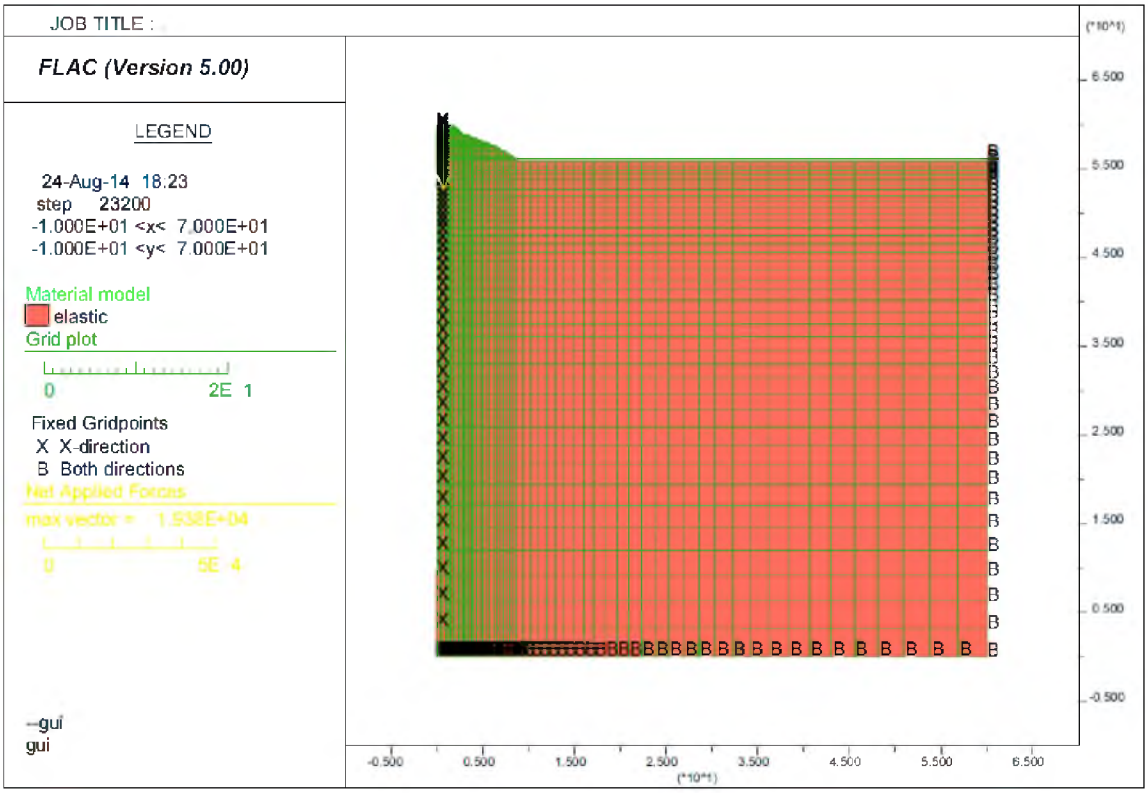

Figure 4.7 FDM Intermediate Mesh (m)

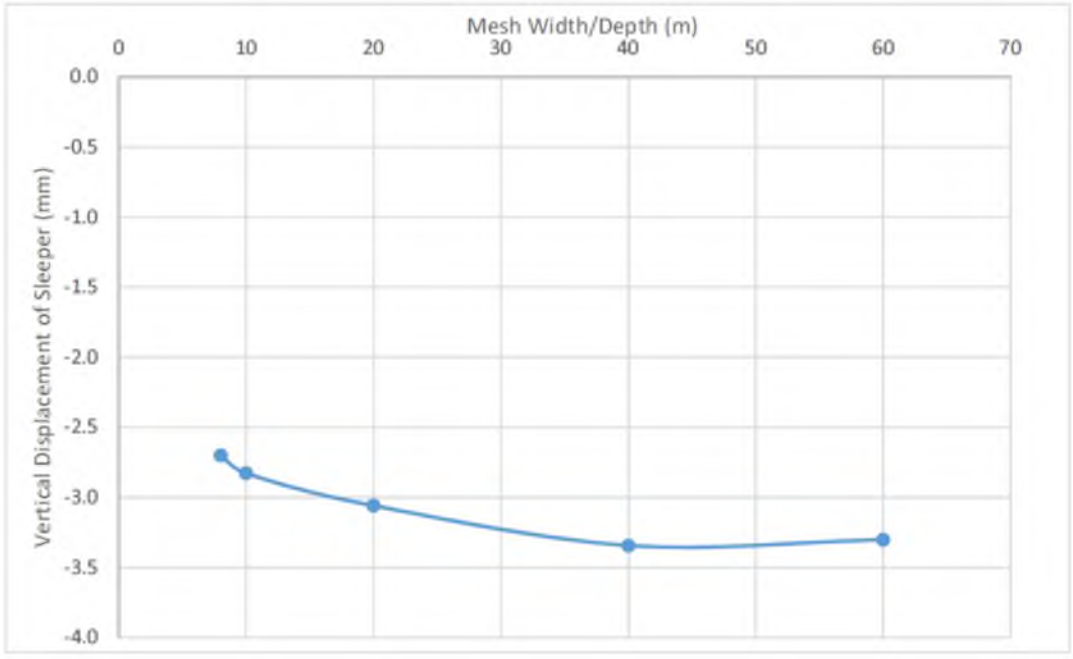

Figure 4.8 Mesh Size's Influence on Vertical Displacement of Sleeper

4.2.3 3D Solution

4.2.3.1 Field Test Result

After the new bridge was completed, static load tests were carried out by the Norwegian Public Roads Administration (NPRA) in order to measure the vertical displacement of the rail and sleeps due to the train loads using precision survey techniques (Frydenlund et al., 1987). For that purpose, a locomotive with wheel configurations as shown in Figure 4.9 was used. Deflections were measured (1988-08-31) on the bolts in the concrete slab above the EPS-blocks at different stationings along the embankment (see Figure 4.10). The results are between 2 and 3 mm of vertical deflection for the west rail (i.e., right side of Figure 4.6)

4.2.3.2 FDM Solution (FLAC)

Figures 4.5 and 4.6 were used to create the geometry for the 3D FLAC model. Key measurements of the system have been previously stated in the Problem Statement Section of this report. The remaining dimensions used for this model were obtained based on scaling from these figures. In the 3D model, only the west half of the system was analyzed because the system is reasonably symmetrical. Figures 4.11 and 4.12 show the mesh developed for the FLAC modeling.

The length of the mesh in the longitudinal (y) direction was taken as that of the locomotive. In the vertical (z) and lateral (x) directions, the dimensions of the mesh were set at 60 m because the results of the two-dimensional analyses indicated that this should be sufficient to eliminate the boundary effects. Smaller elements were used near the track

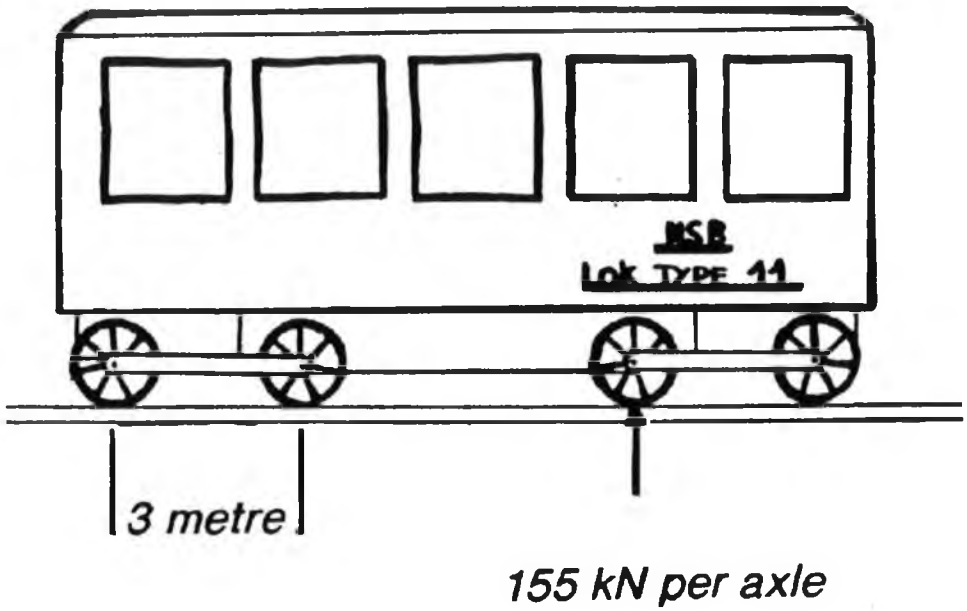

Figure 4.9 Load Configuration

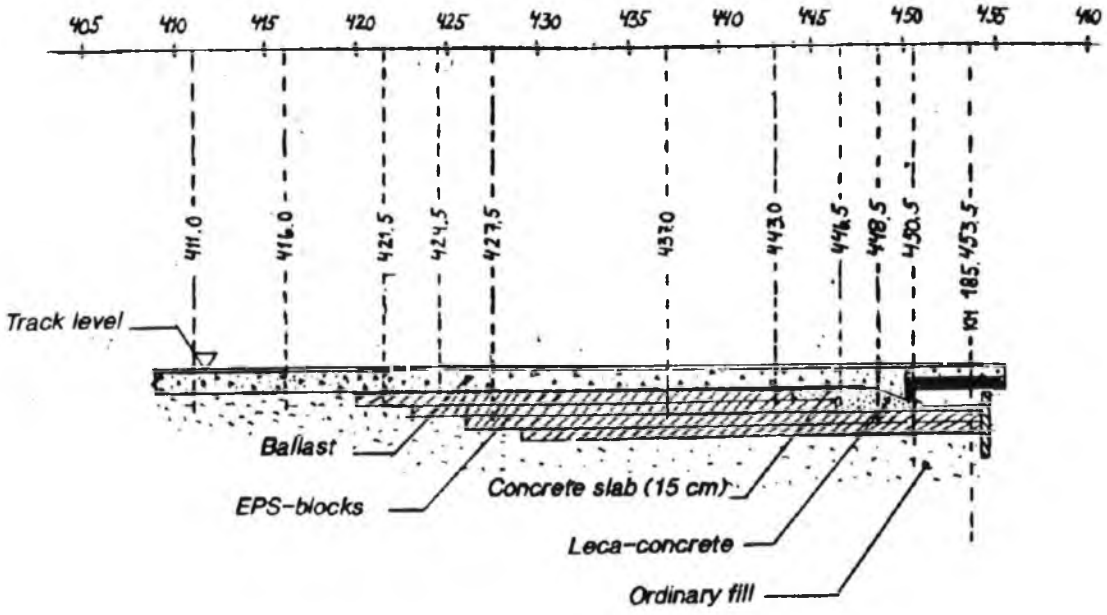

Figure 4.10 Stationings of the Embankment

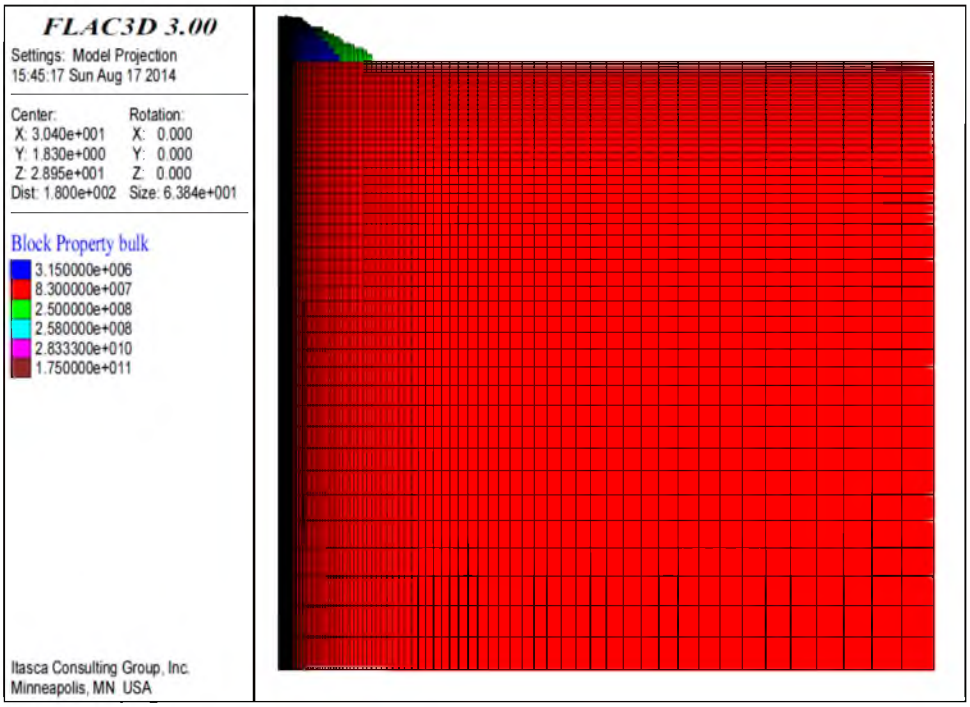

Figure 4.11 Cross-section View of Model Mesh

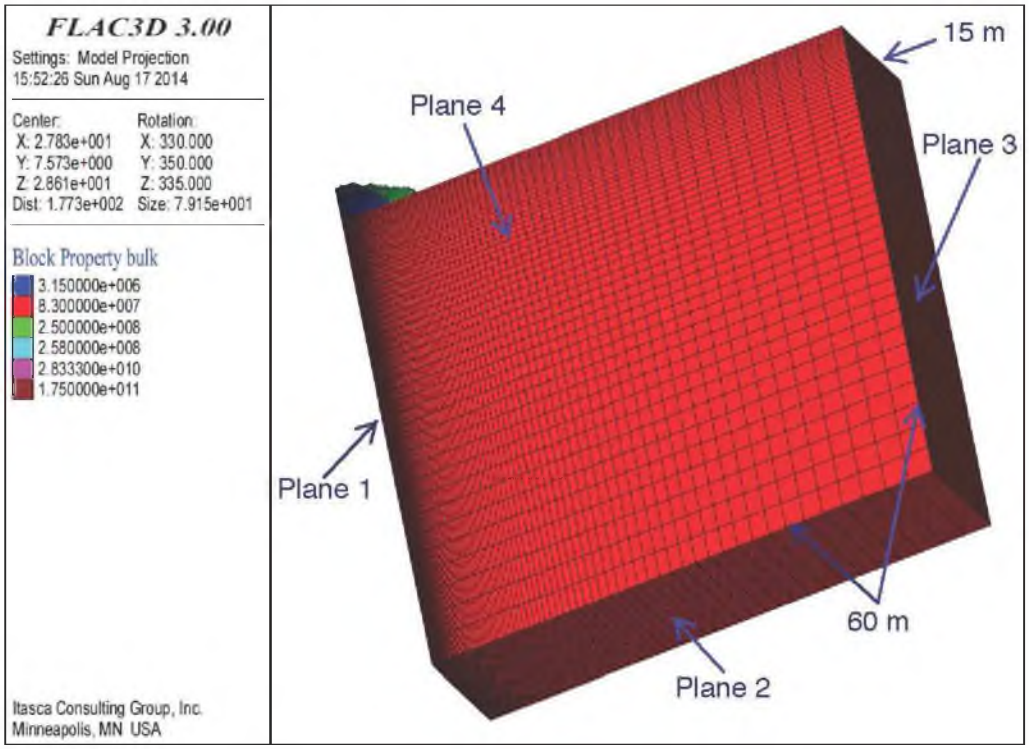

Figure 4.12 3D view of Model Mesh

where the changes of stresses and strains were expected to be the greatest. The bottom and far-lateral boundaries (Plane 2 and 3 in Figure 4.12) were prevented from movement in all three directions. The longitudinal boundaries (Plane 4 in Figure 4.12) were fixed in the x direction only. The center plane (Plane 1 in Figure 4.12) was fixed in the y direction only.

The loading conditions for this case are illustrated in Figure 4.13. The properties of each material are shown in Table 4.2. Estimates of the shear modulus (G) and bulk modulus (K) were calculated based on the E and v values in this table using elastic theory and input in the FLAC model for the respective materials. See Figure 4.11 and Figure 12 for plots of the properties used in the model.

The vertical displacement contours are shown in Figures. 4.14 through 4.17. The maximum vertical rail displacement calculated by FLAC is 2.3 mm, which occurs directly under the wheels. In addition, FLAC3D indicates that the concrete slab has a vertical displacement ranging from 1.8 mm to 2.3 mm. (Compare Figures. 4.14 and 4.15 with Figures. 4.16 and 4.17.) Based on this, it is obvious that the railway embankment

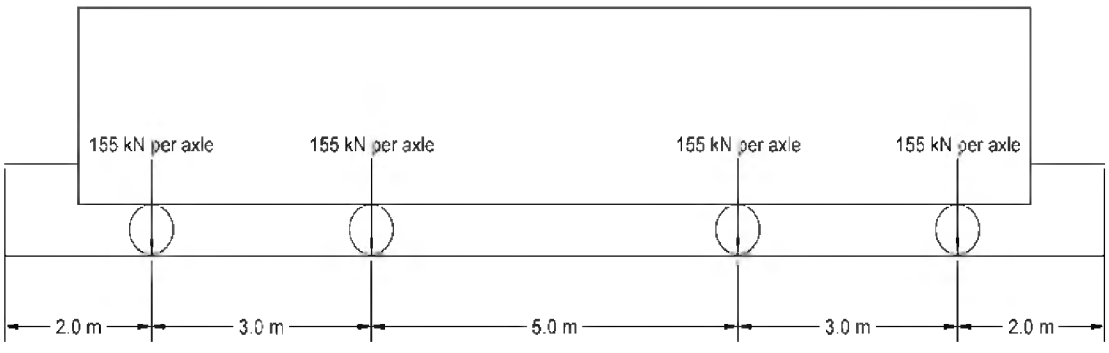

Figure 4.13 Loading Conditions

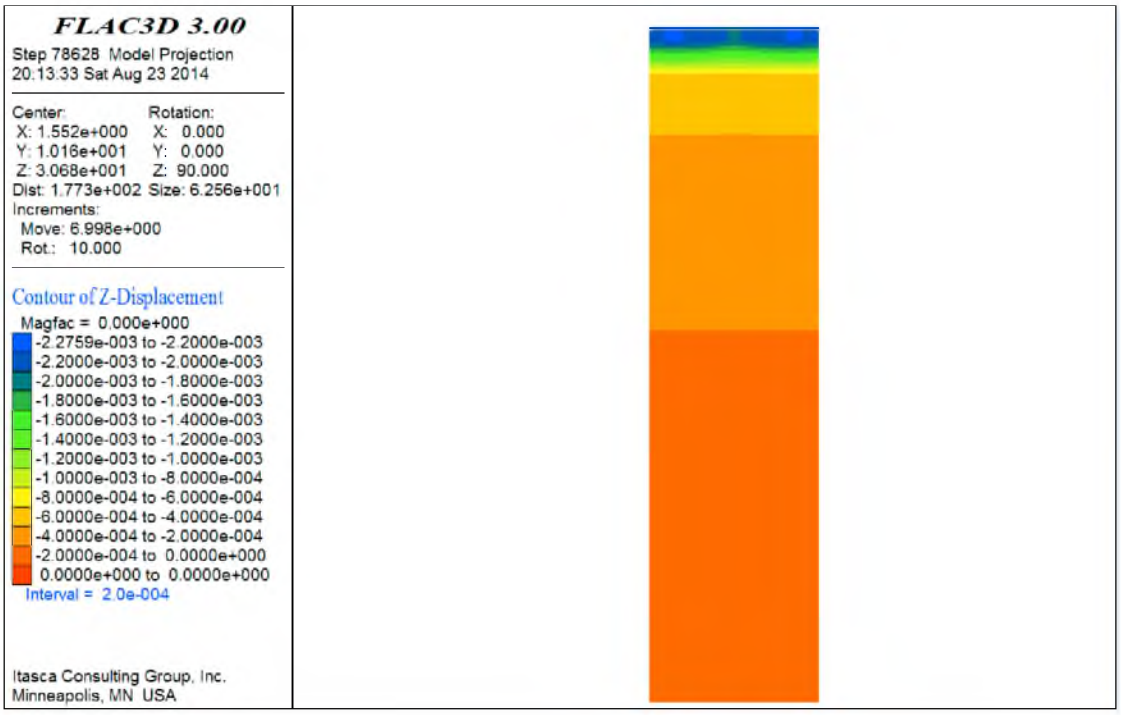

Figure 4.14 Full Model Profile View of Vertical Displacement Contours (m)

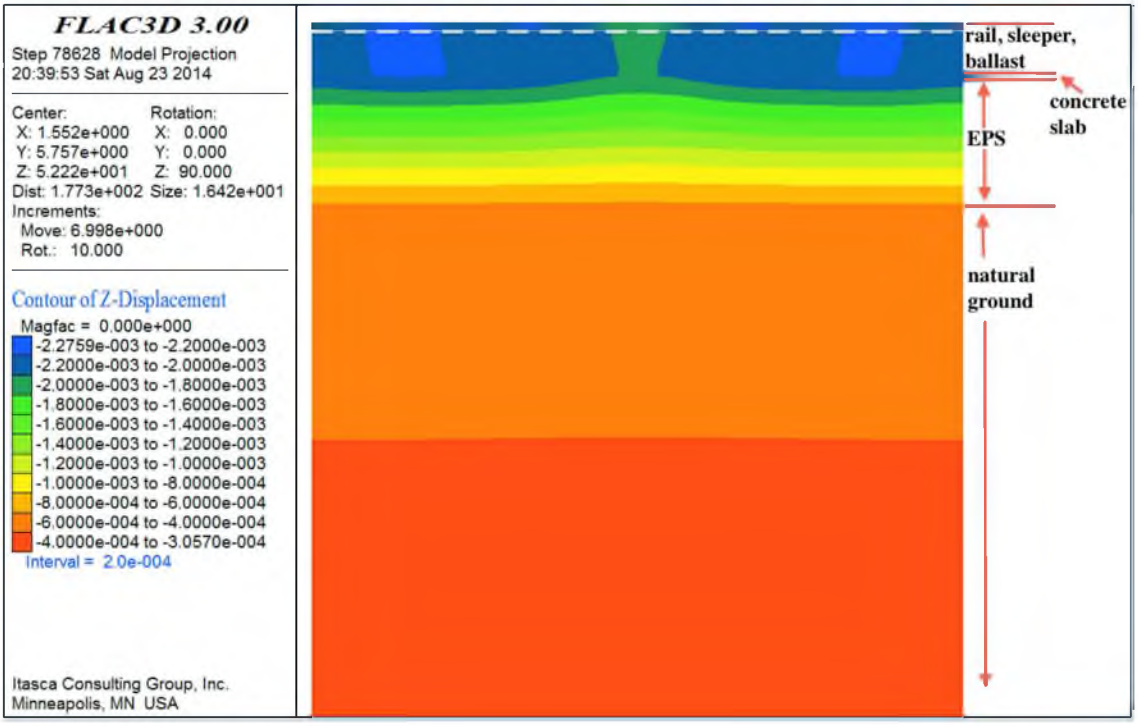

Figure 4.15 Zoomed-in Profile View of Vertical Displacement Contours (m)

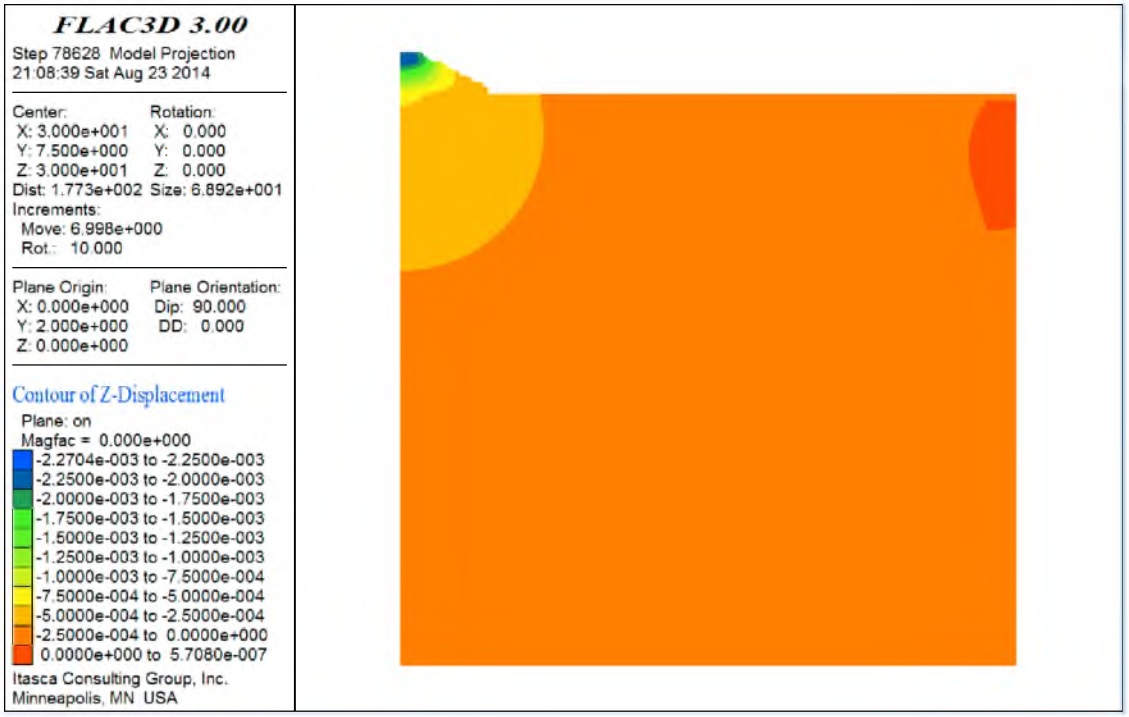

Figure 4.16 Full Model Cross-section View of Vertical Displacement Contours (m)

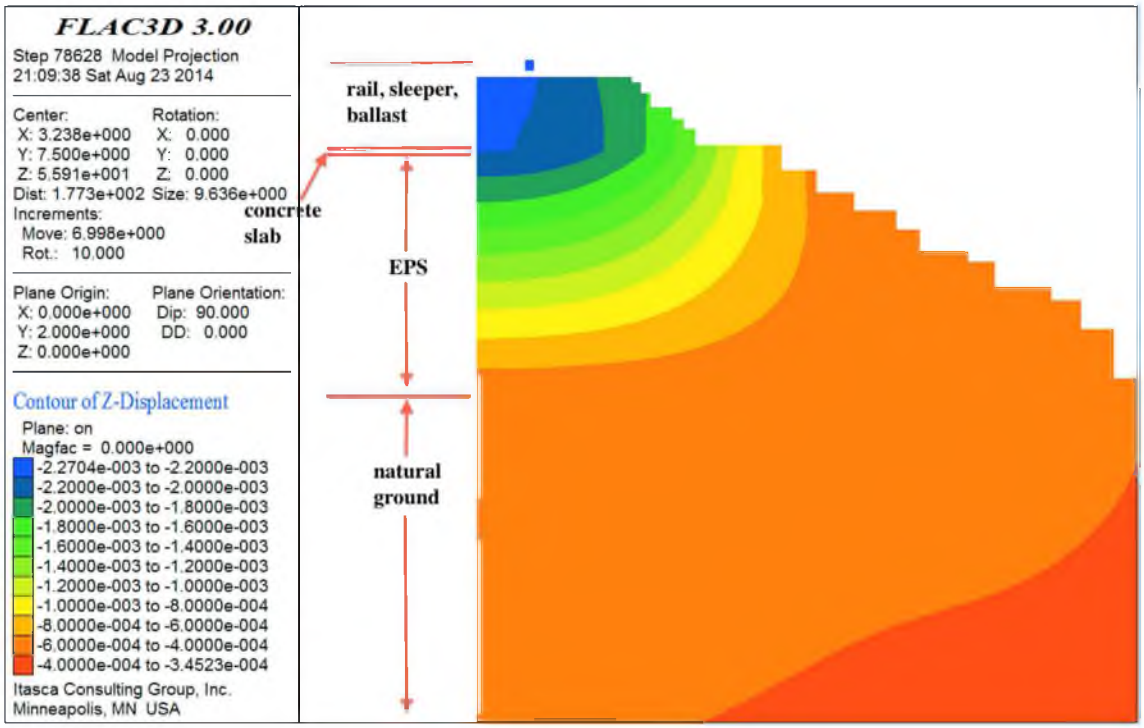

Figure 4.17 Zoomed-in Cross-section View of Vertical Displacement Contours (m)

system settles much more uniformly in the longitudinal (y) direction than in the lateral (x) direction. In addition, even though the thickness of the EPS layer is only approximately 5% of the full depth of the embankment model, approximately 60% of the vertical deformation occurs in the EPS. This is due to the fact that the EPS has a much lower bulk and shear moduli than other materials (i.e., rail, sleeper, ballast, concrete slab, natural ground, etc.).

Figures. 4.18 and 4.19 show the lateral (x direction) and longitudinal (y direction) displacement of the railway embankment system. The system has a maximum lateral displacement of 0.2 mm, and a maximum longitudinal displacement of 0.02 mm, both of which are relatively insignificant compared with the magnitude of the predicted vertical displacement.

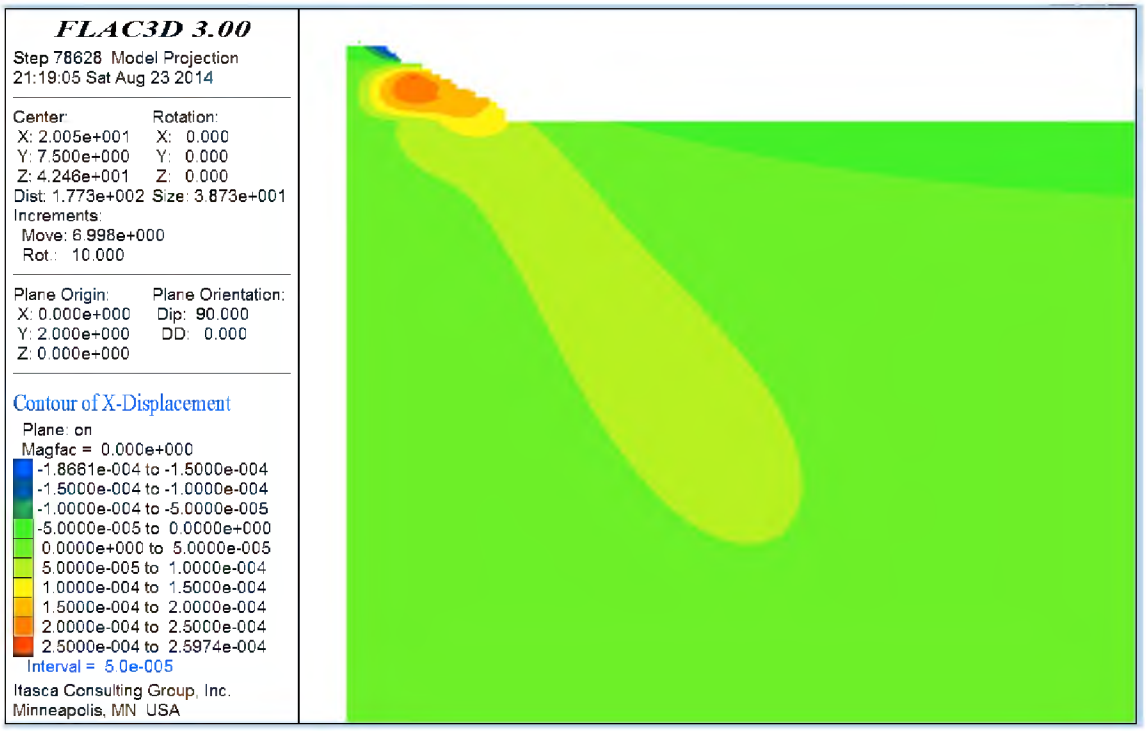

Figure 4.18 Lateral Displacement Contours in X Direction (m)

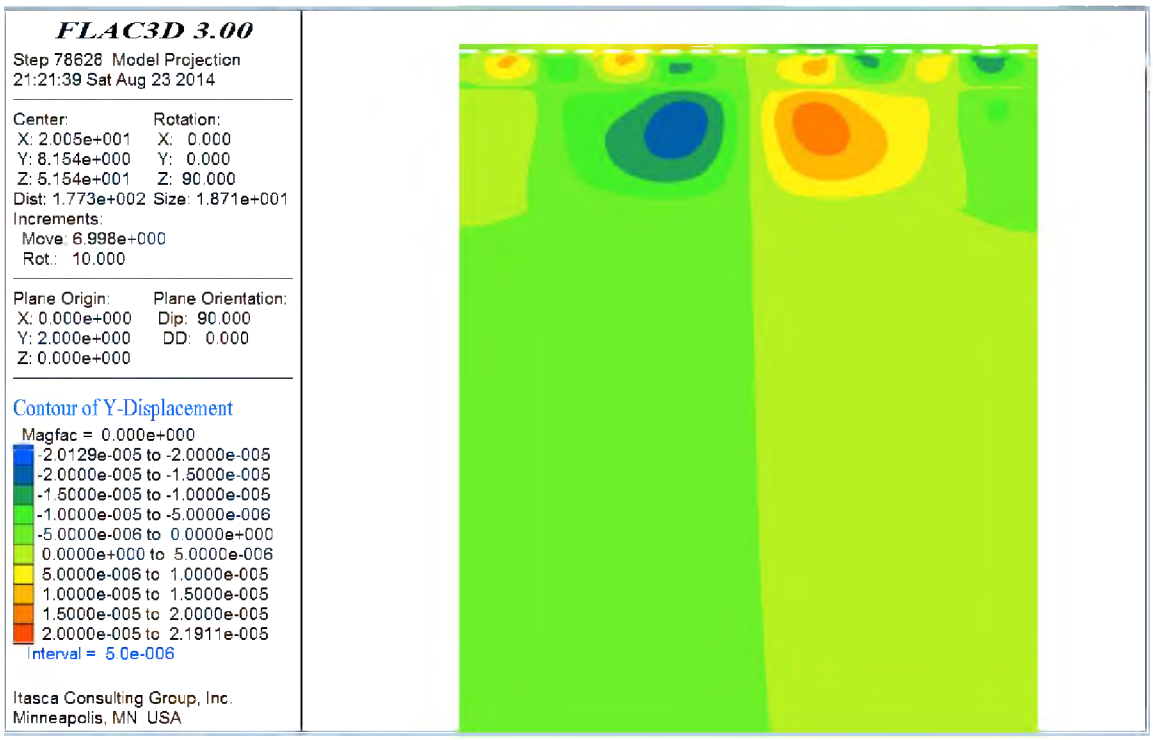

Figure 4.19 Longitudinal Displacement Contours in Y Direction (m)

Figure 4.20 shows the vertical stress contours of the railway embankment system. Figures 4.21 and 4.22 show the horizontal stress contours of the railway embankment system in lateral (x) direction and longitudinal (y) direction. Figures 4.23 and 4.24 show the shear stress contours of the railway embankment system. Using the results of these plots, one can observe that the normal and shear stresses within the system are distributed relatively uniformly by the rail-sleeper-ballast-concrete slab system. This is due to the high stiffness (i.e., high bulk and shear moduli) of these materials in relation to the underlying EPS and soil materials.

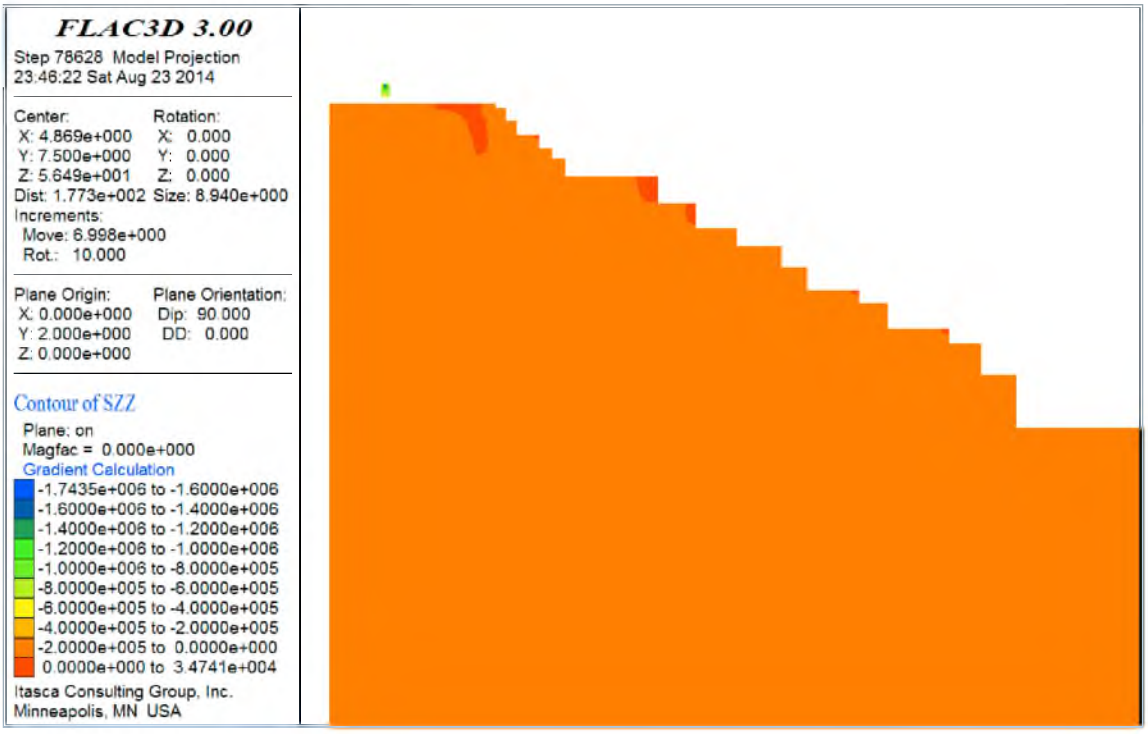

Figure 4.20 Vertical Stress Contours (Pa)

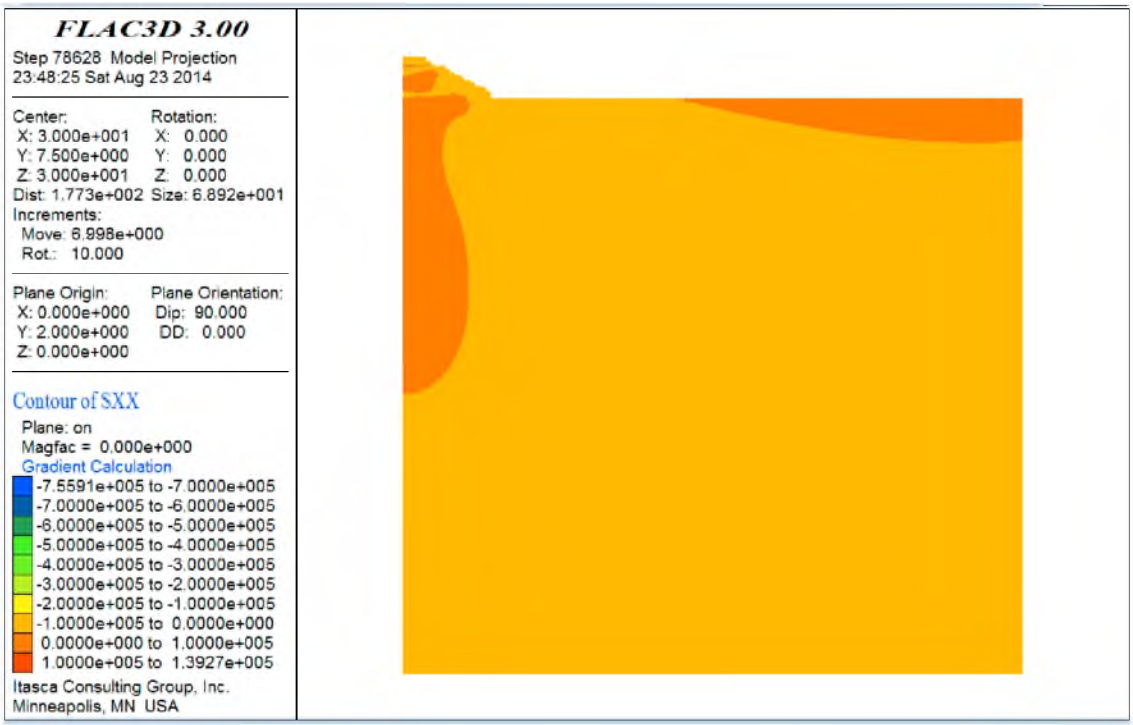

Figure 4.21 Horizontal Stress Contours in Lateral (x) Direction (Pa)

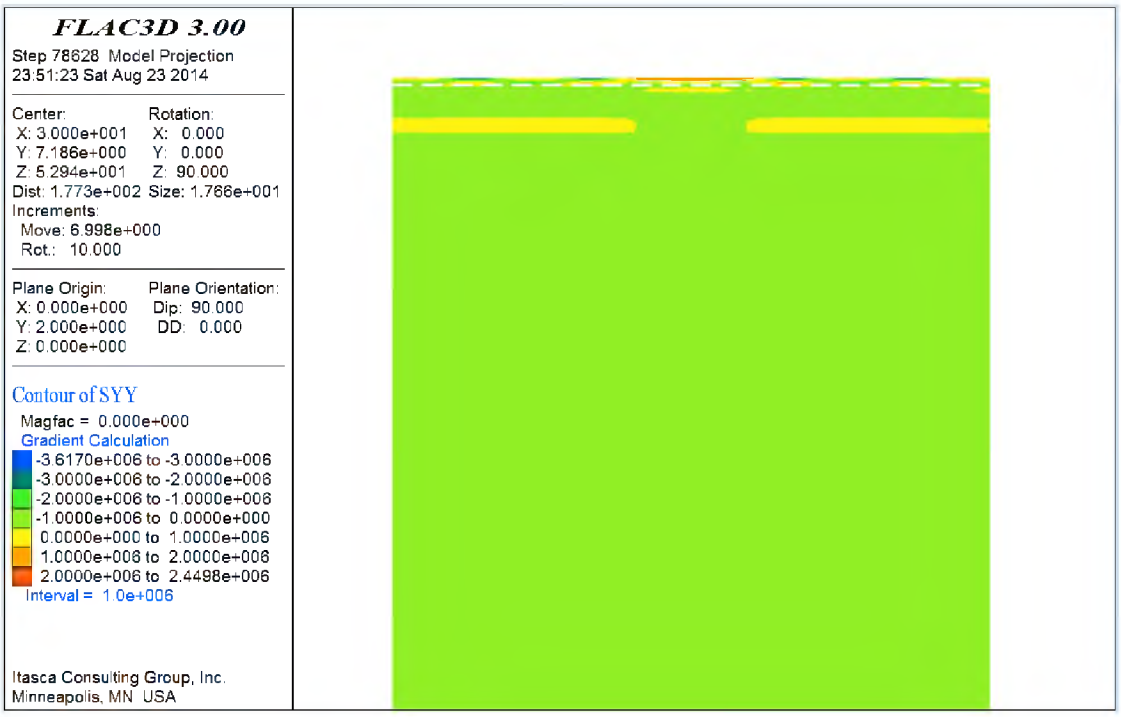

Figure 4.22 Horizontal Stress Contours in Longitudinal (y) Direction (Pa)

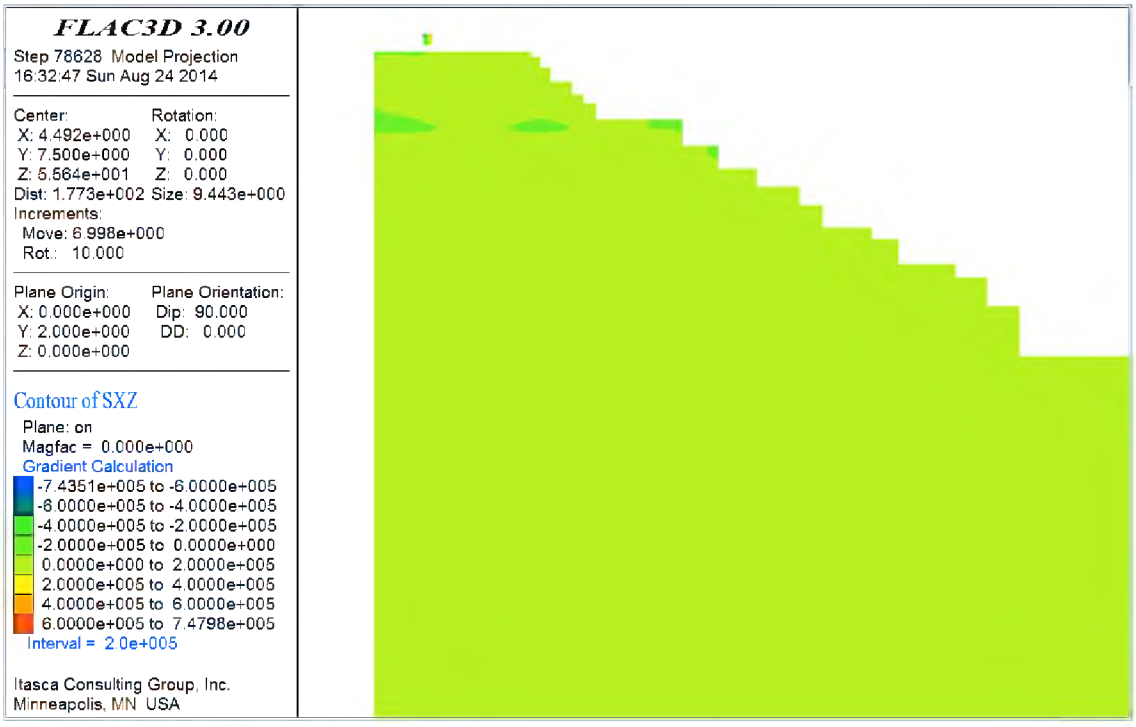

Figure 4.23 Cross-section View of Shear Stress Contours (Pa)

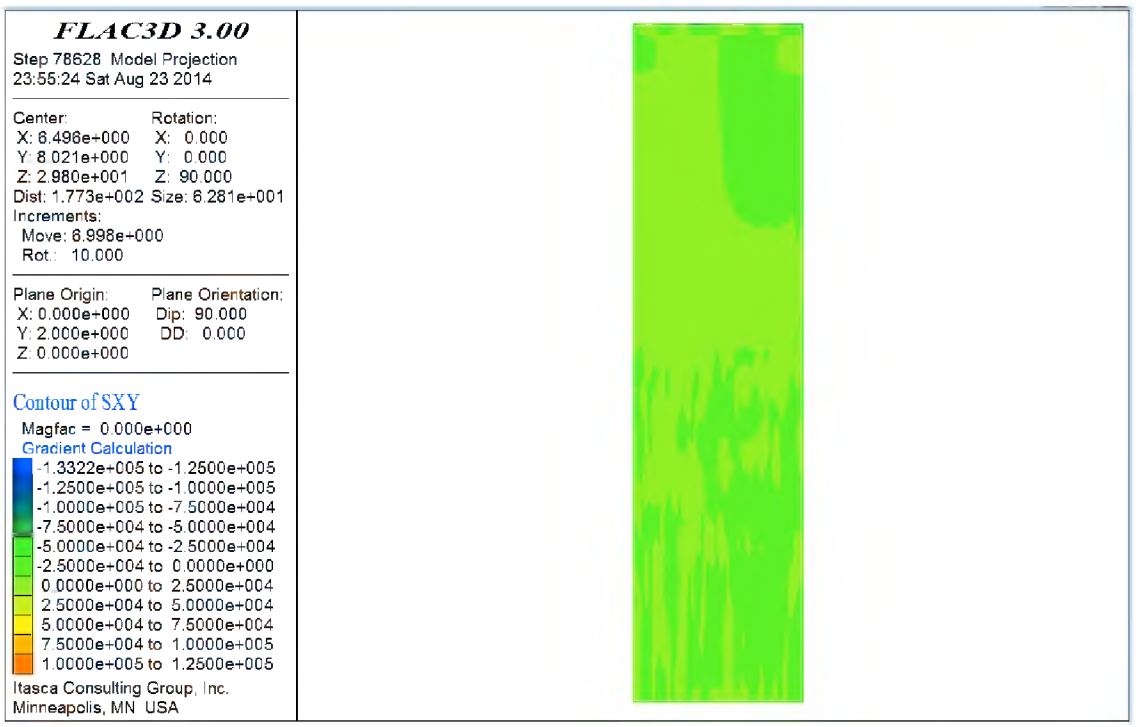

Figure 4.24 Profile View of Shear Stress Contours (Pa)

4.2.4 Comparison and Verification

Vertical deflections were measured by Frydenlund et al. (1987) on bolts found in the concrete slab which was constructed atop the EPS-blocks. The field measurements ranged from 2 to 3 mm on the west rail. This half of the railway embankment system was modeled by FLAC3D. The model produced vertical deflections ranging from 1.8 to 2.3 mm. This range of results appears to be a reasonable estimate of the lower range of the field measurements. In addition, further calibration of the model is not recommended given the uncertainties in the embankment and foundation material properties which were not reported by Frydenlund et al., (1987), but were estimated by this study. Therefore, it is concluded that FDM, as implemented in FLAC, can satisfactory estimate the vertical displacement of rails systems constructed atop EPS-supported embankments when

subjected to a static (i.e., stopped) train loading.

4.3 Rail System Supported by EPS Embankment in Draper, Utah

4.3.1 Problem Statement

The modeling approach developed in the previous sections will now be implemented to estimate the vertical deflections of an EPS geofoam embankment constructed along the UTA FrontRunner South commuter rail line alignment. Deflection measurements are planned by others as part of research funded by the National Center for Freight and Infrastructure Research and Education (CFIRE). Because the estimates contained in this section were performed before the FrontRunner field measurements, they constitute a prior prediction. Table 4.3 shows the material properties including load distribution slab (LDS), EPS, etc. EPS properties are determined from ASTM D 6817. Young's modulus of ballast is for Iteration 1.

Table 4.3 Material Properties and Geometry Used in FDM Analysis

Description	E / MPa	v	Geometry
Rail	210000	0.3	78 mm wide, 153 mm deep
Sleeper (3D/2D)	31000/11600	0.3	242 mm wide, 200 mm deep
Ballast	310	0.3	308.8 mm thick
Sub-ballast	130	0.49	203.2 mm thick
Structural Fill	400	0.3	914.4 mm thick
LDS	30000	0.18	203.2 mm thick
EPS39	10.3	0.103	top layer
EPS29	7.5	0.103	second to fifth layer
EPS22	5	0.103	sixth to bottom layer
Foundation Soil	174	0.4	20 m thick

The UTA Frontrunner South alignment extends from Salt Lake City to Provo, Utah. The particular EPS fill selected for the modeling is shown in Figures 4.25 and 4.26. These show the cross-section of the EPS-supported embankment at Corner Canyon (Parsons et al., unpublished design drawings, Corner Canyon box culvert, Structure 27, 2009) that will be studied using FDM as implemented in FLAC3D. This EPS embankment was constructed over an extension of a concrete drainage culvert so as to not induce damaging settlement to the culvert and the adjacent Union Pacific Rail Line. The loading conditions are shown in Figure 4.27 (a typical Frontrunner Commuter train).

4.3.2 2D Model Preparatory Study

As previously discussed in the models developed for railway systems supported by both regular earthen embankment (Powrie et al., 2007) and EPS embankment (Frydenlund et al., 1987), the coarse mesh, intermediate mesh, and fine mesh spacing resulted in almost the same estimate of vertical displacement of the concrete sleeper. Thus, mesh density is not a major concern in the modeling process if only vertical displacements are to be predicted. However, a fine mesh was used in both the 2D and 3D modeling of the UTA FrontRunner embankment system.

As shown in Figure 4.25, the UTA FrontRunner embankment system is not plane-symmetrical. Simply modeling half of the system will result in incorrect results.

However, a full 3D model of the embankment system requires a significant amount of computational time and memory and thus is not preferable. As a result, a series of 2D models were developed to investigate simplification methods and evaluate the magnitude of the potential differences caused by the simplifications.

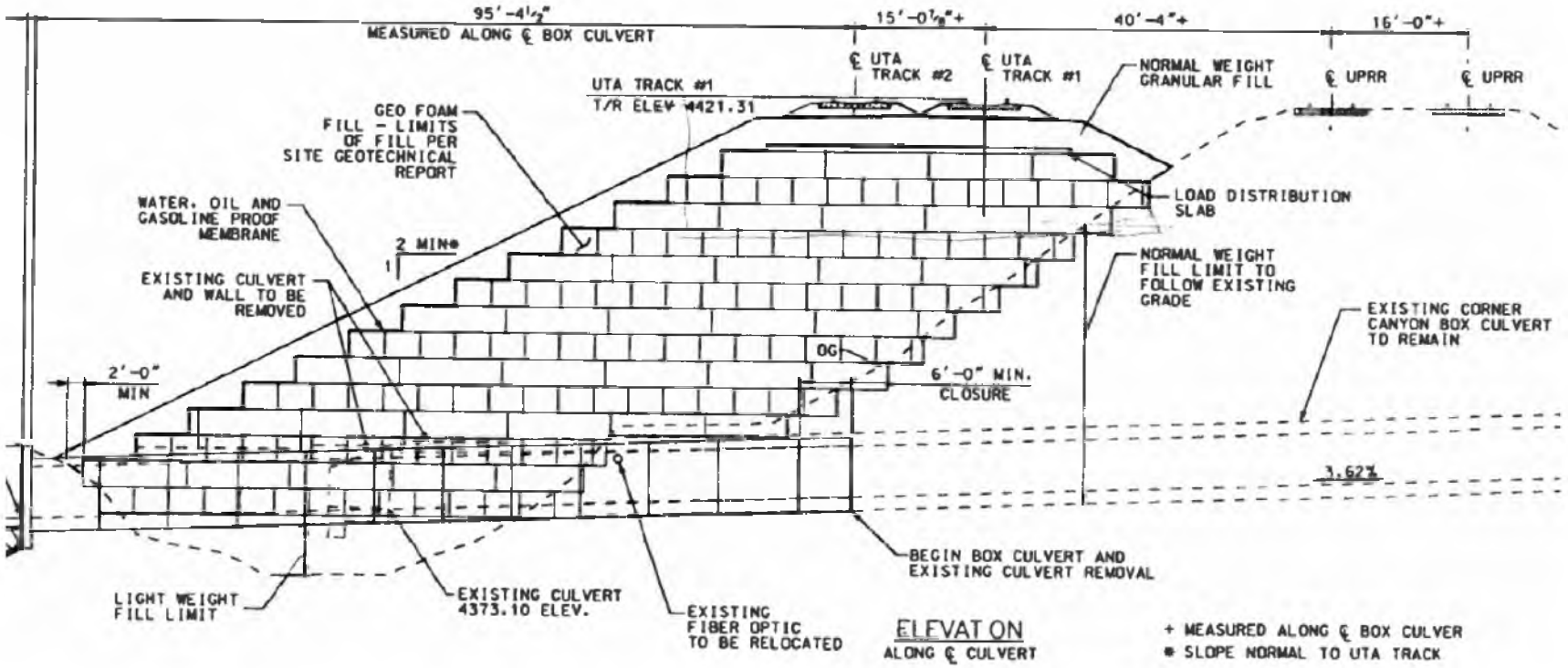

Figure 4.25 Cross-section of the EPS-supported Embankment at Corner Canyon

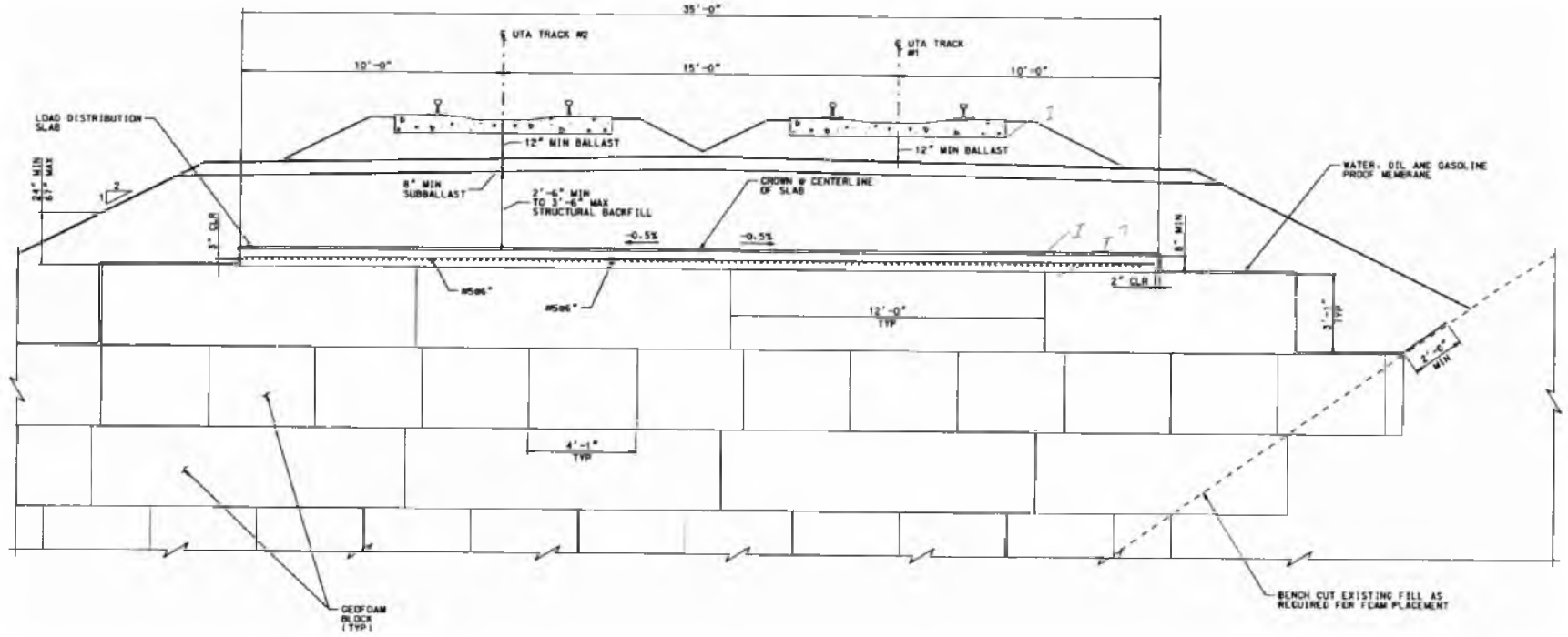

Figure 4.26 EPS Cross-section of the EPS-supported Embankment at Corner Canyon

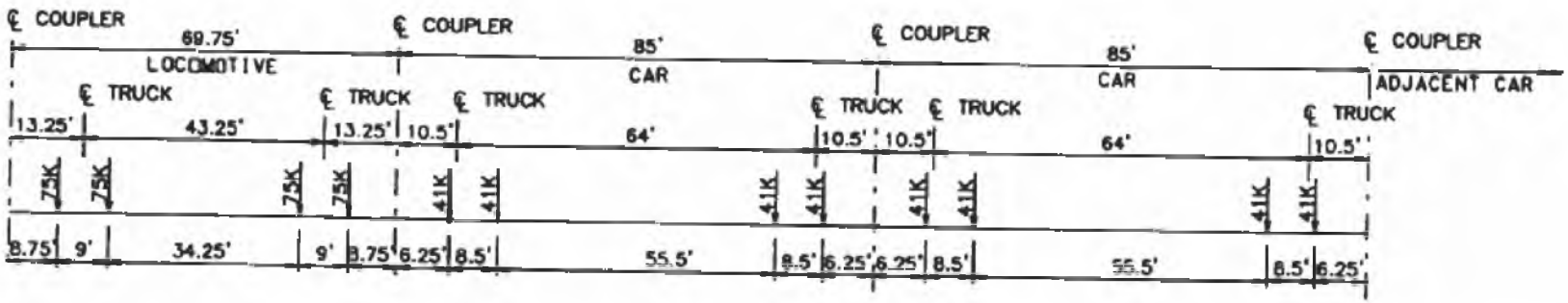

Figure 4.27 Typical Load Conditions for UTA Commuter Rail Train

Firstly, a 2D model of the full embankment system was developed (Figure 4.28 and Figure 4.29). As was done in modeling the regular earthen embankment (Powrie et al., 2007) and the EPS embankment in Norway (Frydenlund et al., 1987), the boundaries on two sides and the bottom were restrained in both the horizontal and vertical directions. A load of 41 kips (182,337 N) per axial for a car is applied on the outer track. In FLAC, since there are two rails with two nodes for each rail top, a vertical force of 45584 N was applied on each node. Figures 4.25 and 4.26 show the geometry used in the FLAC model. See Table 4.3 for details about the material properties and geometry used. Note that Imperial units have been converted to SI units in this table. The length of the sleeper is 2.525 m.

Secondly, the 2D model was cut vertically at the center of the left (i.e., western) outer track (Figures 4.30 and 4.31), similar to what would be done if this represented an axis of symmetry. Thus, in this simplified model, the right boundary was fixed only in the horizontal direction and the left and bottom boundaries were fixed in both directions.

Because the development of a subsequent 3D model was planned, efforts were taken to simplify the 2D cross-section as much as possible. As discussed in modeling the EPS supported embankment system in Norway, much of the vertical deformation occurred within the EPS part of the embankment due to its relatively low stiffness. The corresponding vertical deformation occurring in the foundation soil was reasonably small. However, a comparison of the two EPS supported embankment systems shows that the EPS portion in the FrontRunner system is much thicker than that of the Norwegian system. Because of this increased thickness, the percentage of the total deformation occurring in the EPS is expected to be higher than the Norwegian case, and the

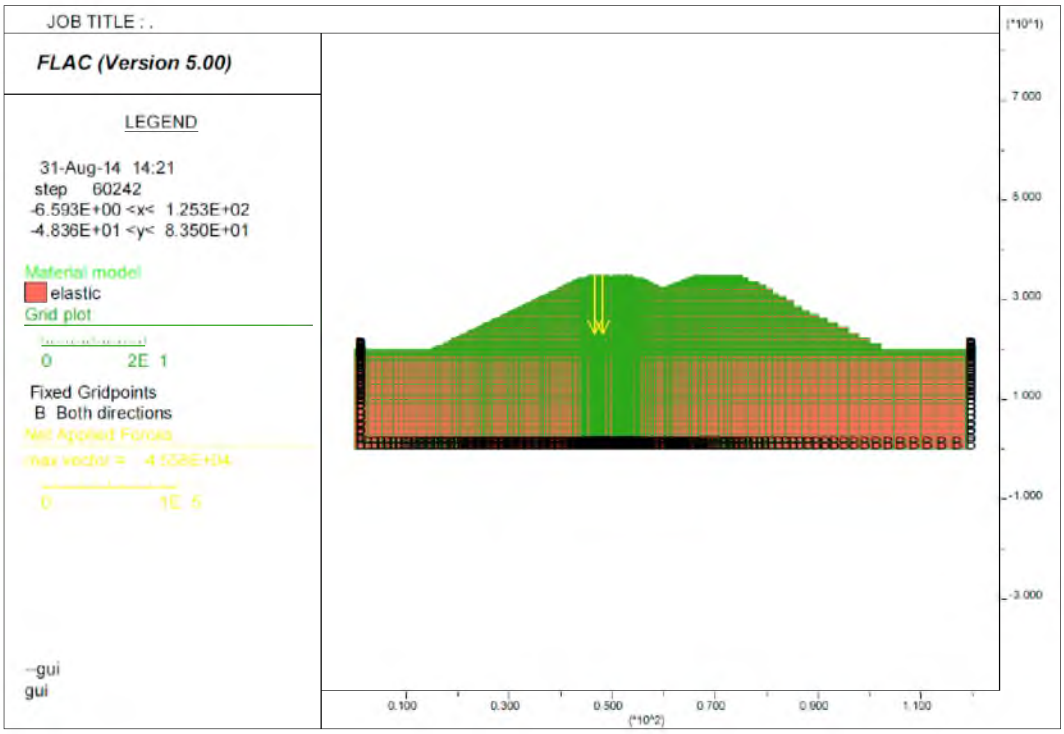

Figure 4.28 Mesh of 2D Model of the Full FrontRunner Embankment System (m)

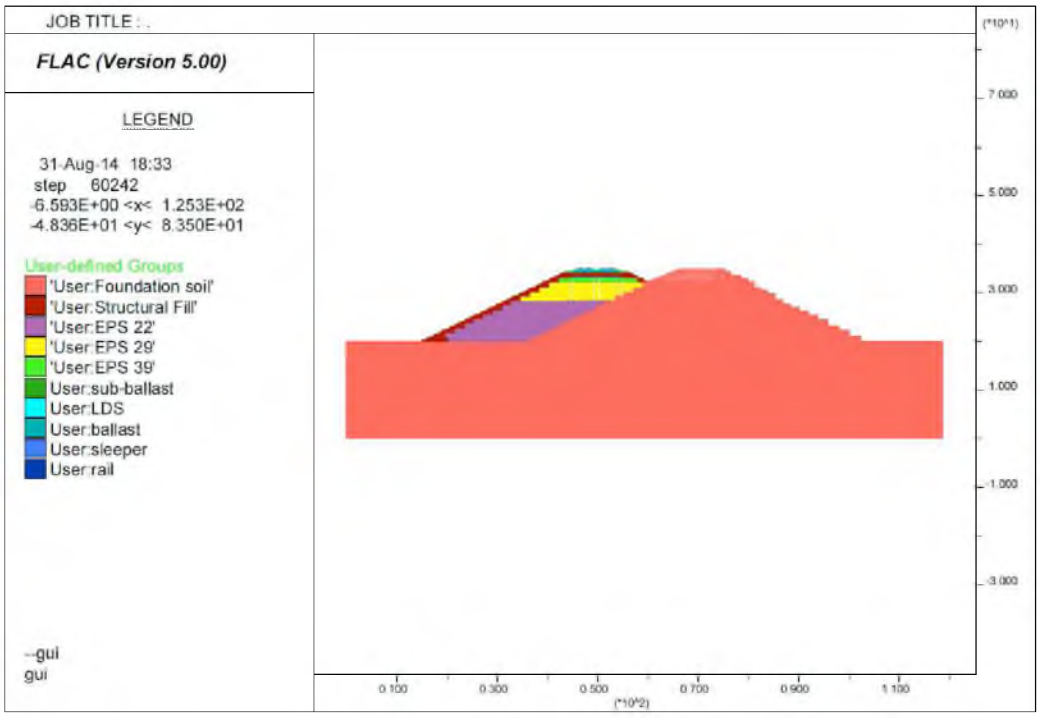

Figure 4.29 Properties of 2D Model of the Full FrontRunner Embankment System (m)

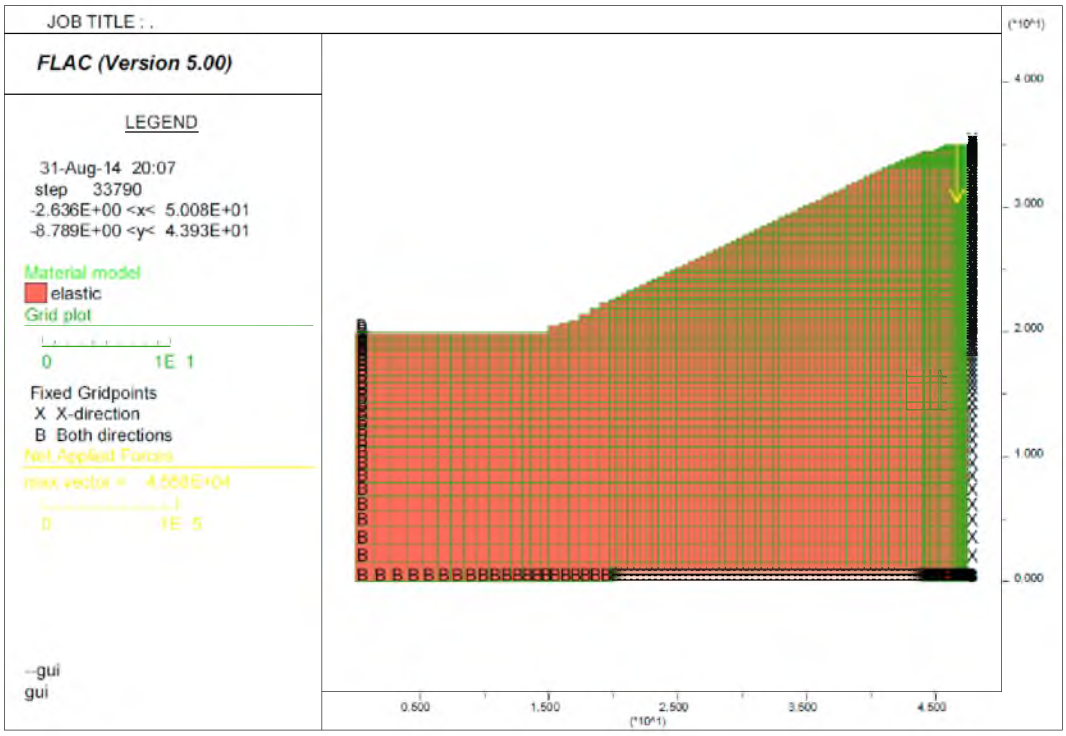

Figure 4.30 Mesh of 2D Model of Initial Simplified FrontRunner Embankment (m)

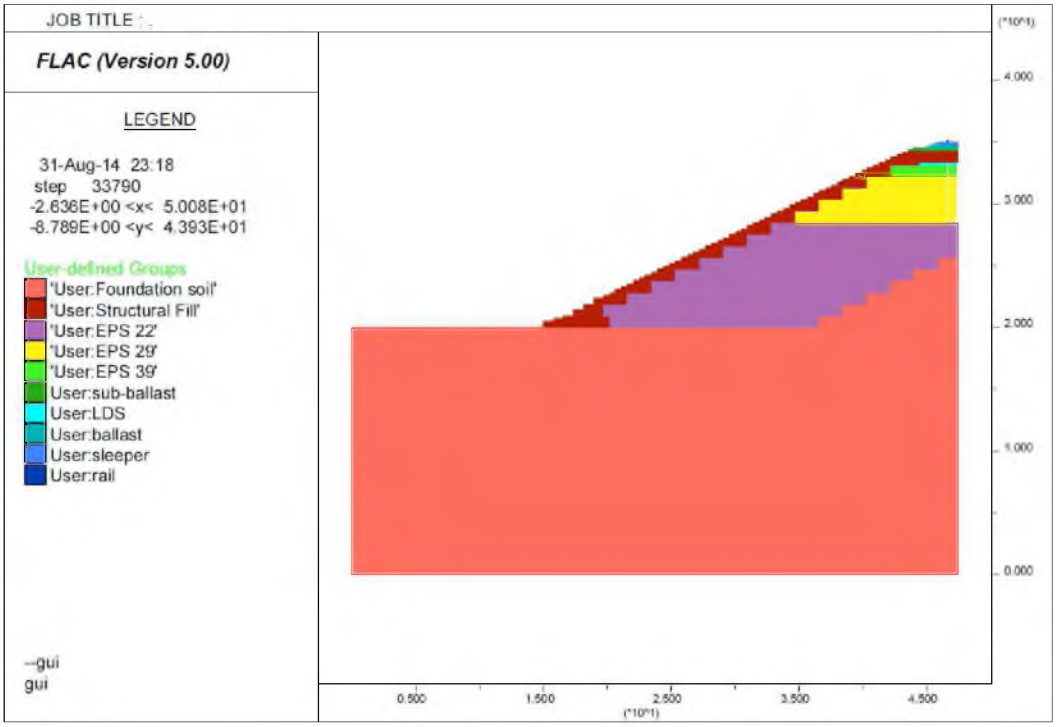

Figure 4.31 Properties of 2D Model of Initial Simplified FrontRunner Embankment (m)

deformation in the foundation soil is expected to be correspondingly less.

A series of 2D models with different dimensions for the foundation soils were developed to investigate the effects of the mesh size and boundaries on the estimated vertical displacement of the rails. Included in these cases were foundation soil dimensions (depth by extended width) of 20 m by 15 m, 10 m by 8 m, 5 m by 3 m, and 0 m by 0 m. Except for the above differences in foundation soil dimension, all other parameters remain the same in these exploratory models. The vertical displacement results for the rails are plotted in Figure 4.32. It is obvious from these exploratory models, which produced almost the same vertical displacement result, that most of the vertical displacement is attributed to the EPS portion of the embankment and not to the foundation soil.

Thus, the simplest model (i.e., depth by extended width: 0 m by 0 m) was used in the subsequent 2D model. The results of this 2D model (Figures 4.33 and 4.34) were compared with the model of the full embankment model (Figures 4.28 and 4.29) under the same conditions (loading, material properties, etc.). The error introduced by the simplifications used in the modeling as represented by Figures 4.33 and 4.34 produced an over-estimation of the vertical displacement of about 11%. Thus, using this simplified method produces a slightly conservative by reasonable result when compared with the full model.

4.3.3 3D Solution (FDM)

Based on the ballast tests discussed previously, it was found that the ballast system had a different Young's modulus according to the strain level used in the tests. To

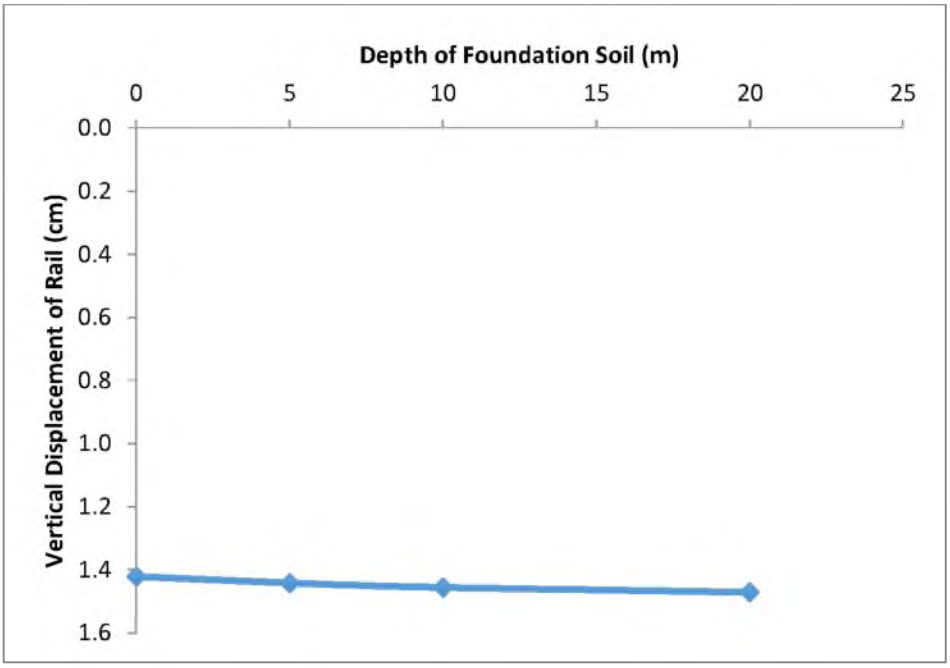

Figure 4.32 Boundary Effect of the Foundation Soils

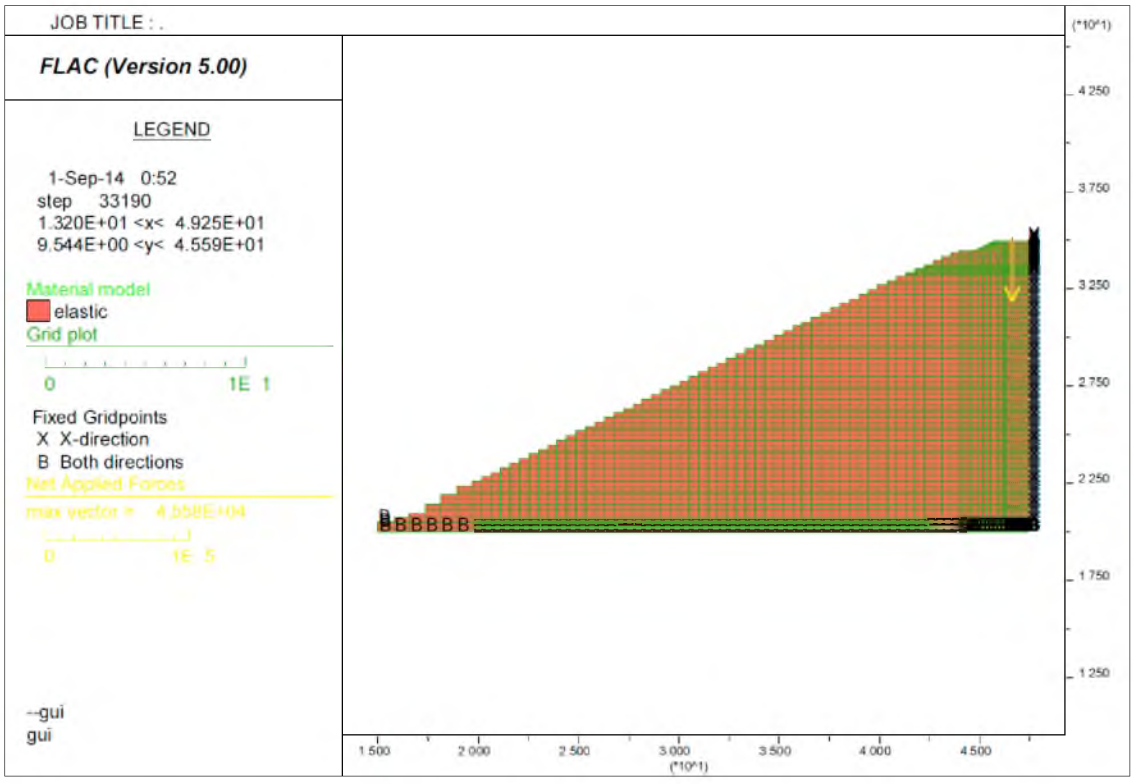

Figure 4.33 Mesh of 2D Model of Final Simplified FrontRunner Embankment (m)

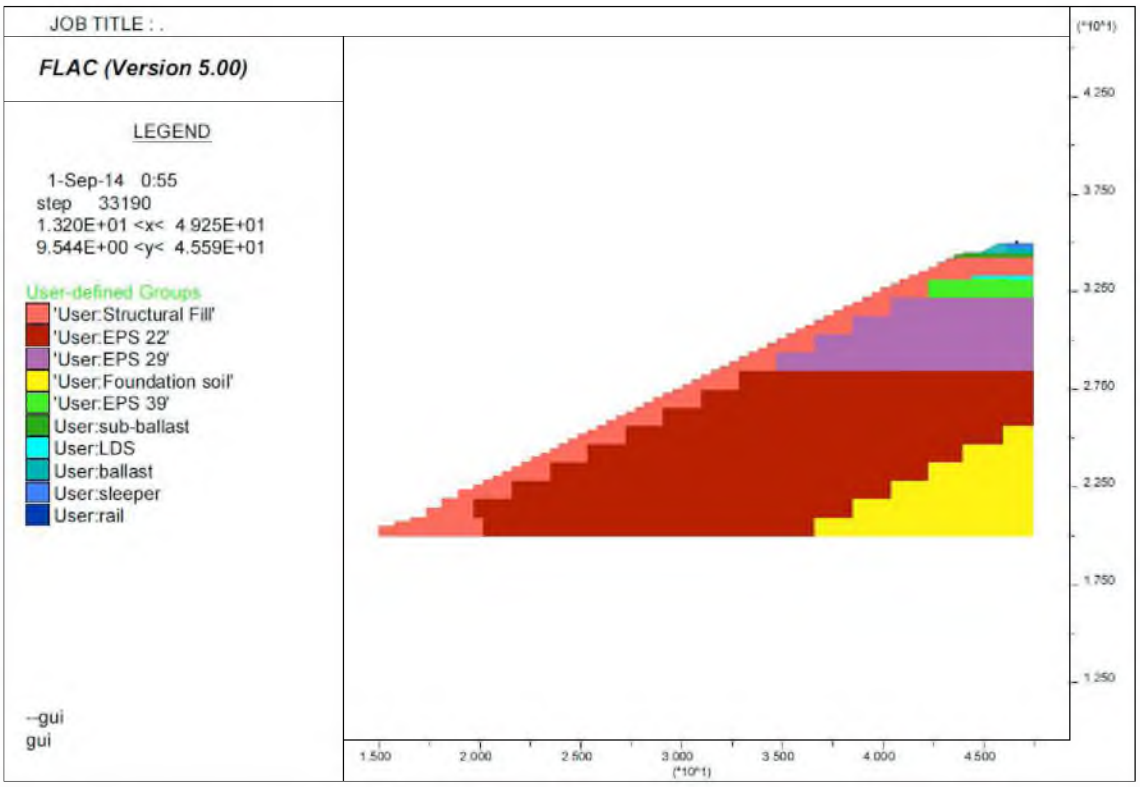

Figure 4.34 Properties of 2D Model of Final Simplified FrontRunner Embankment (m)

incorporate this in the FLAC model, an iterative process was used. First, the value of Young's modulus obtained from the literature was used in the FLAC model (Iteration 1). After the FLAC model had solved for this condition, the strain of the ballast layer was obtained from the output. The strain was then used to calculate the Young's modulus of ballast based on the correlation developed from the ballast test in Chapter 3. This new Young's modulus was used again in the FLAC model (Iteration 2). This process was repeated until the Young's modulus calculated from the strain output is the approximately the same as the Young's modulus input and vertical displacement of the rails are approximately the same as the previous iteration.

Figure 4.35 and Figure 4.36 show the mesh of the 3D model.

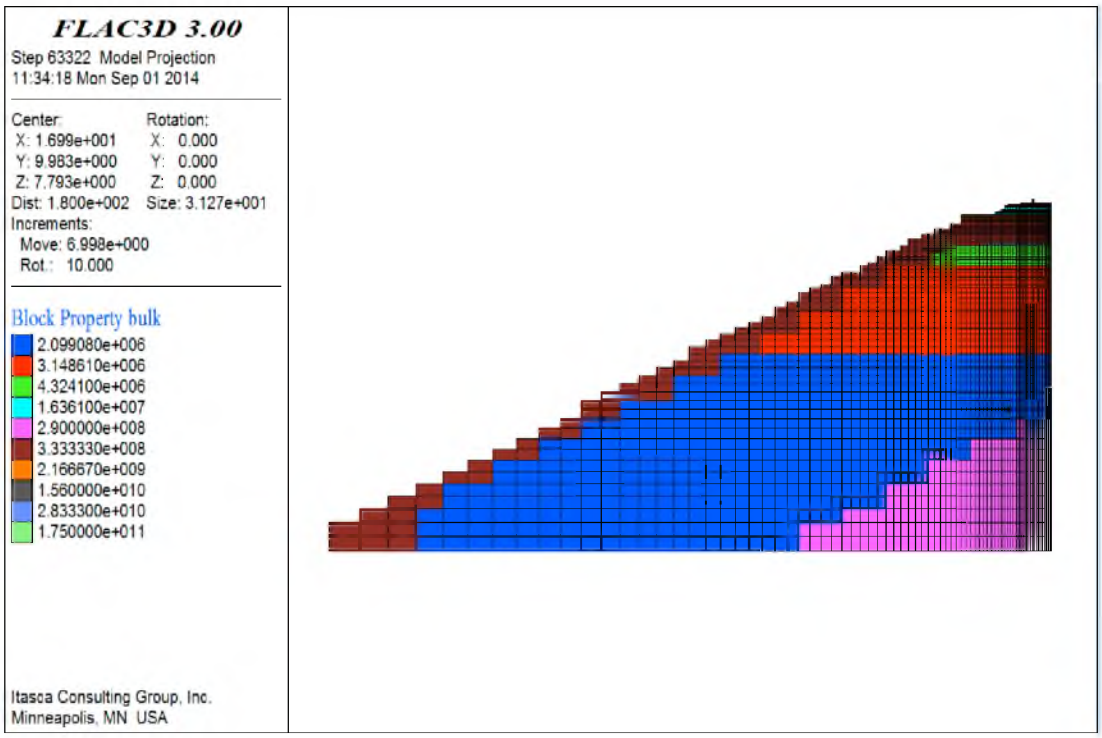

Figure 4.35 Cross-Section View of Model Mesh

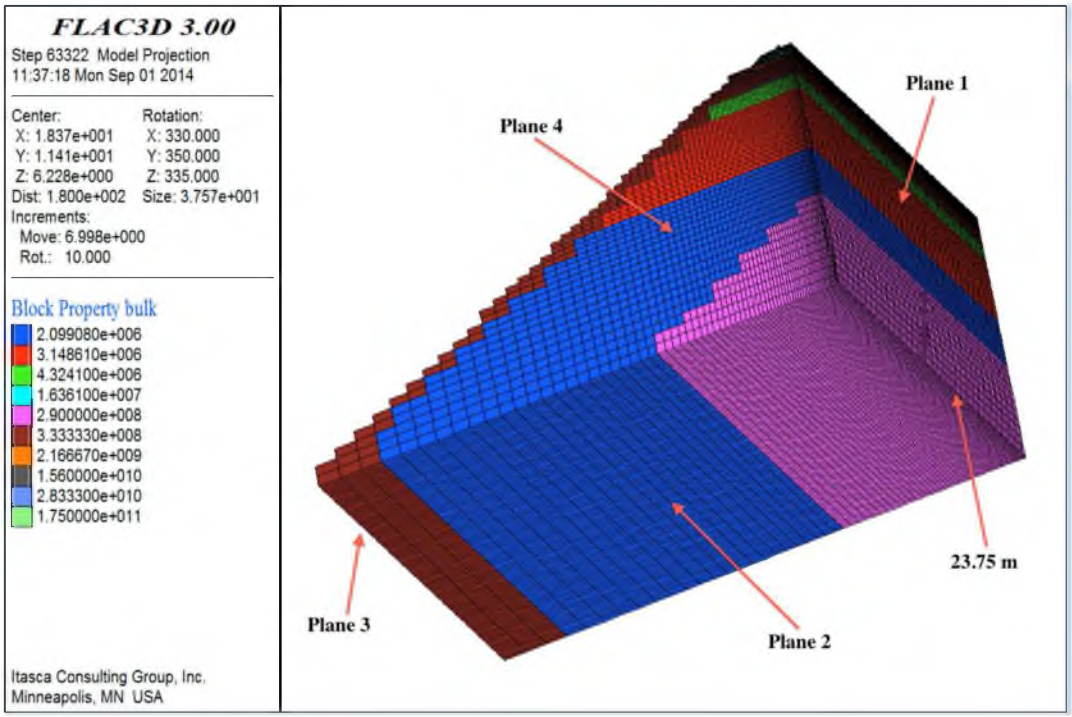

Figure 4.36 3D View of Model Mesh

The length of the mesh in the longitudinal (y) direction was taken as that of half of the locomotive and half of the car (Figure 4.37 and Figure 4.38) as done by Powrie et al. (2007). Smaller elements were used near the rail where the changes of stresses and strains were expected to be the greatest. The bottom and far-lateral boundaries (Plane 2 and 3 in Figure 4.36) were prevented from movement in all three directions. The longitudinal boundaries (Plane 4 in Figure 4.36) were fixed in the x direction only. The center plane (Plane 1 in Figure 4.36) was fixed in the y direction only.

The most critical loading conditions are illustrated in Figure 4.38. The properties of each material are shown in Table 4.3. Values of the shear modulus (G) and bulk modulus (K) for the FLAC3D model were calculated from elastic theory based on values of E and v. See Figures 4.35 and 4.36 for plots of the properties used in the model.

The FLAC3D model produced a maximum vertical rail displacement of 6.1 mm, which occurred directly under the wheels of the locomotive. The vertical displacement contours for this case are shown in Figures 4.39 and 4.40. The pattern of these contours indicates the LDS is effective in distributing the stress of the rail system due to the large bulk and shear moduli used for this slab. In addition, the contours also show that approximately 80% of the vertical deformation occurs in the EPS. Of the remaining components, approximately 15% of the vertical deformation occurs in the support system above LDS (i.e., rail, sleeper, ballast, sub-ballast and structural fill) and approximately 5% of the vertical deformation occurs in the foundation soil. Thus, it is concluded that the vertical displacement of an EPS supported embankment system is mainly controlled by the properties and behavior the EPS for relatively high embankments, such as that modeled herein.

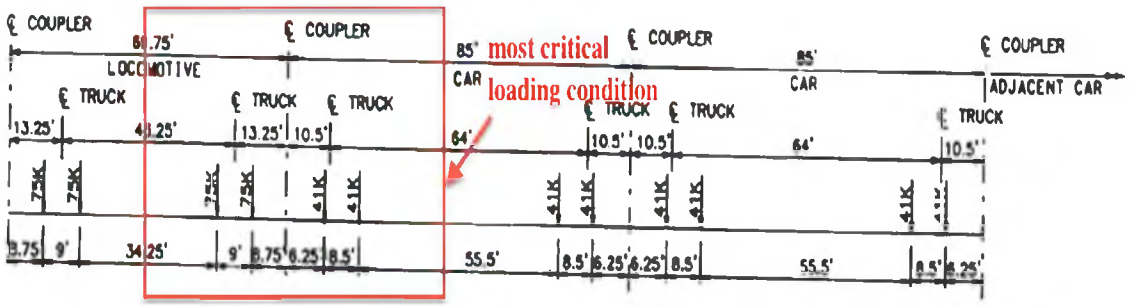

Figure 4.37 Most Critical Loading Condition

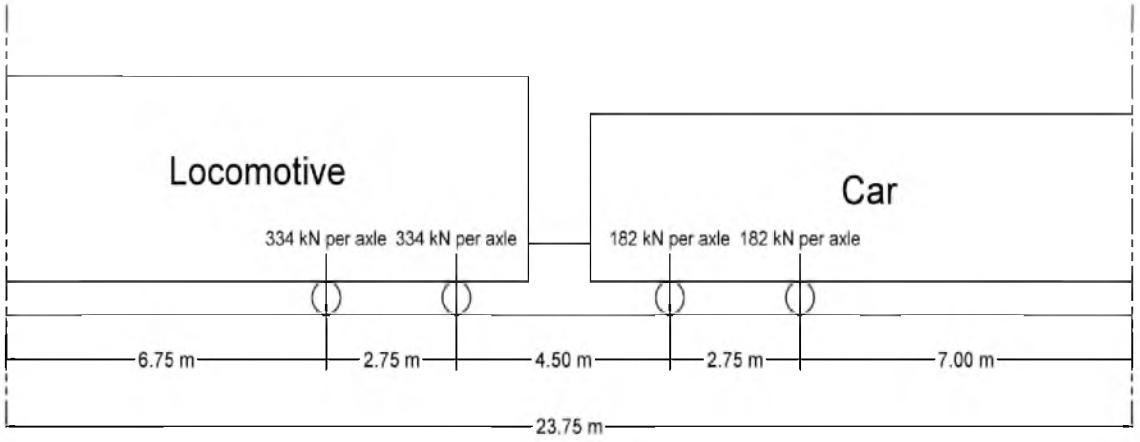

Figure 4.38 Loading Condition Used in 3D Model

Figures 4.41 and 4.42 show the lateral (x direction) and longitudinal (y direction) displacement of the railway embankment model. The model has a maximum lateral displacement of 0.7 mm and a maximum longitudinal displacement of 0.03 mm, both of which are relatively insignificant compared with the magnitude of the vertical displacement.

Figure 4.43 shows the vertical stress contours of the railway embankment model. Figure 4.44 shows the horizontal stress contours of the railway embankment model in the lateral (x) direction.

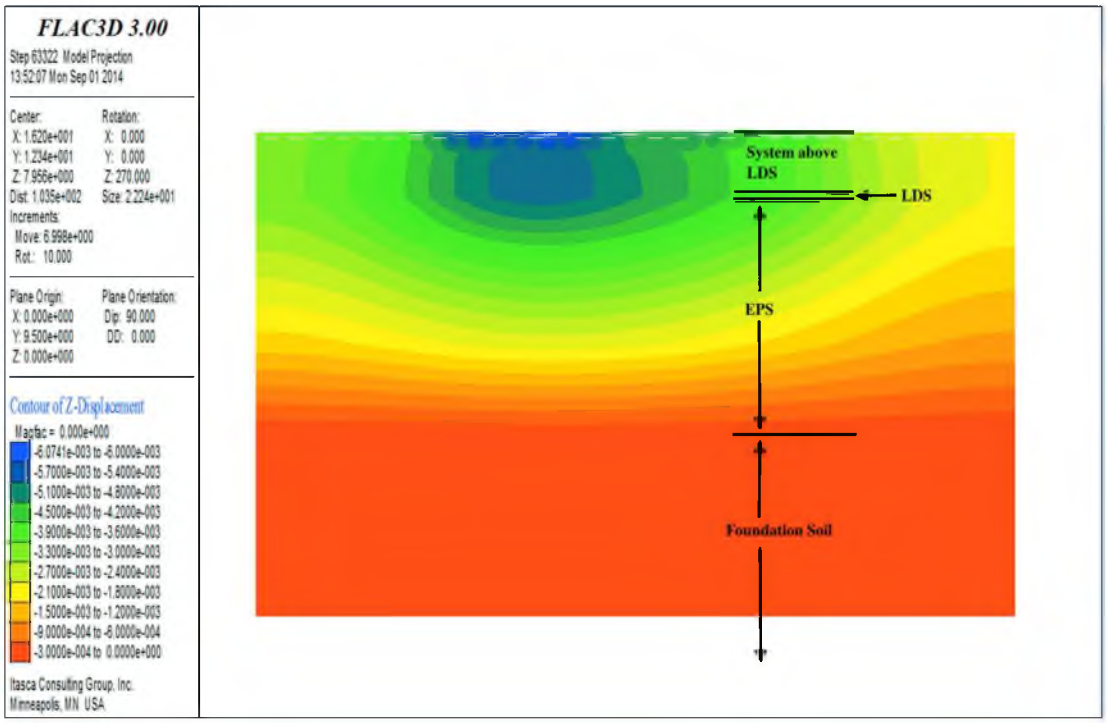

Figure 4.39 Profile View of Vertical Displacement Contours (m)

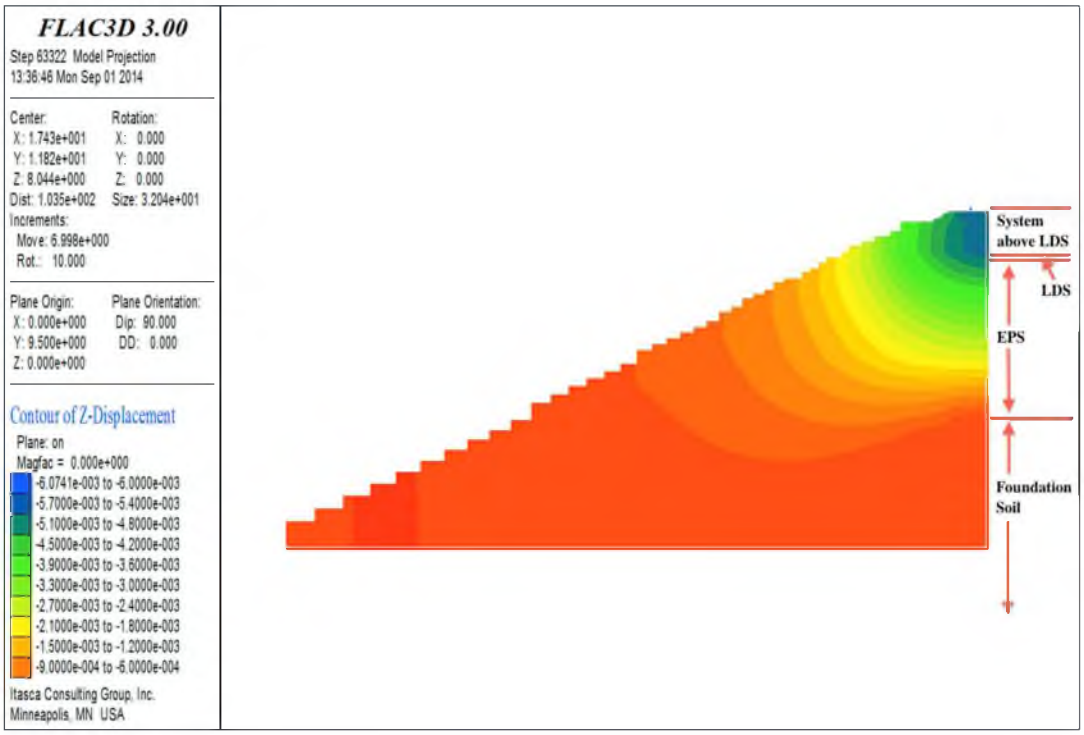

Figure 4.40 Cross-section View of Vertical Displacement Contours (m)

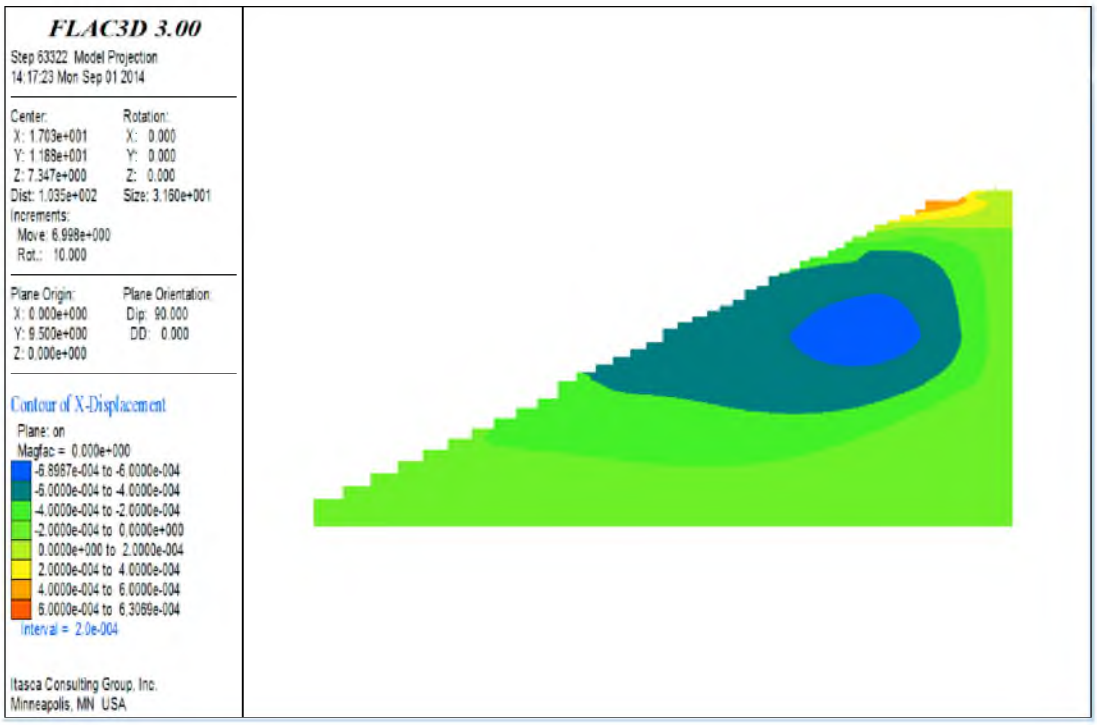

Figure 4.41 Lateral Displacement Contours (m)

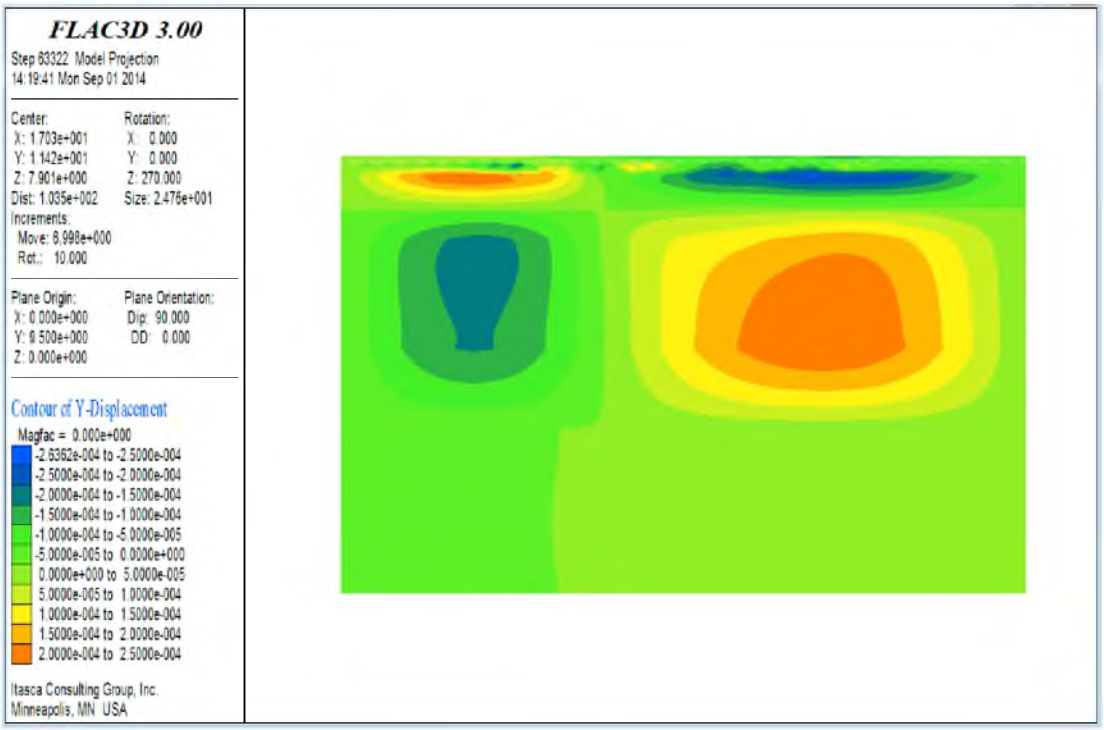

Figure 4.42 Longitudinal Displacement Contours (m)

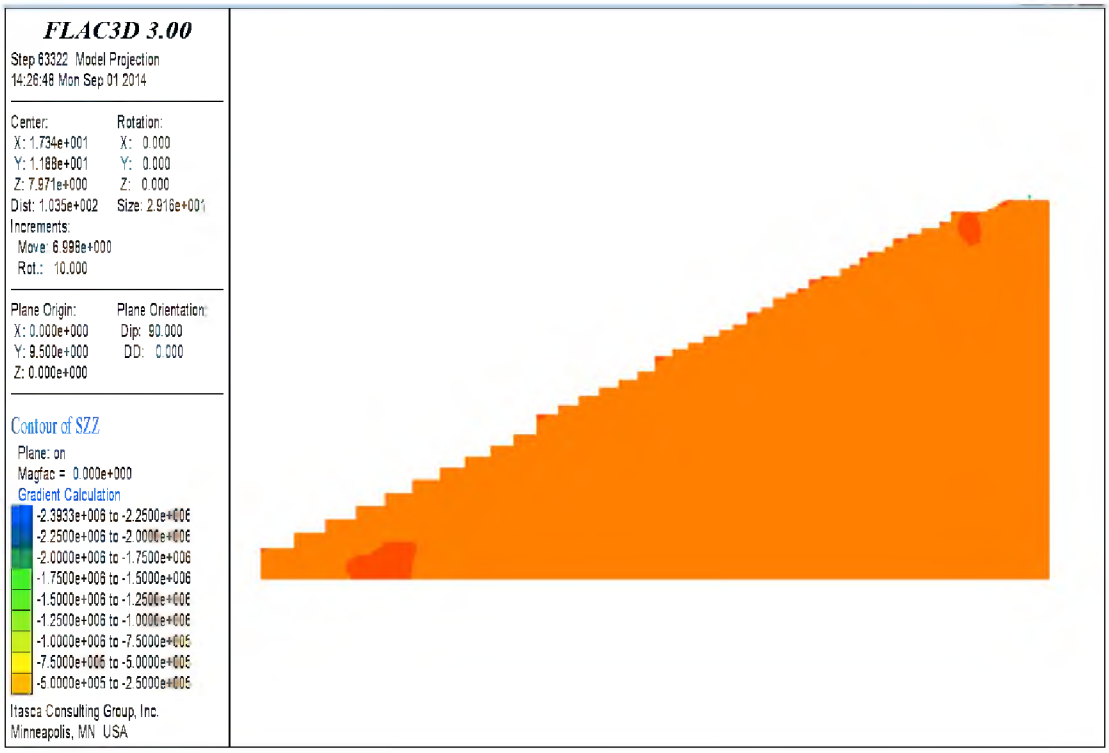

Figure 4.43 Vertical Stress Contours (Pa)

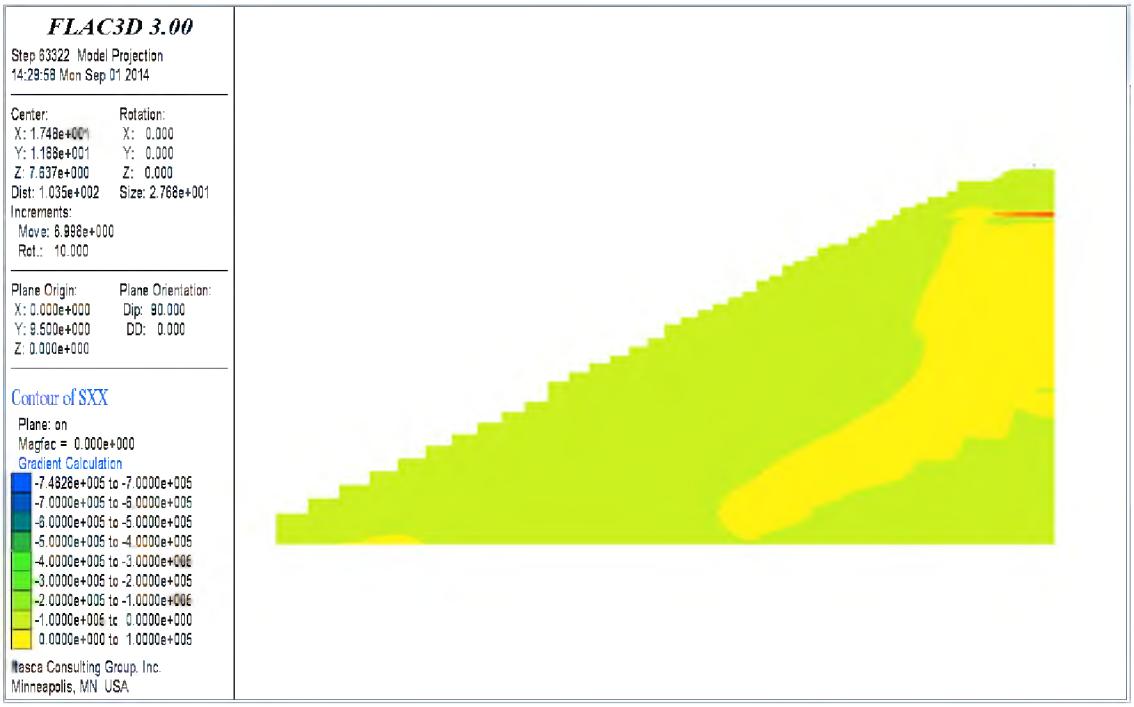

Figure 4.44 Horizontal Stress Contours in Lateral (x) Direction (Pa)

Figure 4.45 show the horizontal stress contours of the railway embankment model in the longitudinal (y) direction.

Figures 4.46 and 4.47 show the shear stress contours of the railway embankment model. According to these plots, one can observe that the normal stress and shear stress within the model are distributed relatively uniformly by the rail-sleeper-ballast (sub-ballast)-structural fill-LDS system. This is due to the high bulk and shear moduli of these materials.

4.3.4 Summary and Discussion

The development of the FLAC modeling approach was based on simplifications, and their potential ramifications were explored and quantified using a 2D model, as discussed

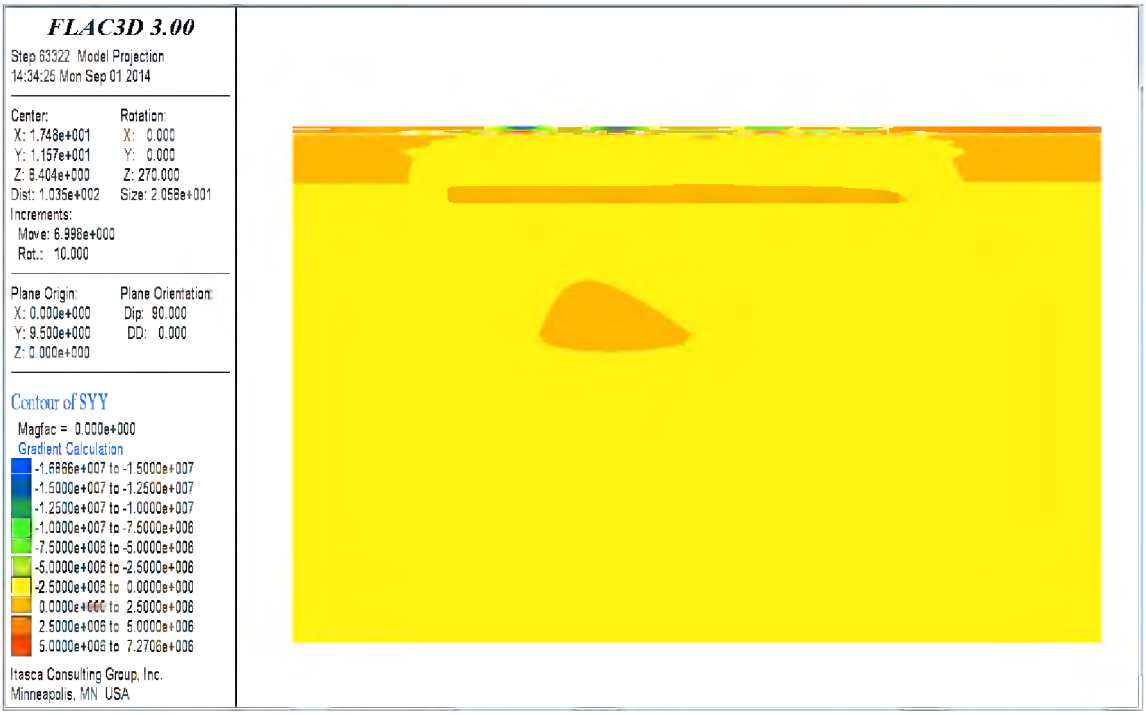

Figure 4.45 Horizontal Stress Contours in Longitudinal (y) Direction (Pa)

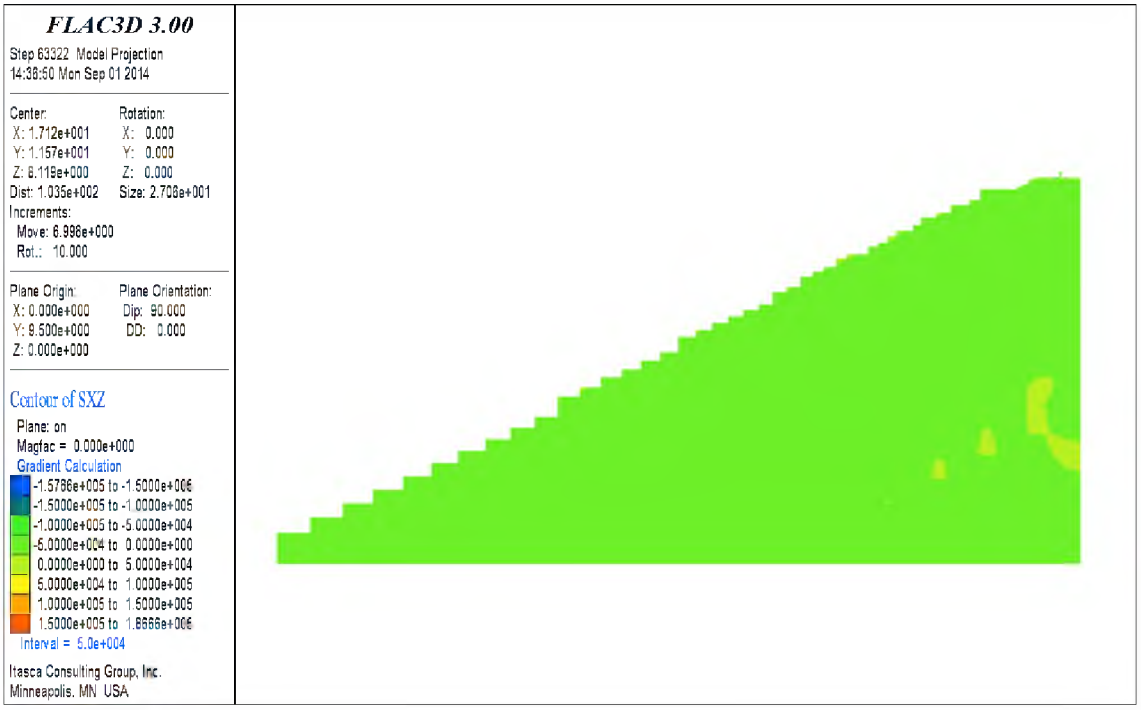

Figure 4.46 Cross-section View of Shear Stress Contours (Pa)

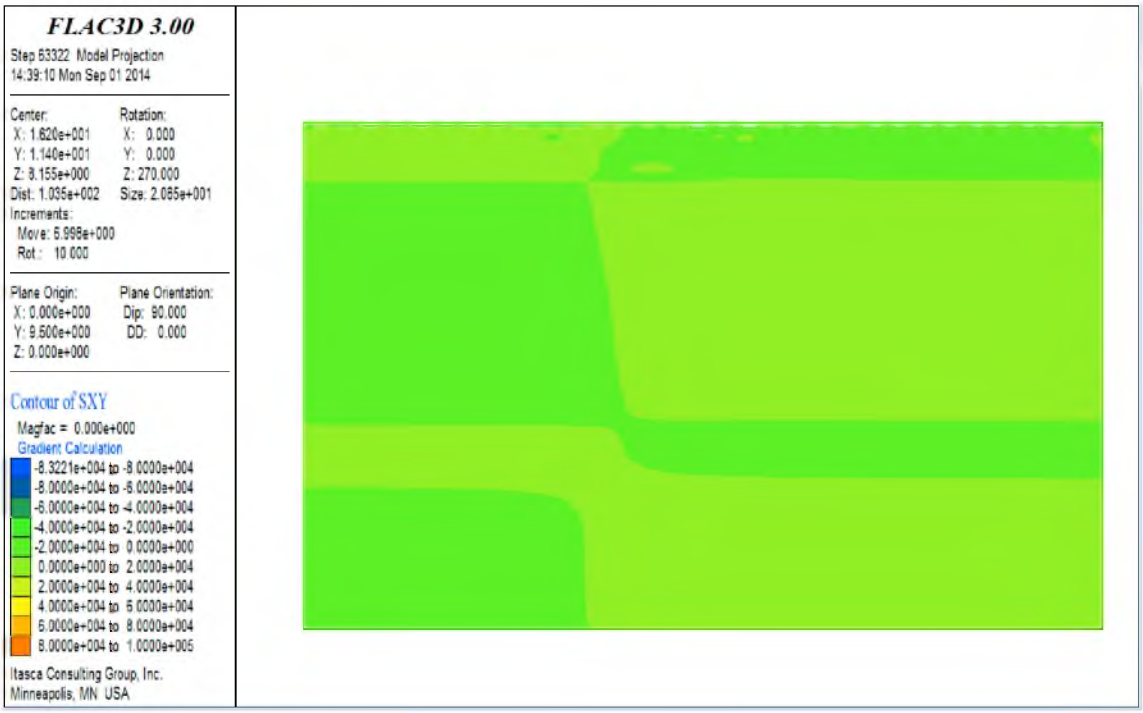

Figure 4.47 Profile View of Shear Stress Contours (Pa)

previously. When evaluated as a 2D model, the simplifications produced a slightly conservative estimate, i.e., slightly overestimated the total vertical displacement of the system, when compared with a more extensive 2D model that incorporated the complete geometry of the system.

When the simplified system was modeled using a 3D geometry, the maximum vertical rail displacement was estimated to be 6.1 mm for the most critical (i.e., highest) loading condition, which occurs directly under the wheels of the locomotive. In addition, based on the developed contours of displacement and stress, it is obvious that the load distribution slab (LDS) effectively distributes the vertical stresses of the system due to the large bulk and shear moduli of this concrete slab. It was also found that approximately 80% of the vertical deformation occurs within the EPS. This is due to the much lower bulk and shear moduli of EPS when compared with other materials and components of the system (i.e., rail, sleeper, ballast, structural fill, foundation soil, etc.). It was estimated that approximately 15% of the vertical deformation of the system occurs above the LDS (i.e., rail, sleeper, ballast, sub-ballast, and structural fill) and approximately 5% of the vertical deformation occurs in the foundation soil. Therefore, the vertical displacement behavior of an EPS supported embankment system is mainly controlled by the properties and behavior the EPS for relatively large embankments, such as that modeled herein.

In addition, it was estimated that the system has a maximum lateral displacement of 0.7 mm and a maximum longitudinal displacement of 0.03 mm, both of which are relatively insignificant compared with the magnitude of the vertical displacement. The normal stress and shear stress within the system are distributed relatively uniformly by

the rail-sleeper-ballast (sub-ballast)-structural fill-LDS system. This is due to the high bulk and shear moduli of these materials.

CHAPTER 5

SUMMARY AND CONCLUSIONS

This research developed a numerical method to evaluate the vertical displacement of rail systems constructed atop EPS geofoam embankments. To achieve this purpose, a complex 2D FLAC modeling approach was developed to analyze the sleeper deflection for a multilayered railway embankment system supported by a regular earthen embankment. The result from this initial effort was checked with FEM analysis conducted by other researchers on the same system. The percentage difference of the estimated sleeper deflection was within 8%, which validated the FLAC model in relation to the FEM modeling approach used in the literature (Powrie et al., 2007).

Additionally, a more complex FLAC3D model was developed to analyze the vertical displacement of an EPS-supported multilayered railway embankment system constructed in Norway. A series of 2D models were first developed to identify the appropriate mesh size and level of discretization required to reasonably estimate the total surface displacement from the train loading. This exploratory modeling was initially performed because 2D models required significantly less computational time and computer memory. This study suggested that fine, intermediate, and coarse meshes produced nearly the same vertical displacement of the sleeper and that a mesh size of 60 m × 60 m (width × depth) was sufficient to produce stable results. A finely graded, nonuniform mesh with a

domain size of 60 m × 60 m (width × depth) was thus used in the 3D modeling.

For the 3D modeling of the Norwegian case, the maximum vertical rail displacement calculated by FLAC3D was 2.3 mm, which occurred directly under the wheels. In addition, FLAC3D indicated that the concrete slab had a vertical displacement ranging from 1.8 mm to 2.3 mm. The vertical displacement of the railway embankment system compressed much more uniformly in the longitudinal (y) direction than in the lateral (x) direction. In addition, even though the thickness of the EPS layer was only approximately 5% of the full depth of the embankment model, approximately 60% of the vertical compression occurred in the EPS. This is due to the fact that the EPS has a much lower bulk and shear moduli than other materials (i.e., rail, sleeper, natural ground, etc.). The system had a maximum predicted lateral displacement of 0.2 mm, and a maximum predicted longitudinal displacement of 0.02 mm, both of which are relatively insignificant compared with the magnitude of the predicted vertical displacement. The normal and shear stresses within the system are distributed relatively uniformly by the rail-sleeper-ballast-concrete slab system. This is due to the high stiffness (i.e., high bulk and shear moduli) of these materials in relation to the underlying EPS and soil materials.

To confirm the above modeling results, surveyed vertical deflections were used as reported by Frydenlund et al. (1987). These measurements were made on bolts found in the concrete slab constructed atop the EPS-blocks. The field measurements ranged from 2 to 3 mm on the west rail. This half of the railway embankment system was modeled by FLAC3D. The model produced vertical deflections ranging from 1.8 to 2.3 mm. This range of results was deemed to be a reasonable estimate of the lower range of the field measurements. Therefore, it was concluded that FDM, as implemented in FLAC, can

satisfactory estimate the static vertical displacement of rails systems constructed atop EPS-supported embankments when subjected to a static (i.e., stopped) train loading.

Finally, a more complex FLAC3D model was developed to analyze the vertical displacement of the EPS-supported UTA FrontRunner embankment system in Corner Canyon, Draper, Utah. One-dimensional compression tests were conducted on the ballast and Young's modulus was obtained for use in the model. In the models developed for railway systems supported by both regular earthen embankment (Powrie et al., 2007) and EPS embankment (Frydenlund et al., 1987), the coarse mesh, intermediate mesh, and fine mesh spacing resulted in almost the same estimate of vertical displacement of the concrete sleeper. Thus, it was concluded that mesh density is not a major factor in the modeling process if only vertical displacements are to be predicted. However, a fine mesh was used in both the 2D and 3D modeling of the UTA FrontRunner embankment system.

This system is not plane-symmetrical. It was found that simply modeling half of the system would not result in correct results. However, a full 3D model of the embankment system require significant amount of computational time and memory and thus is not preferable. As a result, a series of 2D models were developed to investigate simplification methods and evaluate the magnitude of the potential differences caused by the simplifications. Firstly, a 2D model of the full embankment system was developed. Secondly, the 2D model was cut vertically at the center of the left (i.e., western) outer track, similar to what would be done if this represented an axis of symmetry. Thirdly, a series of 2D models with different dimensions for the foundation soils were developed to investigate the effects of the mesh size and boundaries on the estimated vertical

displacement of the rails. Included in these cases were foundation soil dimensions (depth by extended width) of 20 m by 15 m, 10 m by 8 m, 5 m by 3 m, and 0 m by 0 m, which produced almost the same vertical displacement result. Finally, the results of the simplest model (i.e., depth by extended width: 0 m by 0 m) were compared with the model of the full embankment model under the same conditions (loading, material properties, etc.). The error introduced by the simplifications used in the modeling produced an over-estimation of the vertical displacement of about 11%. Using this simplified method produced a slightly conservative but reasonable result when compared with the full model. Thus, this simplest 2D model was used as a representative cross-section of the 3D model.

The FLAC3D model produced a maximum vertical rail displacement of 6.1 mm, which occurred directly under the wheels of the locomotive. The pattern of the vertical displacement contours indicated the load distribution slab (LDS) is effective in distributing the stress of the rail system due to the large bulk and shear moduli used for this slab. In addition, the contours also showed that approximately 80% of the vertical deformation occurred in the EPS. Of the remaining components, approximately 15% of the vertical deformation occurred in the support system above LDS (i.e., rail, sleeper, ballast, sub-ballast and structural fill), and approximately 5% of the vertical deformation occurred in the foundation soil. Thus, it was concluded that the vertical displacement of an EPS supported embankment system is mainly controlled by the properties and behavior the EPS for relatively high embankments, such as that modeled herein.

The model had a maximum lateral displacement of 0.7 mm and a maximum longitudinal displacement of 0.03 mm, both of which are relatively insignificant

compared with the magnitude of the vertical displacement. The normal stress and shear stress within the model were distributed relatively uniformly by the rail-sleeper-ballast (sub-ballast)-structural fill-LDS system. This was due to the high bulk and shear moduli of these materials.

Deflection measurements are planned by others as part of research funded by the National Center for Freight and Infrastructure Research and Education (CFIRE). Because the estimates contained in this section haven performed before the FrontRunner field measurements were obtained, they constitute a prior prediction of the deflection behavior of this system.

APPENDIX A

COMPARISON OF POINT LOAD ON HOMOGENEOUS ELASTIC HALF SPACE USING ELASTIC THEORY AND FINITE DIFFERENCE METHOD (FDM)

A.1 Problem Statement

A vertical point load of 10 kN is applied at the surface of a semi-infinite soil mass as indicated in Figure A.1. Assume that the soil is linear elastic with E = 1E7 kPa and v = 0.3.

The point load is applied on semi-infinite homogeneous, linearly elastic, and isotropic half space.

A.2 Solution

A.2.1 Elastic Theory Solution (Boussinesq, 1883)

For the case of a vertical point load P applied at the origin of the coordinate system (Figure A.1), the vertical stress increase at any point (x, y, z) within the semi-infinite soil mass is given by

$$\Delta\sigma = \frac{3P}{2\pi}\frac{z^3}{(x^2+y^2+z^2)^{\frac{5}{2}}} \qquad \textbf{(A.1)}$$

where P is the intensity of the point load given in force units and x, y, and z are the coordinates of the point at which the increase of vertical stress is calculated.

To calculate the increase in vertical stress directly under the applied load for z = 0 to 1 m, we substitute x = 0 and y = 0 into Equation (A.1). To calculate the increase in vertical stress directly at x = 0.1 m for z = 0 to 1 m, we substitute x = 0.1 and y = 0 into Equation (A.1). Using this equation, we can calculate the increase in vertical stress as a function of z. The results are plotted in Figure A.2.

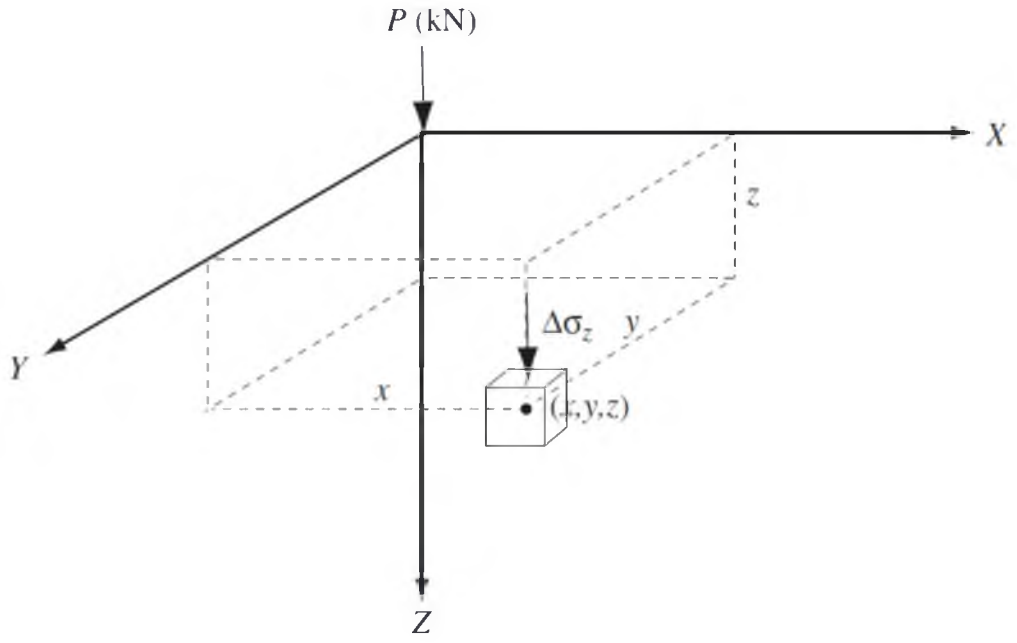

Figure A.1 Vertical Stresses Caused by a Point Load

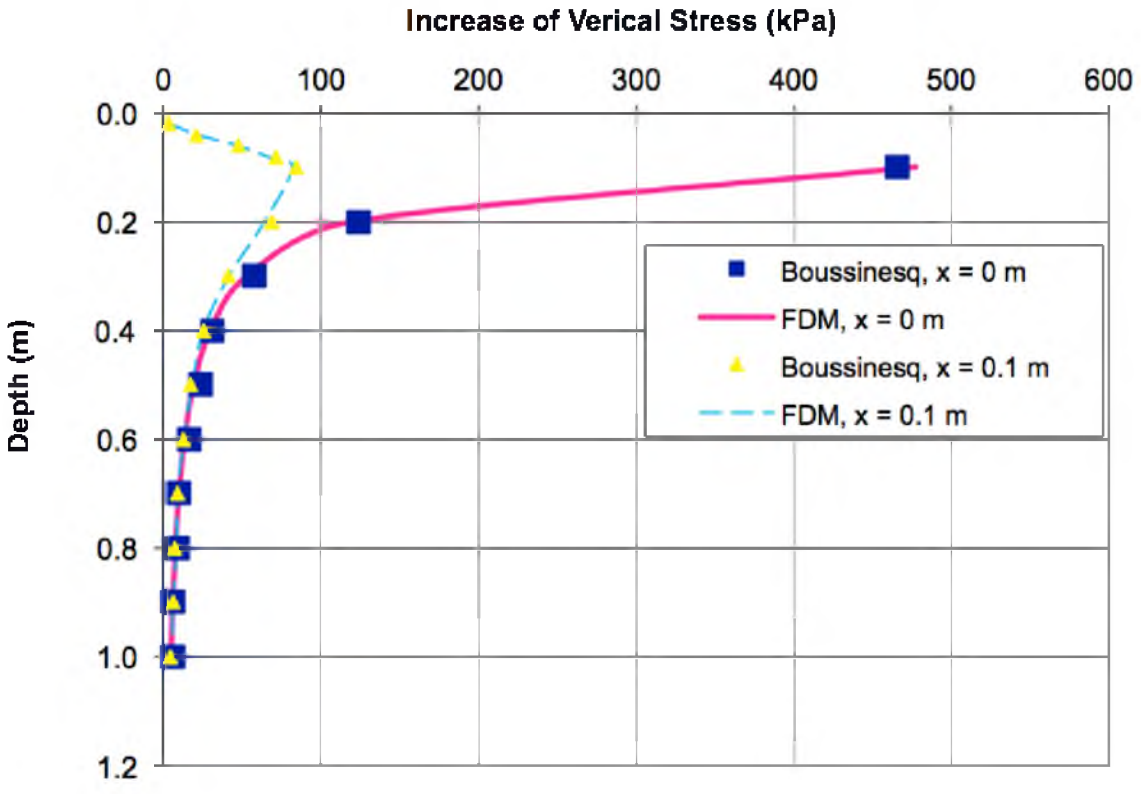

Figure A.2 Comparison of Increase of Vertical Stress Caused by Point Load

A.2.2 FDM Solution (FLAC)

For simplicity, the semi-infinite soil mass is assumed to be a cylinder 1 m in radius and 2 m in height, as shown in Figure A.3. The reason of using a cylindrical shape in this simulation is to take advantage of axisymmetry, in which we can utilize axisymmetric two-dimensional analysis instead of three-dimensional analysis. The mesh is made finer in the zone around the point load where stress concentration is expected.

Assume the soil at the bottom of the model cannot move in both direction; thus, fix in both the x and y direction in the model (z direction in reality) at the bottom. Assume the soil on the side of the model can only move in the vertical direction but cannot move in the horizontal direction; thus, fix only in the x direction on the side.

Treat point load 10 kN as equivalent stress over a small circular area with radius

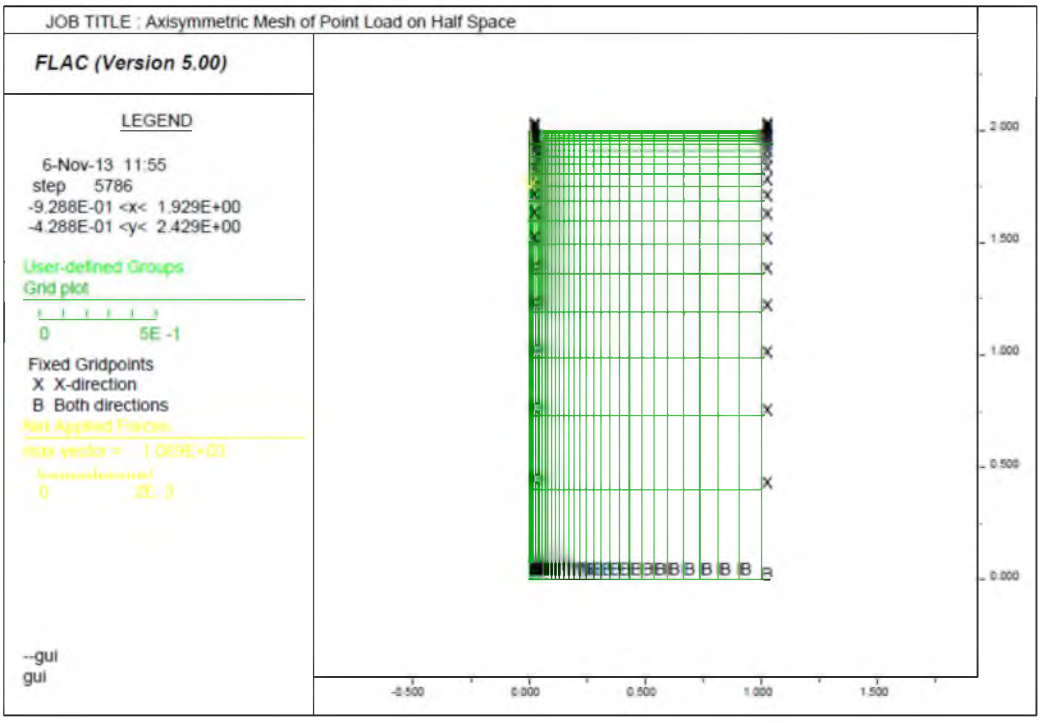

Figure A.3 Axisymmetric Mesh of Point Load on Half Space

6E-3 m, which is the first mesh from center. The soil is assumed to be linear elastic with E = 1E7 kPa and v = 0.3, based on which shear modulus (G) and bulk modulus can be calculated: G = 3.85E9 and K = 8.33E9. Also assume soil has a dry density of 2000 kg/m^3.

The results are also shown in Figure A.2.

A.3 Comparison, Conclusion, and Discussion

Figure A.2 shows excellent agreement between the stresses calculated using the Boussinesq and FDM solutions.

A.4 FLAC Codes

```
config axisymmetry
grid 30,20
model elastic
;
;model geometry, a cylinder 2 m in height, 1 meter in radius; "ratio" defines distribution of mesh
gen 0,0 0,2 1,2 1,0 ratio (1.1,0.8)
;
;model properties, assume the soil is linear elastic with E=1E7 kPa and v=0.3, the following properties are calculated:
prop density=2000.0 bulk=8.33333E9 shear=3.84615E9
;
;boundary conditions
fix  x y j 1; fix in both x and y direction at bottom
fix  x i 31; fix only in the x direction on side
;
;loading condition, treat point load 10 kN as stress over a small circular area with radius 6E-3 m, which is the first mesh from center
apply syy -8.8419416E7 from 1,21 to 2,21
;
solve
```

APPENDIX B

COMPARISON OF LINE LOAD ON HOMOGENEOUS ELASTIC HALF SPACE USING FINITE ELEMENT METHOD (FEM) AND ELASTIC THEORY

B.1 Problem Statement

A vertical line load of 10 kN/m is applied at the surface of a semi-infinite soil mass as indicated in Figure B.1. Assume that the soil is linear elastic with E = 1E7 kPa and $\nu = 0.3$.

The line load is applied on semi-infinite homogeneous, linearly elastic, and isotropic half space.

B.2 Solution

B.2.1 Elastic Theory Solution

Due to the nature of line load (Helwany, 2007), the resulting stresses in the x–z plane are independent of y (i.e., we will get the same stresses in any x-z plane as we travel along the y-axis). This type of loading–geometry is termed plane strain. The vertical stress increase at any point (x, z) is given as

$$\Delta\sigma = \frac{2qz^3}{\pi(x^2 + z^2)^2} \tag{B.1}$$

where q is the line load (force/unit length) and x and z are the coordinates at which the stress increase is calculated.

To calculate the increase in vertical stress directly under the applied load for z = 0 to 0.3 m, we substitute $x = 0$ into (B.1). Using this equation, we can calculate the increase in vertical stress as a function of z. The results are plotted in Figure B.2.

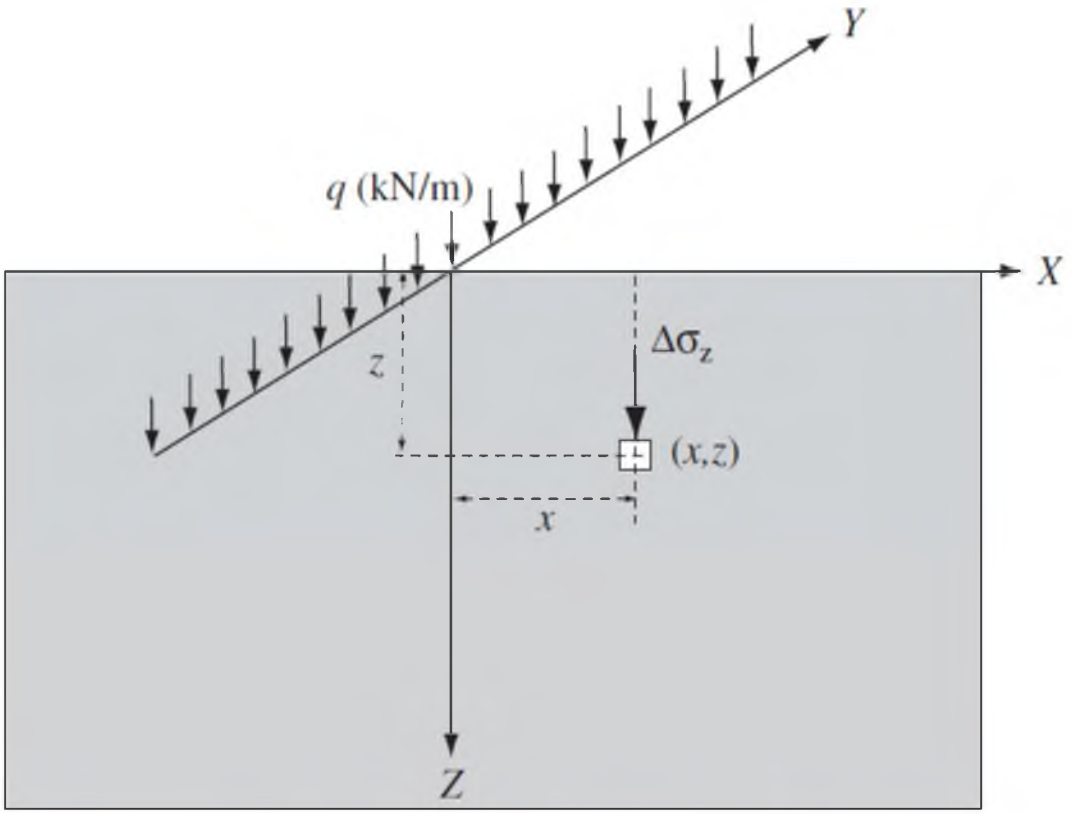

Figure B.1 Stresses Caused by a Line Load

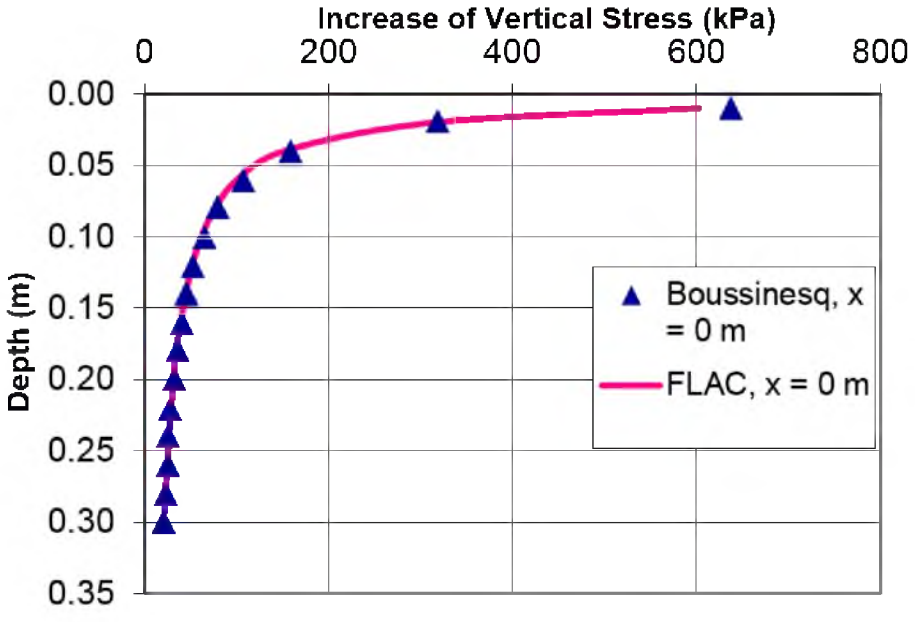

Figure B.2 Comparison of Increase of Vertical Stress Caused by Line Load

B.2.2 FDM Solution (FLAC)

A plane strain condition is assumed in which the semi-infinite soil mass is represented by a 1 m × 2 m (x-z) plane, as shown in Figure B.3. The two-dimensional plane strain mesh used has 30 elements in the x-direction and 20 elements in the z-direction. The mesh is made finer in the zone around the point load where stress concentration is expected.

Assume the soil at the bottom of the model cannot move in both direction; thus, fix in both the x and y direction in the model (z direction in reality) at the bottom. Assume the soil on the side of the model can only move in the vertical direction but cannot move in the horizontal direction; thus, fix only in the x direction on the side.

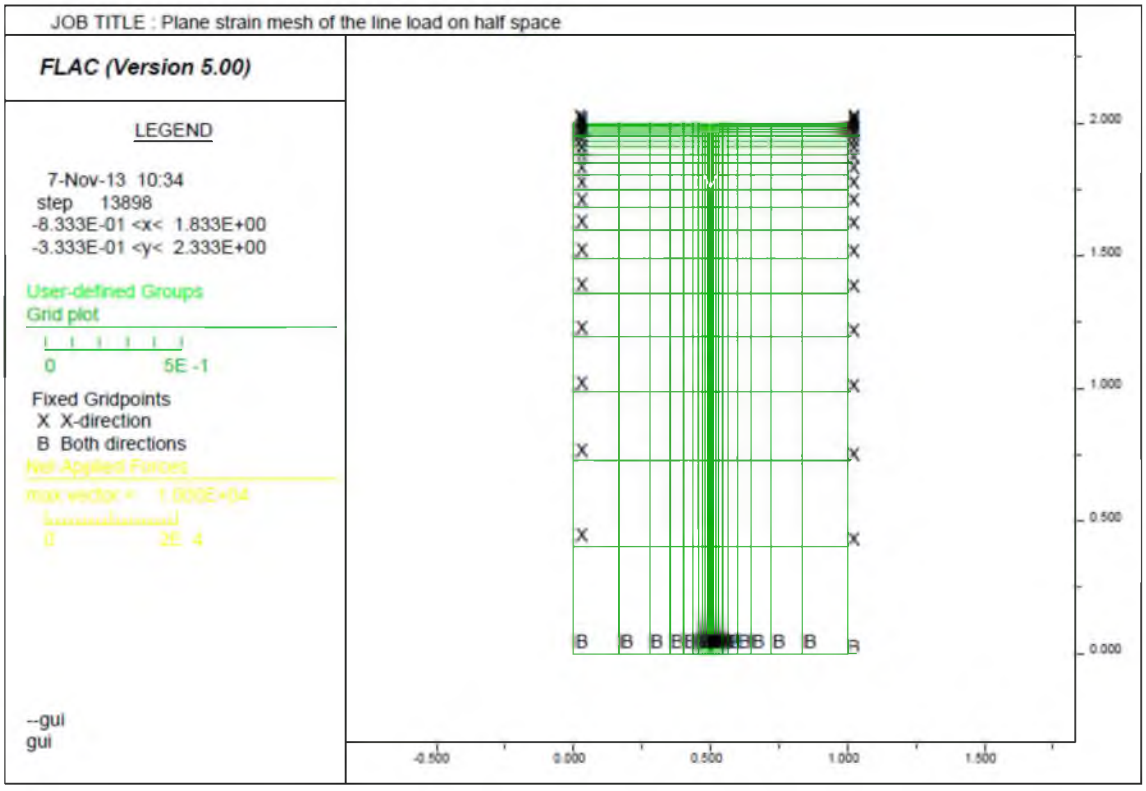

Figure B.3 Plane Strain Mesh of the Line Load on Half Space

Apply a line load of 10 kN/m. In the model, use a force of 10 kN because of the plain strain assumption.

The soil is assumed to be linear elastic with E = 1E7 kPa and v = 0.3, based on which shear modulus (G) and bulk modulus (K) can be calculated: G = 3.85E9 and K = 8.33E9. Also assume soil has a dry density of 2000 kg/m^3.

The results are also shown in Figure B.2.

B.3 Comparison, Conclusion, and Discussion

Figure B.2 shows excellent agreement between the stresses calculated using the analytical solution using Equation (B.1) and FDM solutions.

B.4 FLAC Codes

```
config
grid 30,20
model elastic
;
;model geometry, 1 m × 2 m (x–z) plane; "ratio" defines distribution of mesh
gen 0,0 0,2 0.5,2 0.5,0 ratio (0.667,0.8) i=1,16 j=1,21 ;left half
gen 0.5,0 0.5,2 1,2 1,0 ratio (1.5,0.8) i=16,31 j=1,21 ;right half
;
;model properties, assume the soil is linear elastic with E=1E7 kPa and v=0.3, the following properties are calculated:
prop density=2000.0 bulk=8.33333E9 shear=3.84615E9
;
;boundary conditions
fix  x y j 1 ;fix in both x and y direction at bottom
fix  x i 31 ;fix only in x direction on side
fix  x i 1 ;fix only in x direction on side
;
;loading condition:Apply a line load of 10 kN/m. In the model, use a force of 10 kN because of the plain strain assumption.
apply yforce -10000.0 from 16,21 to 16,21
;
solve
```

APPENDIX C

COMPARISON OF CIRCULAR LOAD ON LAYERED SOIL SYSTEM USING FINITE ELEMENT METHOD (FEM) AND FINITE DIFFERENCE METHOD (FDM)

C.1 Problem Statement

Consider a system with four layers of varying stiffness and thickness, as shown in Figure C.1. A pressure of 10 kPa is uniformly distributed on a circular area with $R = 0.5$ m.

The soil is homogenous within each layer.

C.2 Solution

C.2.1 FEM Solution

A FEM analysis was conducted by Helwany (2007) on the same problem. Results are plotted in Figure C.2 along with the Boussinesq solution for one layer soil system assuming that the soil is linear elastic with E = 1E7 kPa and $v = 0.3$.

C.2.2 FDM Solution (FLAC)

Assume that the semi-infinite soil mass is a cylinder 50 m in radius and 50 m in height. The 10 kPa pressure is applied at the top surface on a circular area with 0.5 m radius. The purpose of the analysis is to calculate the increase in vertical stress within the stratified soil mass due to the application of a uniformly distributed load on a circular area. The two-dimensional axisymmetric mesh used has 30 elements in the x-direction and 30 elements in the y-direction (z direction in reality), as shown in Figure C.3. The mesh includes four layers with the elastic moduli shown in Figure C.1. The mesh is made finer in the zone around the pressurized circle, where stress concentration is expected. The increase in vertical stress under the center of the pressurized circle is plotted as a function of depth, as shown in Figure C.2.

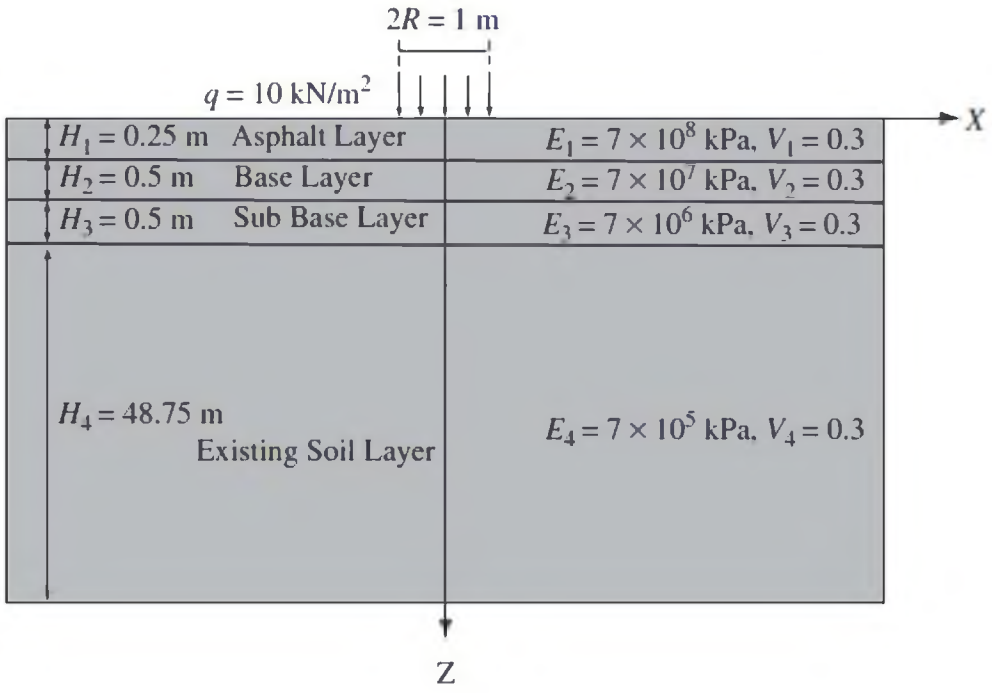

Figure C.1 Stress Increase in a Layered Soil System with a Uniformly Circular Load

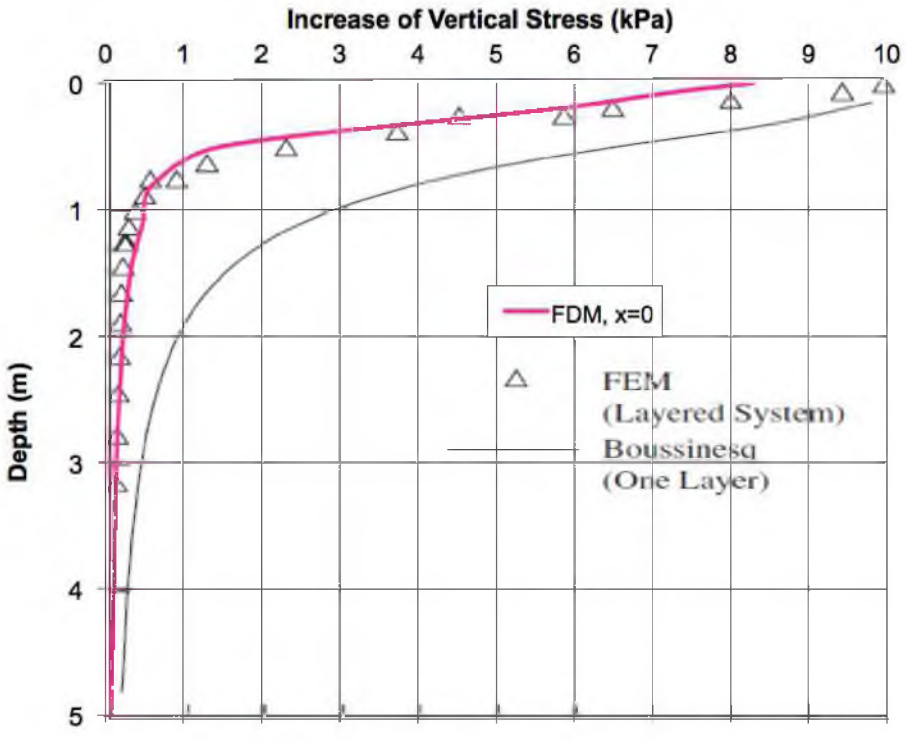

Figure C.2 Comparison of Increase of Vertical Stress Caused by Circular Load

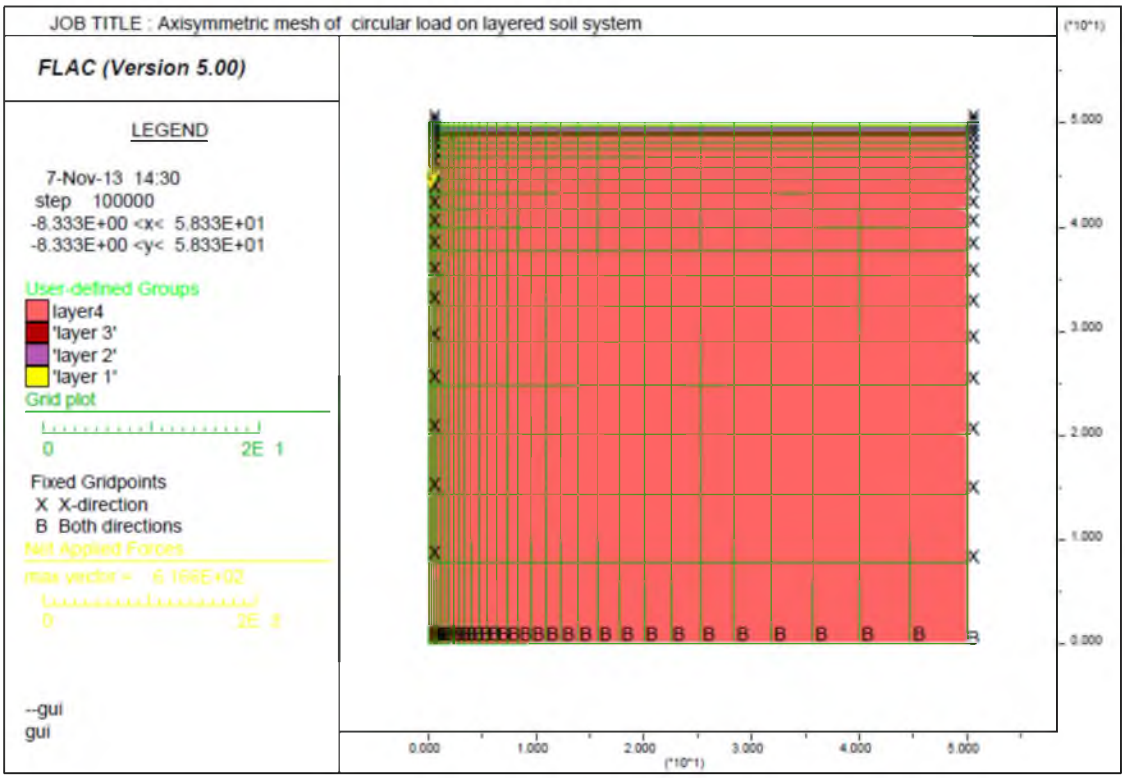

Figure C.3 Axisymmetric Mesh of Circular Load on Layered Soil System

Assume the soil at the bottom of the model cannot move in both directions; thus, fix in both the x and y direction in the model (z direction in reality) at the bottom. Assume the soil on the side of the model can only move in the vertical direction but cannot move in the horizontal direction; thus, fix only in the x direction on the side.

The 10 kPa pressure is applied at the top surface on a circular area with 0.5 m radius.

The properties of each layer are shown in Figure C.1. Shear modulus (G) and bulk modulus (K) can be calculated based on E and v. Also assume soil has a dry density of 2000 kg/m^3

The results are also shown in Figure C.2.

C.3 Comparison, Conclusion, and Discussion

Figure C.2 shows excellent agreement between the FEM and FDM solutions.

C.4 FLAC Codes

```
config axisymmetry
grid 30,20
model elastic
;
;model geometry, a cylinder 50 m in height, 50 m in radius
;"ratio" defines distribution of mesh
;the horizontal mesh is adjusted so that the first two meshes have a width of 0.5 m
gen 0,0 0,50 50,50 50,0 ratio (1.113,0.85)
;
; boundary condition,
fix  x y j 1; fix in both x and y direction at bottom
fix  x i 31; fix only in the x direction on side
;
;loading condition, The 10 kPa pressure is applied at the top surface on a circular area with
0.5 m radius.
apply syy -10000.0 from 1,21 to 3,21
;
;model properties
group 'layer 1' j 20
model elastic group 'layer 1'
prop density=2000.0 bulk=5.83333E11 shear=2.69231E11 group 'layer 1'
group 'layer 2' j 19
model mohr group 'layer 2'
prop density=2000.0 bulk=5.83333E10 shear=2.69231E10 group 'layer 2'
group 'layer 3' j 18
model elastic group 'layer 3'
prop density=2000.0 bulk=5.83333E9 shear=2.69231E9 group 'layer 3'
group 'layer4' j 1 17
model elastic group 'layer4'
prop density=2000.0 bulk=5.83333E8 shear=2.69231E8 group 'layer4'
;
solve
```

APPENDIX D

FLAC CODE OF FDM MODEL FOR RAIL SYSTEMS SUPPORTED BY REGULAR EARTH EMBANKMENT DUE TO TRAIN LOAD

```
config
grid 45,48
gen (0.0,0.0) (0.0,60.0) (0.661,60.0) (0.661,0.0) ratio 0.9,0.87 i 1 6 j 1 36
gen (0.0,60.0) (0.0,60.5) (0.661,60.5) (0.661,60.0) ratio 0.9,0.90000004 i 1 6 j 36 40
gen (0.0,60.5) (0.0,60.7) (0.661,60.7) (0.661,60.5) ratio 0.9,0.8999999 i 1 6 j 40 42
gen (0.0,60.7) (0.0,61.0) (0.661,61.0) (0.661,60.7) ratio 0.9,0.9 i 1 6 j 42 45
gen (0.0,61.0) (0.0,61.2) (0.661,61.2) (0.661,61.0) ratio 0.9,0.8999999 i 1 6 j 45 47
gen (0.0,61.2) (0.0,61.353) (0.661,61.353) (0.661,61.2) ratio 0.9,1.0 i 1 6 j 47 49
gen (0.661,0.0) (0.661,60.0) (0.739,60.0) (0.739,0.0) ratio 1.0,0.87 i 6 7 j 1 36
gen (0.661,60.0) (0.661,60.5) (0.739,60.5) (0.739,60.0) ratio 1.0,0.90000004 i 6 7 j 36 40
gen (0.661,60.5) (0.661,60.7) (0.739,60.7) (0.739,60.5) ratio 1.0,0.8999999 i 6 7 j 40 42
gen (0.661,60.7) (0.661,61.0) (0.739,61.0) (0.739,60.7) ratio 1.0,0.9 i 6 7 j 42 45
gen (0.661,61.0) (0.661,61.2) (0.739,61.2) (0.739,61.0) ratio 1.0,0.8999999 i 6 7 j 45 47
gen (0.661,61.2) (0.661,61.353) (0.739,61.353) (0.739,61.2) i 6 7 j 47 49
gen (0.739,0.0) (0.739,60.0) (1.21,60.0) (1.21,0.0) ratio 1.1,0.87 i 7 11 j 1 36
gen (0.739,60.0) (0.739,60.5) (1.21,60.5) (1.21,60.0) ratio 1.1,0.90000004 i 7 11 j 36 40
gen (0.739,60.5) (0.739,60.7) (1.21,60.7) (1.21,60.5) ratio 1.1,0.8999999 i 7 11 j 40 42
gen (0.739,60.7) (0.739,61.0) (1.21,61.0) (1.21,60.7) ratio 1.1,0.9 i 7 11 j 42 45
gen (0.739,61.0) (0.739,61.2) (1.21,61.2) (1.21,61.0) ratio 1.1,0.8999999 i 7 11 j 45 47
gen (0.739,61.2) (0.739,61.353) (1.21,61.353) (1.21,61.2) ratio 1.1,1.0 i 7 11 j 47 49
gen (1.21,0.0) (1.21,60.0) (2.21,60.0) (2.21,0.0) ratio 1.1,0.87 i 11 18 j 1 36
gen (1.21,60.0) (1.21,60.5) (2.21,60.5) (2.21,60.0) ratio 1.1,0.90000004 i 11 18 j 36 40
gen (1.21,60.5) (1.21,60.7) (2.21,60.7) (2.21,60.5) ratio 1.1,0.8999999 i 11 18 j 40 42
gen (1.21,60.7) (1.21,61.0) (2.21,61.0) (2.21,60.7) ratio 1.1,0.9 i 11 18 j 42 45
gen (1.21,61.0) (1.21,61.2) (2.21,61.2) (2.21,61.0) ratio 1.1,0.8999999 i 11 18 j 45 47
gen (1.21,61.2) (1.21,61.353) (2.21,61.353) (2.21,61.2) ratio 1.1,1.0 i 11 18 j 47 49
gen (2.21,0.0) (2.21,60.0) (3.717,60.0) (3.717,0.0) ratio 1.1,0.87 i 18 26 j 1 36
gen (2.21,60.0) (2.21,60.5) (3.717,60.5) (3.717,60.0) ratio 1.1,0.90000004 i 18 26 j 36 40
gen (2.21,60.5) (2.21,60.7) (3.717,60.7) (3.717,60.5) ratio 1.1,0.8999999 i 18 26 j 40 42
gen (2.21,60.7) (2.21,61.0) (3.717,61.0) (3.717,60.7) ratio 1.1,0.9 i 18 26 j 42 45
gen (2.21,61.0) (2.21,61.2) (3.717,61.2) (3.717,61.0) ratio 1.1,0.8999999 i 18 26 j 45 47
gen (2.21,61.2) (2.21,61.353) (3.717,61.353) (3.717,61.2) ratio 1.1,1.0 i 18 26 j 47 49
gen (3.717,0.0) (3.717,60.0) (60.0,60.0) (60.0,0.0) ratio 1.3,0.87 i 26 46 j 1 36
gen (3.717,60.0) (3.717,60.5) (60.0,60.5) (60.0,60.0) ratio 1.3,0.90000004 i 26 46 j 36 40
gen (3.717,60.5) (3.717,60.7) (60.0,60.7) (60.0,60.5) ratio 1.3,0.8999999 i 26 46 j 40 42
gen (3.717,60.7) (3.717,61.0) (60.0,61.0) (60.0,60.7) ratio 1.3,0.9 i 26 46 j 42 45
gen (3.717,61.0) (3.717,61.2) (60.0,61.2) (60.0,61.0) ratio 1.3,0.8999999 i 26 46 j 45 47
gen (3.717,61.2) (3.717,61.353) (60.0,61.353) (60.0,61.2) ratio 1.3,1.0 i 26 46 j 47 49
model elastic i=1,45 j=1,48
model null i 1 5 j 47 48
group 'null' i 1 5 j 47 48
group delete 'null'
model null i 7 30 j 47 48
group 'null' i 7 30 j 47 48
group delete 'null'
model null i 31 36 j 47 48
group 'null' i 31 36 j 47 48
group delete 'null'
model null i 37 40 j 47 48
group 'null' i 37 40 j 47 48
group delete 'null'
```

```
model null i 41 43 j 47 48
group 'null' i 41 43 j 47 48
group delete 'null'
model null i 44 45 j 47 48
group 'null' i 44 45 j 47 48
group delete 'null'
model null i 18 26 j 42 46
group 'null' i 18 26 j 42 46
group delete 'null'
model null i 27 j 42 45
group 'null' i 27 j 42 45
group delete 'null'
model null i 27 35 j 45 46
group 'null' i 27 35 j 45 46
group delete 'null'
model null i 28 35 j 42 44
group 'null' i 28 35 j 42 44
group delete 'null'
model null i 36 42 j 42 46
group 'null' i 36 42 j 42 46
group delete 'null'
model null i 43 45 j 42 46
group 'null' i 43 45 j 42 46
group delete 'null'
model null i 26 35 j 36 41
group 'null' i 26 35 j 36 41
group delete 'null'
model null i 36 39 j 36 41
group 'null' i 36 39 j 36 41
group delete 'null'
model null i 40 44 j 36 41
group 'null' i 40 44 j 36 41
group delete 'null'
model null i 45 j 36 41
group 'null' i 45 j 36 41
group delete 'null'
gen 1.21,60.7 1.21,61.2 1.41,61.3 2.21,60.7 ratio 1.1,0.9626995 i 11 18 j 42 47
gen 2.21,60.0 2.21,60.7 2.667,60.7 3.717,60.0 ratio 1.1,0.91918045 i 18 26 j 36 42
group 'User:rail' i 6 j 47 48
model elastic group 'User:rail'
prop density=7842.0 bulk=1.75E11 shear=8.07692E10 group 'User:rail'
group 'User:sleeper' i 1 10 j 45 46
model elastic group 'User:sleeper'
prop density=2398.0 bulk=1.08333E10 shear=5E9 group 'User:sleeper'
group 'User:ballast' i 1 17 j 42 44
model elastic group 'User:ballast'
prop density=1698.0 bulk=2.58333E8 shear=1.19231E8 group 'User:ballast'
group 'User:ballast' i 11 17 j 45 46
model elastic group 'User:ballast'
prop density=1698.0 bulk=2.58333E8 shear=1.19231E8 group 'User:ballast'
group 'User:sub-ballast' i 1 25 j 40 41
```

```
model elastic group 'User:sub-ballast'
prop density=2298.0 bulk=2.16666E9 shear=4.36242E7 group 'User:sub-ballast'
group 'User:prepared subgrade' i 1 25 j 36 39
model elastic group 'User:prepared subgrade'
prop density=1998.0 bulk=1.66667E9 shear=3.3557E7 group 'User:prepared subgrade'
group 'User:natural ground' i 1 38 j 17 35
model elastic group 'User:natural ground'
prop density=1998.0 bulk=5.00001E8 shear=1.00671E7 group 'User:natural ground'
group 'User:natural ground' i 39 44 j 11 35
model elastic group 'User:natural ground'
prop density=1998.0 bulk=5.00001E8 shear=1.00671E7 group 'User:natural ground'
group 'User:natural ground' i 45 j 15 35
model elastic group 'User:natural ground'
prop density=1998.0 bulk=5.00001E8 shear=1.00671E7 group 'User:natural ground'
group 'User:natural ground' i 1 38 j 4 16
model elastic group 'User:natural ground'
prop density=1998.0 bulk=5.00001E8 shear=1.00671E7 group 'User:natural ground'
group 'User:natural ground' i 1 38 j 1 3
model elastic group 'User:natural ground'
prop density=1998.0 bulk=5.00001E8 shear=1.00671E7 group 'User:natural ground'
group 'User:natural ground' i 39 45 j 1 10
model elastic group 'User:natural ground'
prop density=1998.0 bulk=5.00001E8 shear=1.00671E7 group 'User:natural ground'
group 'User:natural ground' i 45 j 11 14
model elastic group 'User:natural ground'
prop density=1998.0 bulk=5.00001E8 shear=1.00671E7 group 'User:natural ground'
fix x y j 1
fix x i 1
fix x y i 46
set gravity=9.81
solve
ini xdis 0 ydis 0
ini xvel 0 yvel 0
history 999 unbalanced
apply yforce -62500.0 from 6,49 to 6,49
apply yforce -62500.0 from 7,49 to 7,49
solve
```

APPENDIX E

FLAC CODE OF FDM MODEL FOR VERTICAL DISPLACEMENT OF A RAILWAY SYSTEM SUPPORTED BY EPS EMBANKMENT IN NORWAY DUE TO TRAIN LOAD

E.1 2D Model

The codes presented here are for the model with intermediate mesh. Both the depth and width of the foundation soil are 60 m.

```
config
grid 68,63
gen (0.0,0.0) (0.0,56.187) (0.661,56.187) (0.661,0.0) ratio 1.0,0.95 i 1 5 j 1 41
gen (0.0,56.187) (0.0,56.337) (0.661,56.337) (0.661,56.187) i 1 5 j 41 42
gen (0.0,56.337) (0.0,56.937) (0.661,56.937) (0.661,56.337) i 1 5 j 42 45
gen (0.0,56.937) (0.0,57.537) (0.661,57.537) (0.661,56.937) i 1 5 j 45 48
gen (0.0,57.537) (0.0,58.137) (0.661,58.137) (0.661,57.537) i 1 5 j 48 51
gen (0.0,58.137) (0.0,58.737) (0.661,58.737) (0.661,58.137) i 1 5 j 51 54
gen (0.0,58.737) (0.0,58.887) (0.661,58.887) (0.661,58.737) i 1 5 j 54 55
gen (0.0,58.887) (0.0,59.647) (0.661,59.647) (0.661,58.887) i 1 5 j 55 60
gen (0.0,59.647) (0.0,59.847) (0.661,59.847) (0.661,59.647) i 1 5 j 60 62
gen (0.0,59.847) (0.0,60.0) (0.661,60.0) (0.661,59.847) i 1 5 j 62 64
gen (0.661,0.0) (0.661,56.187) (0.739,56.187) (0.739,0.0) ratio 1.0,0.95 i 5 6 j 1 41
gen (0.661,56.187) (0.661,56.337) (0.739,56.337) (0.739,56.187) i 5 6 j 41 42
gen (0.661,56.337) (0.661,56.937) (0.739,56.937) (0.739,56.337) i 5 6 j 42 45
gen (0.661,56.937) (0.661,57.537) (0.739,57.537) (0.739,56.937) i 5 6 j 45 48
gen (0.661,57.537) (0.661,58.137) (0.739,58.137) (0.739,57.537) i 5 6 j 48 51
gen (0.661,58.137) (0.661,58.737) (0.739,58.737) (0.739,58.137) i 5 6 j 51 54
gen (0.661,58.737) (0.661,58.887) (0.739,58.887) (0.739,58.737) i 5 6 j 54 55
gen (0.661,58.887) (0.661,59.647) (0.739,59.647) (0.739,58.887) i 5 6 j 55 60
gen (0.661,59.647) (0.661,59.847) (0.739,59.847) (0.739,59.647) i 5 6 j 60 62
gen (0.661,59.847) (0.661,60.0) (0.739,60.0) (0.739,59.847) i 5 6 j 62 64
gen (0.739,0.0) (0.739,56.187) (1.21,56.187) (1.21,0.0) ratio 1.0,0.95 i 6 9 j 1 41
gen (0.739,56.187) (0.739,56.337) (1.21,56.337) (1.21,56.187) i 6 9 j 41 42
gen (0.739,56.337) (0.739,56.937) (1.21,56.937) (1.21,56.337) i 6 9 j 42 45
gen (0.739,56.937) (0.739,57.537) (1.21,57.537) (1.21,56.937) i 6 9 j 45 48
gen (0.739,57.537) (0.739,58.137) (1.21,58.137) (1.21,57.537) i 6 9 j 48 51
gen (0.739,58.137) (0.739,58.737) (1.21,58.737) (1.21,58.137) i 6 9 j 51 54
gen (0.739,58.737) (0.739,58.887) (1.21,58.887) (1.21,58.737) i 6 9 j 54 55
gen (0.739,58.887) (0.739,59.647) (1.21,59.647) (1.21,58.887) i 6 9 j 55 60
gen (0.739,59.647) (0.739,59.847) (1.21,59.847) (1.21,59.647) i 6 9 j 60 62
gen (0.739,59.847) (0.739,60.0) (1.21,60.0) (1.21,59.847) i 6 9 j 62 64
gen (1.21,0.0) (1.21,56.187) (1.88,56.187) (1.88,0.0) ratio 1.0,0.95 i 9 13 j 1 41
gen (1.21,56.187) (1.21,56.337) (1.88,56.337) (1.88,56.187) i 9 13 j 41 42
gen (1.21,56.337) (1.21,56.937) (1.88,56.937) (1.88,56.337) i 9 13 j 42 45
gen (1.21,56.937) (1.21,57.537) (1.88,57.537) (1.88,56.937) i 9 13 j 45 48
gen (1.21,57.537) (1.21,58.137) (1.88,58.137) (1.88,57.537) i 9 13 j 48 51
gen (1.21,58.137) (1.21,58.737) (1.88,58.737) (1.88,58.137) i 9 13 j 51 54
gen (1.21,58.737) (1.21,58.887) (1.88,58.887) (1.88,58.737) i 9 13 j 54 55
gen (1.21,58.887) (1.21,59.647) (1.88,59.647) (1.88,58.887) i 9 13 j 55 60
gen (1.21,59.647) (1.21,59.847) (1.88,59.847) (1.88,59.647) i 9 13 j 60 62
gen (1.21,59.847) (1.21,60.0) (1.88,60.0) (1.88,59.847) i 9 13 j 62 64
gen (1.88,0.0) (1.88,56.187) (2.88,56.187) (2.88,0.0) ratio 1.0,0.95 i 13 18 j 1 41
gen (1.88,56.187) (1.88,56.337) (2.88,56.337) (2.88,56.187) i 13 18 j 41 42
```

```
gen (1.88,56.337) (1.88,56.937) (2.88,56.937) (2.88,56.337) i 13 18 j 42 45
gen (1.88,56.937) (1.88,57.537) (2.88,57.537) (2.88,56.937) i 13 18 j 45 48
gen (1.88,57.537) (1.88,58.137) (2.88,58.137) (2.88,57.537) i 13 18 j 48 51
gen (1.88,58.137) (1.88,58.737) (2.88,58.737) (2.88,58.137) i 13 18 j 51 54
gen (1.88,58.737) (1.88,58.887) (2.88,58.887) (2.88,58.737) i 13 18 j 54 55
gen (1.88,58.887) (1.88,59.647) (2.88,59.647) (2.88,58.887) i 13 18 j 55 60
gen (1.88,59.647) (1.88,59.847) (2.88,59.847) (2.88,59.647) i 13 18 j 60 62
gen (1.88,59.847) (1.88,60.0) (2.88,60.0) (2.88,59.847) i 13 18 j 62 64
gen (2.88,0.0) (2.88,56.187) (3.5,56.187) (3.5,0.0) ratio 1.0,0.95 i 18 22 j 1 41
gen (2.88,56.187) (2.88,56.337) (3.5,56.337) (3.5,56.187) i 18 22 j 41 42
gen (2.88,56.337) (2.88,56.937) (3.5,56.937) (3.5,56.337) i 18 22 j 42 45
gen (2.88,56.937) (2.88,57.537) (3.5,57.537) (3.5,56.937) i 18 22 j 45 48
gen (2.88,57.537) (2.88,58.137) (3.5,58.137) (3.5,57.537) i 18 22 j 48 51
gen (2.88,58.137) (2.88,58.737) (3.5,58.737) (3.5,58.137) i 18 22 j 51 54
gen (2.88,58.737) (2.88,58.887) (3.5,58.887) (3.5,58.737) i 18 22 j 54 55
gen (2.88,58.887) (2.88,59.647) (3.5,59.647) (3.5,58.887) i 18 22 j 55 60
gen (2.88,59.647) (2.88,59.847) (3.5,59.847) (3.5,59.647) i 18 22 j 60 62
gen (2.88,59.847) (2.88,60.0) (3.5,60.0) (3.5,59.847) i 18 22 j 62 64
gen (3.5,0.0) (3.5,56.187) (4.0,56.187) (4.0,0.0) ratio 1.0,0.95 i 22 25 j 1 41
gen (3.5,56.187) (3.5,56.337) (4.0,56.337) (4.0,56.187) i 22 25 j 41 42
gen (3.5,56.337) (3.5,56.937) (4.0,56.937) (4.0,56.337) i 22 25 j 42 45
gen (3.5,56.937) (3.5,57.537) (4.0,57.537) (4.0,56.937) i 22 25 j 45 48
gen (3.5,57.537) (3.5,58.137) (4.0,58.137) (4.0,57.537) i 22 25 j 48 51
gen (3.5,58.137) (3.5,58.737) (4.0,58.737) (4.0,58.137) i 22 25 j 51 54
gen (3.5,58.737) (3.5,58.887) (4.0,58.887) (4.0,58.737) i 22 25 j 54 55
gen (3.5,58.887) (3.5,59.647) (4.0,59.647) (4.0,58.887) i 22 25 j 55 60
gen (3.5,59.647) (3.5,59.847) (4.0,59.847) (4.0,59.647) i 22 25 j 60 62
gen (3.5,59.847) (3.5,60.0) (4.0,60.0) (4.0,59.847) i 22 25 j 62 64
gen (4.0,0.0) (4.0,56.187) (4.5,56.187) (4.5,0.0) ratio 1.0,0.95 i 25 27 j 1 41
gen (4.0,56.187) (4.0,56.337) (4.5,56.337) (4.5,56.187) i 25 27 j 41 42
gen (4.0,56.337) (4.0,56.937) (4.5,56.937) (4.5,56.337) i 25 27 j 42 45
gen (4.0,56.937) (4.0,57.537) (4.5,57.537) (4.5,56.937) i 25 27 j 45 48
gen (4.0,57.537) (4.0,58.137) (4.5,58.137) (4.5,57.537) i 25 27 j 48 51
gen (4.0,58.137) (4.0,58.737) (4.5,58.737) (4.5,58.137) i 25 27 j 51 54
gen (4.0,58.737) (4.0,58.887) (4.5,58.887) (4.5,58.737) i 25 27 j 54 55
gen (4.0,58.887) (4.0,59.647) (4.5,59.647) (4.5,58.887) i 25 27 j 55 60
gen (4.0,59.647) (4.0,59.847) (4.5,59.847) (4.5,59.647) i 25 27 j 60 62
gen (4.0,59.847) (4.0,60.0) (4.5,60.0) (4.5,59.847) i 25 27 j 62 64
gen (4.5,0.0) (4.5,56.187) (5.0,56.187) (5.0,0.0) ratio 1.0,0.95 i 27 29 j 1 41
gen (4.5,56.187) (4.5,56.337) (5.0,56.337) (5.0,56.187) i 27 29 j 41 42
gen (4.5,56.337) (4.5,56.937) (5.0,56.937) (5.0,56.337) i 27 29 j 42 45
gen (4.5,56.937) (4.5,57.537) (5.0,57.537) (5.0,56.937) i 27 29 j 45 48
gen (4.5,57.537) (4.5,58.137) (5.0,58.137) (5.0,57.537) i 27 29 j 48 51
gen (4.5,58.137) (4.5,58.737) (5.0,58.737) (5.0,58.137) i 27 29 j 51 54
gen (4.5,58.737) (4.5,58.887) (5.0,58.887) (5.0,58.737) i 27 29 j 54 55
gen (4.5,58.887) (4.5,59.647) (5.0,59.647) (5.0,58.887) i 27 29 j 55 60
gen (4.5,59.647) (4.5,59.847) (5.0,59.847) (5.0,59.647) i 27 29 j 60 62
gen (4.5,59.847) (4.5,60.0) (5.0,60.0) (5.0,59.847) i 27 29 j 62 64
gen (5.0,0.0) (5.0,56.187) (8.3,56.187) (8.3,0.0) ratio 1.0,0.95 i 29 38 j 1 41
gen (5.0,56.187) (5.0,56.337) (8.3,56.337) (8.3,56.187) i 29 38 j 41 42
gen (5.0,56.337) (5.0,56.937) (8.3,56.937) (8.3,56.337) i 29 38 j 42 45
```

```
gen (5.0,56.937) (5.0,57.537) (8.3,57.537) (8.3,56.937) i 29 38 j 45 48
gen (5.0,57.537) (5.0,58.137) (8.3,58.137) (8.3,57.537) i 29 38 j 48 51
gen (5.0,58.137) (5.0,58.737) (8.3,58.737) (8.3,58.137) i 29 38 j 51 54
gen (5.0,58.737) (5.0,58.887) (8.3,58.887) (8.3,58.737) i 29 38 j 54 55
gen (5.0,58.887) (5.0,59.647) (8.3,59.647) (8.3,58.887) i 29 38 j 55 60
gen (5.0,59.647) (5.0,59.847) (8.3,59.847) (8.3,59.647) i 29 38 j 60 62
gen (5.0,59.847) (5.0,60.0) (8.3,60.0) (8.3,59.847) i 29 38 j 62 64
gen (8.3,0.0) (8.3,56.187) (8.6,56.187) (8.6,0.0) ratio 1.0,0.95 i 38 39 j 1 41
gen (8.3,56.187) (8.3,56.337) (8.6,56.337) (8.6,56.187) i 38 39 j 41 42
gen (8.3,56.337) (8.3,56.937) (8.6,56.937) (8.6,56.337) i 38 39 j 42 45
gen (8.3,56.937) (8.3,57.537) (8.6,57.537) (8.6,56.937) i 38 39 j 45 48
gen (8.3,57.537) (8.3,58.137) (8.6,58.137) (8.6,57.537) i 38 39 j 48 51
gen (8.3,58.137) (8.3,58.737) (8.6,58.737) (8.6,58.137) i 38 39 j 51 54
gen (8.3,58.737) (8.3,58.887) (8.6,58.887) (8.6,58.737) i 38 39 j 54 55
gen (8.3,58.887) (8.3,59.647) (8.6,59.647) (8.6,58.887) i 38 39 j 55 60
gen (8.3,59.647) (8.3,59.847) (8.6,59.847) (8.6,59.647) i 38 39 j 60 62
gen (8.3,59.847) (8.3,60.0) (8.6,60.0) (8.6,59.847) i 38 39 j 62 64
gen (8.6,0.0) (8.6,56.187) (60.0,56.187) (60.0,0.0) ratio 1.05,0.95 i 39 69 j 1 41
gen (8.6,56.187) (8.6,56.337) (60.0,56.337) (60.0,56.187) ratio 1.05,1.0 i 39 69 j 41 42
gen (8.6,56.337) (8.6,56.937) (60.0,56.937) (60.0,56.337) ratio 1.05,1.0 i 39 69 j 42 45
gen (8.6,56.937) (8.6,57.537) (60.0,57.537) (60.0,56.937) ratio 1.05,1.0 i 39 69 j 45 48
gen (8.6,57.537) (8.6,58.137) (60.0,58.137) (60.0,57.537) ratio 1.05,1.0 i 39 69 j 48 51
gen (8.6,58.137) (8.6,58.737) (60.0,58.737) (60.0,58.137) ratio 1.05,1.0 i 39 69 j 51 54
gen (8.6,58.737) (8.6,58.887) (60.0,58.887) (60.0,58.737) ratio 1.05,1.0 i 39 69 j 54 55
gen (8.6,58.887) (8.6,59.647) (60.0,59.647) (60.0,58.887) ratio 1.05,1.0 i 39 69 j 55 60
gen (8.6,59.647) (8.6,59.847) (60.0,59.847) (60.0,59.647) ratio 1.05,1.0 i 39 69 j 60 62
gen (8.6,59.847) (8.6,60.0) (60.0,60.0) (60.0,59.847) ratio 1.05,1.0 i 39 69 j 62 64
model elastic i=1,68 j=1,63
model null i 39 49 j 41 63
group 'null' i 39 49 j 41 63
group delete 'null'
model null i 50 59 j 41 63
group 'null' i 50 59 j 41 63
group delete 'null'
model null i 60 66 j 41 63
group 'null' i 60 66 j 41 63
group delete 'null'
model null i 67 68 j 41 63
group 'null' i 67 68 j 41 63
group delete 'null'
model null i 18 34 j 55 63
group 'null' i 18 34 j 55 63
group delete 'null'
model null i 35 38 j 55 63
group 'null' i 35 38 j 55 63
group delete 'null'
model null i 22 29 j 54
group 'null' i 22 29 j 54
group delete 'null'
model null i 30 37 j 54
group 'null' i 30 37 j 54
```

```
group delete 'null'
model null i 38 j 54
group 'null' i 38 j 54
group delete 'null'
model null i 6 17 j 62 63
group 'null' i 6 17 j 62 63
group delete 'null'
model null i 1 4 j 62 63
group 'null' i 1 4 j 62 63
group delete 'null'
model null i 38 j 42 53
group 'null' i 38 j 42 53
group delete 'null'
model null i 37 j 43 53
group 'null' i 37 j 43 53
group delete 'null'
model null i 36 j 44 53
group 'null' i 36 j 44 53
group delete 'null'
model null i 35 j 45 53
group 'null' i 35 j 45 53
group delete 'null'
model null i 34 j 46 53
group 'null' i 34 j 46 53
group delete 'null'
model null i 33 j 47 53
group 'null' i 33 j 47 53
group delete 'null'
model null i 32 j 48 53
group 'null' i 32 j 48 53
group delete 'null'
model null i 31 j 49 53
group 'null' i 31 j 49 53
group delete 'null'
model null i 30 j 50 53
group 'null' i 30 j 50 53
group delete 'null'
model null i 29 j 51 53
group 'null' i 29 j 51 53
group delete 'null'
model null i 28 j 52 53
group 'null' i 28 j 52 53
group delete 'null'
model null i 27 j 53
group 'null' i 27 j 53
group delete 'null'
model null i 26 j 53
group 'null' i 26 j 53
group delete 'null'
model null i 24 25 j 53
group 'null' i 24 25 j 53
```

```
    group delete 'null'
    model null i 26 27 j 52
    group 'null' i 26 27 j 52
    group delete 'null'
    model null i 28 j 51
    group 'null' i 28 j 51
    group delete 'null'
    gen 1.3775,58.887 1.3775,59.847 1.88,59.847 2.88,58.887 ratio 1.0330254,0.96044856 i 10
18 j 55 62
    group 'User:rail' i 5 j 62 63
    model elastic group 'User:rail'
    prop density=7820.0 bulk=1.75E11 shear=8.08E10 group 'User:rail'
    group 'User:sleeper' i 1 8 j 60 61
    model elastic group 'User:sleeper'
    prop density=2398.0 bulk=1.08330E10 shear=5E9 group 'User:sleeper'
    group 'User:ballast' i 1 17 j 55 59
    model elastic group 'User:ballast'
    prop density=2300.0 bulk=2.5833E8 shear=1.1923E8 group 'User:ballast'
    group 'User:ballast' i 9 17 j 60 61
    model elastic group 'User:ballast'
    prop density=2300.0 bulk=2.5833E8 shear=1.1923E8 group 'User:ballast'
    group 'User:reinforced concrete slab' i 1 21 j 54
    model elastic group 'User:reinforced concrete slab'
    prop density=2400.0 bulk=2.22222E10 shear=1.6667E10 group 'User:reinforced concrete
slab'
    group 'User:EPS29' i 1 21 j 51 53
    model elastic group 'User:EPS29'
    prop density=30.0 bulk=3.1486E6 shear=3.3998E6 group 'User:EPS29'
    group 'User:EPS29' i 1 24 j 48 50
    model elastic group 'User:EPS29'
    prop density=30.0 bulk=3.1486E6 shear=3.3998E6 group 'User:EPS29'
    group 'User:EPS29' i 1 26 j 45 47
    model elastic group 'User:EPS29'
    prop density=30.0 bulk=3.1486E6 shear=3.3998E6 group 'User:EPS29'
    group 'User:EPS29' i 1 28 j 42 44
    model elastic group 'User:EPS29'
    prop density=30.0 bulk=3.1486E6 shear=3.3998E6 group 'User:EPS29'
    group 'User:drainage(gravel/sand)' i 1 38 j 41
    model elastic group 'User:drainage(gravel/sand)'
    prop density=2000.0 bulk=2.5E8 shear=1.15E8 group 'User:drainage(gravel/sand)'
    group 'User:fill' notnull i 22 27 j 51 53
    model elastic notnull group 'User:fill'
    prop density=2000.0 bulk=2.5E8 shear=1.15E8 notnull group 'User:fill'
    group 'User:fill' notnull i 25 31 j 48 50
    model elastic notnull group 'User:fill'
    prop density=2000.0 bulk=2.5E8 shear=1.15E8 notnull group 'User:fill'
    group 'User:fill' notnull i 27 34 j 45 47
    model elastic notnull group 'User:fill'
    prop density=2000.0 bulk=2.5E8 shear=1.15E8 notnull group 'User:fill'
    group 'User:fill' notnull i 29 37 j 42 44
    model elastic notnull group 'User:fill'
```

```
prop density=2000.0 bulk=2.5E8 shear=1.15E8 notnull group 'User:fill'
group 'User:fill' j 37 40
model elastic group 'User:fill'
prop density=2000.0 bulk=2.5E8 shear=1.15E8 group 'User:fill'
group 'User:sand' j 16 36
model elastic group 'User:sand'
prop density=2000.0 bulk=8.3333E7 shear=3.8462E7 group 'User:sand'
group 'User:sand' j 1 15
model elastic group 'User:sand'
prop density=2000.0 bulk=8.3333E7 shear=3.8462E7 group 'User:sand'
fix  x y j 1
fix  x y i 69 j 1 41
fix  x i 1 j 1 62
apply yforce -19375.0 from 5,64 to 5,64
apply yforce -19375.0 from 6,64 to 6,64
solve
```

E.2 3D Model

```
;set mechanical ratio 1e-4
gen zone brick size 100 60 100 p0 0,0,0 p1 60,0,0 p2 0,15,0 p3 0,0,60 ratio 1.05 1.0 0.95;
model elas
;
model null range x 0 0.661 z 59.847 60 ; inside of rail
model null range x 0.739 60 z 59.847 60 ; outside of rail
model null range x 1.2 60 z 59.747 59.847 ; outside of upper  sleeper
model null range x 2.05 60 z 59.687 59.847 ; slope outside of ballast 1
model null range x 2.21 60 z 59.527 59.687 ; slope outside of ballast 2
model null range x 2.38 60 z 59.367 59.527 ; slope outside of ballast 3
model null range x 2.55 60 z 59.207 59.367 ; slope outside of ballast 4
model null range x 2.71 60 z 59.047 59.207 ; slope outside of ballast 5
model null range x 2.88 60 z 58.887 59.047 ; slope outside of ballast 6
model null range x 4.01 60 z 58.737 58.887 ; slope outside of load distribution slab
model null range x 4.01 60 z 58.482 58.737 ; slope outside of EPS 1
model null range x 4.52 60 z 58.227 58.482 ; slope outside of EPS 2
model null range x 5.03 60 z 57.972 58.227 ; slope outside of EPS 3
model null range x 5.54 60 z 57.717 57.972 ; slope outside of EPS 4
model null range x 6.05 60 z 57.462 57.717 ; slope outside of EPS 5
model null range x 6.56 60 z 57.207 57.462 ; slope outside of EPS 6
model null range x 7.07 60 z 56.952 57.207 ; slope outside of EPS 7
model null range x 7.58 60 z 56.697 56.952 ; slope outside of EPS 8
model null range x 8.09 60 z 56.442 56.697 ; slope outside of EPS 9
model null range x 8.60 60 z 55.737 56.442 ; slope outside of EPS 10
model null range y 0.249 0.751 z 59.747 59.847 ; gap under rail between sleepers
model null range y 0.999 1.501 z 59.747 59.847 ; gap under rail between sleepers
model null range y 1.749 2.251 z 59.747 59.847 ; gap under rail between sleepers
model null range y 2.499 3.001 z 59.747 59.847 ; gap under rail between sleepers
model null range y 3.249 3.751 z 59.747 59.847 ; gap under rail between sleepers
model null range y 3.999 4.501 z 59.747 59.847 ; gap under rail between sleepers
```

```
    model null range y 4.749 5.251 z 59.747 59.847 ; gap under rail between sleepers
    model null range y 5.499 6.001 z 59.747 59.847 ; gap under rail between sleepers
    model null range y 6.249 6.751 z 59.747 59.847 ; gap under rail between sleepers
    model null range y 6.999 7.501 z 59.747 59.847 ; gap under rail between sleepers
    model null range y 7.749 8.251 z 59.747 59.847 ; gap under rail between sleepers
    model null range y 8.499 9.001 z 59.747 59.847 ; gap under rail between sleepers
    model null range y 9.249 9.751 z 59.747 59.847 ; gap under rail between sleepers
    model null range y 9.999 10.501 z 59.747 59.847 ; gap under rail between sleepers
    model null range y 10.749 11.251 z 59.747 59.847 ; gap under rail between sleepers
    model null range y 11.499 12.001 z 59.747 59.847 ; gap under rail between sleepers
    model null range y 12.249 12.751 z 59.747 59.847 ; gap under rail between sleepers
    model null range y 12.999 13.501 z 59.747 59.847 ; gap under rail between sleepers
    model null range y 13.749 14.251 z 59.747 59.847 ; gap under rail between sleepers
    model null range y 14.499 15.001 z 59.747 59.847 ; gap under rail between sleepers
    ;
    prop bulk 175000e6 shear 80769e6 range z 59.847 60; rail steel
    prop bulk 258e6 shear 118e6 range x 0 60 z 0 59.647; ballast under sleeper
    prop bulk 258e6 shear 118e6 range x 0 60 z 59.647 59.747; ballast between sleeper
    ;prop bulk 10833e6 shear 5000e6 range x 0 1.21 z 59.647 59.847 ; sleeper concrete
continuous
    prop bulk 28333e6 shear 13077e6 range x 0 1.21 y -0.001 0.251 z 59.647 59.847 ; sleeper
concrete 1
    prop bulk 28333e6 shear 13077e6 range x 0 1.21 y 0.749 1.001 z 59.647 59.847 ; sleeper
concrete 2
    prop bulk 28333e6 shear 13077e6 range x 0 1.21 y 1.499 1.751 z 59.647 59.847 ; sleeper
concrete 3
    prop bulk 28333e6 shear 13077e6 range x 0 1.21 y 2.249 2.501 z 59.647 59.847 ; sleeper
concrete 4
    prop bulk 28333e6 shear 13077e6 range x 0 1.21 y 2.999 3.251 z 59.647 59.847 ; sleeper
concrete 5
    prop bulk 28333e6 shear 13077e6 range x 0 1.21 y 3.749 4.001 z 59.647 59.847 ; sleeper
concrete 6
    prop bulk 28333e6 shear 13077e6 range x 0 1.21 y 4.499 4.751 z 59.647 59.847 ; sleeper
concrete 7
    prop bulk 28333e6 shear 13077e6 range x 0 1.21 y 5.249 5.501 z 59.647 59.847 ; sleeper
concrete 8
    prop bulk 28333e6 shear 13077e6 range x 0 1.21 y 5.999 6.251 z 59.647 59.847 ; sleeper
concrete 9
    prop bulk 28333e6 shear 13077e6 range x 0 1.21 y 6.749 7.001 z 59.647 59.847 ; sleeper
concrete 10
    prop bulk 28333e6 shear 13077e6 range x 0 1.21 y 7.449 7.751 z 59.647 59.847 ; sleeper
concrete 11
    prop bulk 28333e6 shear 13077e6 range x 0 1.21 y 8.249 8.501 z 59.647 59.847 ; sleeper
concrete 12
    prop bulk 28333e6 shear 13077e6 range x 0 1.21 y 8.999 9.251 z 59.647 59.847 ; sleeper
concrete 13
    prop bulk 28333e6 shear 13077e6 range x 0 1.21 y 9.749 10.001 z 59.647 59.847 ; sleeper
concrete 14
    prop bulk 28333e6 shear 13077e6 range x 0 1.21 y 10.499 10.751 z 59.647 59.847 ; sleeper
concrete 15
    prop bulk 28333e6 shear 13077e6 range x 0 1.21 y 11.249 11.501 z 59.647 59.847 ; sleeper
```

```
concrete 16
    prop bulk 28333e6 shear 13077e6 range x 0 1.21 y 11.999 12.251 z 59.647 59.847 ; sleeper
concrete 17
    prop bulk 28333e6 shear 13077e6 range x 0 1.21 y 12.749 13.001 z 59.647 59.847 ; sleeper
concrete 18
    prop bulk 28333e6 shear 13077e6 range x 0 1.21 y 13.499 13.751 z 59.647 59.847 ; sleeper
concrete 19
    prop bulk 28333e6 shear 13077e6 range x 0 1.21 y 14.249 14.501 z 59.647 59.847 ; sleeper
concrete 20
    prop bulk 258e6 shear 119e6 range x 1.21 1.88  z 59.647 59.747 ; ballast outside of sleeper
    prop bulk 28333e6 shear 13077e6 range x 0 4.01 z 58.737 58.887; load distribution slab
    prop bulk 250e6 shear 115e6 range z 55.737 58.737 ; fill in shoulder of slope EPS
    prop bulk 3.15e6 shear 3.4e6 range x 0 3.5 z 58.137 58.737 ; EPS29
    prop bulk 3.15e6 shear 3.4e6 range x 0 4.0 z 57.537 58.137 ; EPS29
    prop bulk 3.15e6 shear 3.4e6 range x 0 4.5 z 56.937 57.537 ; EPS29
    prop bulk 3.15e6 shear 3.4e6 range x 0 5.0 z 56.337 56.937 ; EPS29
    prop bulk 3.15e6 shear 3.4e6 range x 0 5.5 z 55.737 56.337 ; EPS29
    prop bulk 83e6 shear 38e6 range z 0 55.737; foundation soil
    ;
    ;boundary conditions
    ;
    fix x y z range z -.01 .01 ; fixes base
    fix x y z range x 59.99 60.01 ; fixes right boundary
    fix y range y -0.01 0.01 ; fixes front face in y direction (axis of symmetry)
    fix y range y 14.99 15.01 ; fixes back face in y direction (axis of symmetry)
    fix x range x -0.01 0.01; fixes left boundary in x direction (axis of symmetry)
    ;
    apply zforce -77.5e3 range z 59.99 60.01 x 0.701 0.703 y 1.999 2.001 ; axle load 1
    apply zforce -77.5e3 range z 59.99 60.01 x 0.701 0.703 y 4.999 5.001 ; axle load 2
    apply zforce -77.5e3 range z 59.99 60.01 x 0.701 0.703 y 9.999 10.001; axle load 3
    apply zforce -77.5e3 range z 59.99 60.01 x 0.701 0.703 y 12.999 13.001; axle load 4
    ;
    hist unbal
    ;step 40000
    Solve
    ;
    plot create PROPV ; shows properties in X section
    plot set color On
    plot set caption On
    plot set caption left
    plot set caption size 26
    plot set title On
    plot set title top
    plot set foreground black
    plot set background white
    plot set window position (0.00,0.00) size(1.00,0.89)
    plot set plane normal (0.000,1.000,0.000)
    plot set plane origin (30.0000e+000,7.500e+000,30.0000e+000)
    plot set mode model
    plot set center (30.0000e+000,6.000e+000,30.0000e+000)
    plot set rotation (0.00, 0.00, 0.00)
```

```
plot set distance 180
plot set angle 22
plot set magnification  1.0e+000
plot add block prop bulk
plot add contour zdisp
;
save Norway-EPS.sav
```

APPENDIX F

FLAC CODE OF FDM MODEL FOR VERTICAL DISPLACEMENT OF UTA FRONTRUNNER RAILWAY SYSTEM SUPPORTED BY EPS EMBANKMENT IN CORNER CANYON DUE TO TRAIN LOAD

F.1 2D Model

The codes presented here are for the model with 0 m depth and extended width of the foundation soil.

```
config
grid 216,106
;generate raw mesh
gen (0.0,0.0) (0.0,20.0) (15.0,20.0) (15.0,0.0) ratio 0.95,0.93 i 1 16 j 1 31
gen (0.0,20.0) (0.0,33.1572) (15.0,33.1572) (15.0,20.0) ratio 0.95,1.0 i 1 16 j 31 87
gen (0.0,33.1572) (0.0,33.3604) (15.0,33.3604) (15.0,33.1572) ratio 0.95,1.0 i 1 16 j 87 89
gen (0.0,33.3604) (0.0,34.2748) (15.0,34.2748) (15.0,33.3604) ratio 0.95,1.0 i 1 16 j 89 98
gen (0.0,34.2748) (0.0,34.478) (15.0,34.478) (15.0,34.2748) ratio 0.95,1.0 i 1 16 j 98 100
gen (0.0,34.478) (0.0,34.7828) (15.0,34.7828) (15.0,34.478) ratio 0.95,1.0 i 1 16 j 100 103
gen (0.0,34.7828) (0.0,34.9828) (15.0,34.9828) (15.0,34.7828) ratio 0.95,1.0 i 1 16 j 103 105
gen (0.0,34.9828) (0.0,35.1358) (15.0,35.1358) (15.0,34.9828) ratio 0.95,1.0 i 1 16 j 105 107
gen (15.0,0.0) (15.0,20.0) (19.699,20.0) (19.699,0.0) ratio 1.0,0.93 i 16 22 j 1 31
gen (15.0,20.0) (15.0,33.1572) (19.699,33.1572) (19.699,20.0) i 16 22 j 31 87
gen (15.0,33.1572) (15.0,33.3604) (19.699,33.3604) (19.699,33.1572) i 16 22 j 87 89
gen (15.0,33.3604) (15.0,34.2748) (19.699,34.2748) (19.699,33.3604) i 16 22 j 89 98
gen (15.0,34.2748) (15.0,34.478) (19.699,34.478) (19.699,34.2748) i 16 22 j 98 100
gen (15.0,34.478) (15.0,34.7828) (19.699,34.7828) (19.699,34.478) i 16 22 j 100 103
gen (15.0,34.7828) (15.0,34.9828) (19.699,34.9828) (19.699,34.7828) i 16 22 j 103 105
gen (15.0,34.9828) (15.0,35.1358) (19.699,35.1358) (19.699,34.9828) i 16 22 j 105 107
gen (19.699,0.0) (19.699,20.0) (42.2542,20.0) (42.2542,0.0) ratio 1.0,0.93 i 22 70 j 1 31
gen (19.699,20.0) (19.699,33.1572) (42.2542,33.1572) (42.2542,20.0) i 22 70 j 31 87
gen (19.699,33.1572) (19.699,33.3604) (42.2542,33.3604) (42.2542,33.1572) i 22 70 j 87 89
gen (19.699,33.3604) (19.699,34.2748) (42.2542,34.2748) (42.2542,33.3604) i 22 70 j 89 98
gen (19.699,34.2748) (19.699,34.478) (42.2542,34.478) (42.2542,34.2748) i 22 70 j 98 100
gen (19.699,34.478) (19.699,34.7828) (42.2542,34.7828) (42.2542,34.478) i 22 70 j 100 103
gen (19.699,34.7828) (19.699,34.9828) (42.2542,34.9828) (42.2542,34.7828) i 22 70 j 103
105
gen (19.699,34.9828) (19.699,35.1358) (42.2542,35.1358) (42.2542,34.9828) i 22 70 j 105
107
gen (42.2542,0.0) (42.2542,20.0) (43.956,20.0) (43.956,0.0) ratio 1.0,0.93 i 70 74 j 1 31
gen (42.2542,20.0) (42.2542,33.1572) (43.956,33.1572) (43.956,20.0) i 70 74 j 31 87
gen (42.2542,33.1572) (42.2542,33.3604) (43.956,33.3604) (43.956,33.1572) i 70 74 j 87 89
gen (42.2542,33.3604) (42.2542,34.2748) (43.956,34.2748) (43.956,33.3604) i 70 74 j 89 98
gen (42.2542,34.2748) (42.2542,34.478) (43.956,34.478) (43.956,34.2748) i 70 74 j 98 100
gen (42.2542,34.478) (42.2542,34.7828) (43.956,34.7828) (43.956,34.478) i 70 74 j 100 103
gen (42.2542,34.7828) (42.2542,34.9828) (43.956,34.9828) (43.956,34.7828) i 70 74 j 103
105
gen (42.2542,34.9828) (42.2542,35.1358) (43.956,35.1358) (43.956,34.9828) i 70 74 j 105
107
gen (43.956,0.0) (43.956,20.0) (44.7369,20.0) (44.7369,0.0) ratio 1.0,0.93 i 74 79 j 1 31
gen (43.956,20.0) (43.956,33.1572) (44.7369,33.1572) (44.7369,20.0) i 74 79 j 31 87
gen (43.956,33.1572) (43.956,33.3604) (44.7369,33.3604) (44.7369,33.1572) i 74 79 j 87 89
gen (43.956,33.3604) (43.956,34.2748) (44.7369,34.2748) (44.7369,33.3604) i 74 79 j 89 98
gen (43.956,34.2748) (43.956,34.478) (44.7369,34.478) (44.7369,34.2748) i 74 79 j 98 100
```

```
    gen (43.956,34.478) (43.956,34.7828) (44.7369,34.7828) (44.7369,34.478) i 74 79 j 100 103
    gen (43.956,34.7828) (43.956,34.9828) (44.7369,34.9828) (44.7369,34.7828) i 74 79 j 103
105
    gen (43.956,34.9828) (43.956,35.1358) (44.7369,35.1358) (44.7369,34.9828) i 74 79 j 105
107
    gen (44.7369,0.0) (44.7369,20.0) (45.7465,20.0) (45.7465,0.0) ratio 1.0,0.93 i 79 84 j 1 31
    gen (44.7369,20.0) (44.7369,33.1572) (45.7465,33.1572) (45.7465,20.0) i 79 84 j 31 87
    gen (44.7369,33.1572) (44.7369,33.3604) (45.7465,33.3604) (45.7465,33.1572) i 79 84 j 87
89
    gen (44.7369,33.3604) (44.7369,34.2748) (45.7465,34.2748) (45.7465,33.3604) i 79 84 j 89
98
    gen (44.7369,34.2748) (44.7369,34.478) (45.7465,34.478) (45.7465,34.2748) i 79 84 j 98
100
    gen (44.7369,34.478) (44.7369,34.7828) (45.7465,34.7828) (45.7465,34.478) i 79 84 j 100
103
    gen (44.7369,34.7828) (44.7369,34.9828) (45.7465,34.9828) (45.7465,34.7828) i 79 84 j 103
105
    gen (44.7369,34.9828) (44.7369,35.1358) (45.7465,35.1358) (45.7465,34.9828) i 79 84 j 105
107
    gen (45.7465,0.0) (45.7465,20.0) (46.13695,20.0) (46.13695,0.0) ratio 1.0,0.93 i 84 86 j 1 31
    gen (45.7465,20.0) (45.7465,33.1572) (46.13695,33.1572) (46.13695,20.0) i 84 86 j 31 87
    gen (45.7465,33.1572) (45.7465,33.3604) (46.13695,33.3604) (46.13695,33.1572) i 84 86 j
87 89
    gen (45.7465,33.3604) (45.7465,34.2748) (46.13695,34.2748) (46.13695,33.3604) i 84 86 j
89 98
    gen (45.7465,34.2748) (45.7465,34.478) (46.13695,34.478) (46.13695,34.2748) i 84 86 j 98
100
    gen (45.7465,34.478) (45.7465,34.7828) (46.13695,34.7828) (46.13695,34.478) i 84 86 j 100
103
    gen (45.7465,34.7828) (45.7465,34.9828) (46.13695,34.9828) (46.13695,34.7828) i 84 86 j
103 105
    gen (45.7465,34.9828) (45.7465,35.1358) (46.13695,35.1358) (46.13695,34.9828) i 84 86 j
105 107
    gen (46.13695,0.0) (46.13695,20.0) (46.58645,20.0) (46.58645,0.0) ratio 1.0,0.93 i 86 90 j 1
31
    gen (46.13695,20.0) (46.13695,33.1572) (46.58645,33.1572) (46.58645,20.0) i 86 90 j 31 87
    gen (46.13695,33.1572) (46.13695,33.3604) (46.58645,33.3604) (46.58645,33.1572) i 86 90
j 87 89
    gen (46.13695,33.3604) (46.13695,34.2748) (46.58645,34.2748) (46.58645,33.3604) i 86 90
j 89 98
    gen (46.13695,34.2748) (46.13695,34.478) (46.58645,34.478) (46.58645,34.2748) i 86 90 j
98 100
    gen (46.13695,34.478) (46.13695,34.7828) (46.58645,34.7828) (46.58645,34.478) i 86 90 j
100 103
    gen (46.13695,34.7828) (46.13695,34.9828) (46.58645,34.9828) (46.58645,34.7828) i 86 90
j 103 105
    gen (46.13695,34.9828) (46.13695,35.1358) (46.58645,35.1358) (46.58645,34.9828) i 86 90
j 105 107
    gen (46.58645,0.0) (46.58645,20.0) (46.66445,20.0) (46.66445,0.0) ratio 1.0,0.93 i 90 91 j 1
31
    gen (46.58645,20.0) (46.58645,33.1572) (46.66445,33.1572) (46.66445,20.0) i 90 91 j 31 87
```

```
    gen (46.58645,33.1572) (46.58645,33.3604) (46.66445,33.3604) (46.66445,33.1572) i 90 91
j 87 89
    gen (46.58645,33.3604) (46.58645,34.2748) (46.66445,34.2748) (46.66445,33.3604) i 90 91
j 89 98
    gen (46.58645,34.2748) (46.58645,34.478) (46.66445,34.478) (46.66445,34.2748) i 90 91 j
98 100
    gen (46.58645,34.478) (46.58645,34.7828) (46.66445,34.7828) (46.66445,34.478) i 90 91 j
100 103
    gen (46.58645,34.7828) (46.58645,34.9828) (46.66445,34.9828) (46.66445,34.7828) i 90 91
j 103 105
    gen (46.58645,34.9828) (46.58645,35.1358) (46.66445,35.1358) (46.66445,34.9828) i 90 91
j 105 107
    gen (46.66445,0.0) (46.66445,20.0) (48.12445,20.0) (48.12445,0.0) ratio 1.0,0.93 i 91 106 j 1
31
    gen (46.66445,20.0) (46.66445,33.1572) (48.12445,33.1572) (48.12445,20.0) i 91 106 j 31
87
    gen (46.66445,33.1572) (46.66445,33.3604) (48.12445,33.3604) (48.12445,33.1572) i 91 106
j 87 89
    gen (46.66445,33.3604) (46.66445,34.2748) (48.12445,34.2748) (48.12445,33.3604) i 91 106
j 89 98
    gen (46.66445,34.2748) (46.66445,34.478) (48.12445,34.478) (48.12445,34.2748) i 91 106 j
98 100
    gen (46.66445,34.478) (46.66445,34.7828) (48.12445,34.7828) (48.12445,34.478) i 91 106 j
100 103
    gen (46.66445,34.7828) (46.66445,34.9828) (48.12445,34.9828) (48.12445,34.7828) i 91 106
j 103 105
    gen (46.66445,34.9828) (46.66445,35.1358) (48.12445,35.1358) (48.12445,34.9828) i 91 106
j 105 107
    gen (48.12445,0.0) (48.12445,20.0) (48.20245,20.0) (48.20245,0.0) ratio 1.0,0.93 i 106 107 j
1 31
    gen (48.12445,20.0) (48.12445,33.1572) (48.20245,33.1572) (48.20245,20.0) i 106 107 j 31
87
    gen (48.12445,33.1572) (48.12445,33.3604) (48.20245,33.3604) (48.20245,33.1572) i 106
107 j 87 89
    gen (48.12445,33.3604) (48.12445,34.2748) (48.20245,34.2748) (48.20245,33.3604) i 106
107 j 89 98
    gen (48.12445,34.2748) (48.12445,34.478) (48.20245,34.478) (48.20245,34.2748) i 106 107
j 98 100
    gen (48.12445,34.478) (48.12445,34.7828) (48.20245,34.7828) (48.20245,34.478) i 106 107
j 100 103
    gen (48.12445,34.7828) (48.12445,34.9828) (48.20245,34.9828) (48.20245,34.7828) i 106
107 j 103 105
    gen (48.12445,34.9828) (48.12445,35.1358) (48.20245,35.1358) (48.20245,34.9828) i 106
107 j 105 107
    gen (48.20245,0.0) (48.20245,20.0) (48.65795,20.0) (48.65795,0.0) ratio 1.0,0.93 i 107 111 j
1 31
    gen (48.20245,20.0) (48.20245,33.1572) (48.65795,33.1572) (48.65795,20.0) i 107 111 j 31
87
    gen (48.20245,33.1572) (48.20245,33.3604) (48.65795,33.3604) (48.65795,33.1572) i 107
111 j 87 89
    gen (48.20245,33.3604) (48.20245,34.2748) (48.65795,34.2748) (48.65795,33.3604) i 107
```

```
111 j 89 98
    gen (48.20245,34.2748) (48.20245,34.478) (48.65795,34.478) (48.65795,34.2748) i 107 111
j 98 100
    gen (48.20245,34.478) (48.20245,34.7828) (48.65795,34.7828) (48.65795,34.478) i 107 111
j 100 103
    gen (48.20245,34.7828) (48.20245,34.9828) (48.65795,34.9828) (48.65795,34.7828) i 107
111 j 103 105
    gen (48.20245,34.9828) (48.20245,35.1358) (48.65795,35.1358) (48.65795,34.9828) i 107
111 j 105 107
    gen (48.65795,0.0) (48.65795,20.0) (49.0424,20.0) (49.0424,0.0) ratio 1.0,0.93 i 111 113 j 1
31
    gen (48.65795,20.0) (48.65795,33.1572) (49.0424,33.1572) (49.0424,20.0) i 111 113 j 31 87
    gen (48.65795,33.1572) (48.65795,33.3604) (49.0424,33.3604) (49.0424,33.1572) i 111 113
j 87 89
    gen (48.65795,33.3604) (48.65795,34.2748) (49.0424,34.2748) (49.0424,33.3604) i 111 113
j 89 98
    gen (48.65795,34.2748) (48.65795,34.478) (49.0424,34.478) (49.0424,34.2748) i 111 113 j
98 100
    gen (48.65795,34.478) (48.65795,34.7828) (49.0424,34.7828) (49.0424,34.478) i 111 113 j
100 103
    gen (48.65795,34.7828) (48.65795,34.9828) (49.0424,34.9828) (49.0424,34.7828) i 111 113
j 103 105
    gen (48.65795,34.9828) (48.65795,35.1358) (49.0424,35.1358) (49.0424,34.9828) i 111 113
j 105 107
    gen (49.0424,0.0) (49.0424,20.0) (50.3185,20.0) (50.3185,0.0) ratio 1.0,0.93 i 113 119 j 1 31
    gen (49.0424,20.0) (49.0424,33.1572) (50.3185,33.1572) (50.3185,20.0) i 113 119 j 31 87
    gen (49.0424,33.1572) (49.0424,33.3604) (50.3185,33.3604) (50.3185,33.1572) i 113 119 j
87 89
    gen (49.0424,33.3604) (49.0424,34.2748) (50.3185,34.2748) (50.3185,33.3604) i 113 119 j
89 98
    gen (49.0424,34.2748) (49.0424,34.478) (50.3185,34.478) (50.3185,34.2748) i 113 119 j 98
100
    gen (49.0424,34.478) (49.0424,34.7828) (50.3185,34.7828) (50.3185,34.478) i 113 119 j 100
103
    gen (49.0424,34.7828) (49.0424,34.9828) (50.3185,34.9828) (50.3185,34.7828) i 113 119 j
103 105
    gen (49.0424,34.9828) (49.0424,35.1358) (50.3185,35.1358) (50.3185,34.9828) i 113 119 j
105 107
    gen (50.3185,0.0) (50.3185,20.0) (50.70895,20.0) (50.70895,0.0) ratio 1.0,0.93 i 119 121 j 1
31
    gen (50.3185,20.0) (50.3185,33.1572) (50.70895,33.1572) (50.70895,20.0) i 119 121 j 31 87
    gen (50.3185,33.1572) (50.3185,33.3604) (50.70895,33.3604) (50.70895,33.1572) i 119 121
j 87 89
    gen (50.3185,33.3604) (50.3185,34.2748) (50.70895,34.2748) (50.70895,33.3604) i 119 121
j 89 98
    gen (50.3185,34.2748) (50.3185,34.478) (50.70895,34.478) (50.70895,34.2748) i 119 121 j
98 100
    gen (50.3185,34.478) (50.3185,34.7828) (50.70895,34.7828) (50.70895,34.478) i 119 121 j
100 103
    gen (50.3185,34.7828) (50.3185,34.9828) (50.70895,34.9828) (50.70895,34.7828) i 119 121
j 103 105
```

gen (50.3185,34.9828) (50.3185,35.1358) (50.70895,35.1358) (50.70895,34.9828) i 119 121 j 105 107
gen (50.70895,0.0) (50.70895,20.0) (51.15845,20.0) (51.15845,0.0) ratio 1.0,0.93 i 121 125 j 1 31
gen (50.70895,20.0) (50.70895,33.1572) (51.15845,33.1572) (51.15845,20.0) i 121 125 j 31 87
gen (50.70895,33.1572) (50.70895,33.3604) (51.15845,33.3604) (51.15845,33.1572) i 121 125 j 87 89
gen (50.70895,33.3604) (50.70895,34.2748) (51.15845,34.2748) (51.15845,33.3604) i 121 125 j 89 98
gen (50.70895,34.2748) (50.70895,34.478) (51.15845,34.478) (51.15845,34.2748) i 121 125 j 98 100
gen (50.70895,34.478) (50.70895,34.7828) (51.15845,34.7828) (51.15845,34.478) i 121 125 j 100 103
gen (50.70895,34.7828) (50.70895,34.9828) (51.15845,34.9828) (51.15845,34.7828) i 121 125 j 103 105
gen (50.70895,34.9828) (50.70895,35.1358) (51.15845,35.1358) (51.15845,34.9828) i 121 125 j 105 107
gen (51.15845,0.0) (51.15845,20.0) (51.23645,20.0) (51.23645,0.0) ratio 1.0,0.93 i 125 126 j 1 31
gen (51.15845,20.0) (51.15845,33.1572) (51.23645,33.1572) (51.23645,20.0) i 125 126 j 31 87
gen (51.15845,33.1572) (51.15845,33.3604) (51.23645,33.3604) (51.23645,33.1572) i 125 126 j 87 89
gen (51.15845,33.3604) (51.15845,34.2748) (51.23645,34.2748) (51.23645,33.3604) i 125 126 j 89 98
gen (51.15845,34.2748) (51.15845,34.478) (51.23645,34.478) (51.23645,34.2748) i 125 126 j 98 100
gen (51.15845,34.478) (51.15845,34.7828) (51.23645,34.7828) (51.23645,34.478) i 125 126 j 100 103
gen (51.15845,34.7828) (51.15845,34.9828) (51.23645,34.9828) (51.23645,34.7828) i 125 126 j 103 105
gen (51.15845,34.9828) (51.15845,35.1358) (51.23645,35.1358) (51.23645,34.9828) i 125 126 j 105 107
gen (51.23645,0.0) (51.23645,20.0) (52.69645,20.0) (52.69645,0.0) ratio 1.0,0.93 i 126 141 j 1 31
gen (51.23645,20.0) (51.23645,33.1572) (52.69645,33.1572) (52.69645,20.0) i 126 141 j 31 87
gen (51.23645,33.1572) (51.23645,33.3604) (52.69645,33.3604) (52.69645,33.1572) i 126 141 j 87 89
gen (51.23645,33.3604) (51.23645,34.2748) (52.69645,34.2748) (52.69645,33.3604) i 126 141 j 89 98
gen (51.23645,34.2748) (51.23645,34.478) (52.69645,34.478) (52.69645,34.2748) i 126 141 j 98 100
gen (51.23645,34.478) (51.23645,34.7828) (52.69645,34.7828) (52.69645,34.478) i 126 141 j 100 103
gen (51.23645,34.7828) (51.23645,34.9828) (52.69645,34.9828) (52.69645,34.7828) i 126 141 j 103 105
gen (51.23645,34.9828) (51.23645,35.1358) (52.69645,35.1358) (52.69645,34.9828) i 126 141 j 105 107
gen (52.69645,0.0) (52.69645,20.0) (52.77445,20.0) (52.77445,0.0) ratio 1.0,0.93 i 141 142 j

```
1 31
    gen (52.69645,20.0) (52.69645,33.1572) (52.77445,33.1572) (52.77445,20.0) i 141 142 j 31
87
    gen (52.69645,33.1572) (52.69645,33.3604) (52.77445,33.3604) (52.77445,33.1572) i 141
142 j 87 89
    gen (52.69645,33.3604) (52.69645,34.2748) (52.77445,34.2748) (52.77445,33.3604) i 141
142 j 89 98
    gen (52.69645,34.2748) (52.69645,34.478) (52.77445,34.478) (52.77445,34.2748) i 141 142
j 98 100
    gen (52.69645,34.478) (52.69645,34.7828) (52.77445,34.7828) (52.77445,34.478) i 141 142
j 100 103
    gen (52.69645,34.7828) (52.69645,34.9828) (52.77445,34.9828) (52.77445,34.7828) i 141
142 j 103 105
    gen (52.69645,34.9828) (52.69645,35.1358) (52.77445,35.1358) (52.77445,34.9828) i 141
142 j 105 107
    gen (52.77445,0.0) (52.77445,20.0) (53.22395,20.0) (53.22395,0.0) ratio 1.0,0.93 i 142 146 j
1 31
    gen (52.77445,20.0) (52.77445,33.1572) (53.22395,33.1572) (53.22395,20.0) i 142 146 j 31
87
    gen (52.77445,33.1572) (52.77445,33.3604) (53.22395,33.3604) (53.22395,33.1572) i 142
146 j 87 89
    gen (52.77445,33.3604) (52.77445,34.2748) (53.22395,34.2748) (53.22395,33.3604) i 142
146 j 89 98
    gen (52.77445,34.2748) (52.77445,34.478) (53.22395,34.478) (53.22395,34.2748) i 142 146
j 98 100
    gen (52.77445,34.478) (52.77445,34.7828) (53.22395,34.7828) (53.22395,34.478) i 142 146
j 100 103
    gen (52.77445,34.7828) (52.77445,34.9828) (53.22395,34.9828) (53.22395,34.7828) i 142
146 j 103 105
    gen (52.77445,34.9828) (52.77445,35.1358) (53.22395,35.1358) (53.22395,34.9828) i 142
146 j 105 107
    gen (53.22395,0.0) (53.22395,20.0) (53.6144,20.0) (53.6144,0.0) ratio 1.0,0.93 i 146 148 j 1
31
    gen (53.22395,20.0) (53.22395,33.1572) (53.6144,33.1572) (53.6144,20.0) i 146 148 j 31 87
    gen (53.22395,33.1572) (53.22395,33.3604) (53.6144,33.3604) (53.6144,33.1572) i 146 148
j 87 89
    gen (53.22395,33.3604) (53.22395,34.2748) (53.6144,34.2748) (53.6144,33.3604) i 146 148
j 89 98
    gen (53.22395,34.2748) (53.22395,34.478) (53.6144,34.478) (53.6144,34.2748) i 146 148 j
98 100
    gen (53.22395,34.478) (53.22395,34.7828) (53.6144,34.7828) (53.6144,34.478) i 146 148 j
100 103
    gen (53.22395,34.7828) (53.22395,34.9828) (53.6144,34.9828) (53.6144,34.7828) i 146 148
j 103 105
    gen (53.22395,34.9828) (53.22395,35.1358) (53.6144,35.1358) (53.6144,34.9828) i 146 148
j 105 107
    gen (53.6144,0.0) (53.6144,20.0) (55.4049,20.0) (55.4049,0.0) ratio 1.0,0.93 i 148 157 j 1 31
    gen (53.6144,20.0) (53.6144,33.1572) (55.4049,33.1572) (55.4049,20.0) i 148 157 j 31 87
    gen (53.6144,33.1572) (53.6144,33.3604) (55.4049,33.3604) (55.4049,33.1572) i 148 157 j
87 89
    gen (53.6144,33.3604) (53.6144,34.2748) (55.4049,34.2748) (55.4049,33.3604) i 148 157 j
```

```
89 98
    gen (53.6144,34.2748) (53.6144,34.478) (55.4049,34.478) (55.4049,34.2748) i 148 157 j 98
100
    gen (53.6144,34.478) (53.6144,34.7828) (55.4049,34.7828) (55.4049,34.478) i 148 157 j 100
103
    gen (53.6144,34.7828) (53.6144,34.9828) (55.4049,34.9828) (55.4049,34.7828) i 148 157 j
103 105
    gen (53.6144,34.9828) (53.6144,35.1358) (55.4049,35.1358) (55.4049,34.9828) i 148 157 j
105 107
    gen (55.4049,0.0) (55.4049,20.0) (57.1067,20.0) (57.1067,0.0) ratio 1.0,0.93 i 157 161 j 1 31
    gen (55.4049,20.0) (55.4049,33.1572) (57.1067,33.1572) (57.1067,20.0) i 157 161 j 31 87
    gen (55.4049,33.1572) (55.4049,33.3604) (57.1067,33.3604) (57.1067,33.1572) i 157 161 j
87 89
    gen (55.4049,33.3604) (55.4049,34.2748) (57.1067,34.2748) (57.1067,33.3604) i 157 161 j
89 98
    gen (55.4049,34.2748) (55.4049,34.478) (57.1067,34.478) (57.1067,34.2748) i 157 161 j 98
100
    gen (55.4049,34.478) (55.4049,34.7828) (57.1067,34.7828) (57.1067,34.478) i 157 161 j 100
103
    gen (55.4049,34.7828) (55.4049,34.9828) (57.1067,34.9828) (57.1067,34.7828) i 157 161 j
103 105
    gen (55.4049,34.9828) (55.4049,35.1358) (57.1067,35.1358) (57.1067,34.9828) i 157 161 j
105 107
    gen (57.1067,0.0) (57.1067,20.0) (59.9261,20.0) (59.9261,0.0) ratio 1.0,0.93 i 161 167 j 1 31
    gen (57.1067,20.0) (57.1067,33.1572) (59.9261,33.1572) (59.9261,20.0) i 161 167 j 31 87
    gen (57.1067,33.1572) (57.1067,33.3604) (59.9261,33.3604) (59.9261,33.1572) i 161 167 j
87 89
    gen (57.1067,33.3604) (57.1067,34.2748) (59.9261,34.2748) (59.9261,33.3604) i 161 167 j
89 98
    gen (57.1067,34.2748) (57.1067,34.478) (59.9261,34.478) (59.9261,34.2748) i 161 167 j 98
100
    gen (57.1067,34.478) (57.1067,34.7828) (59.9261,34.7828) (59.9261,34.478) i 161 167 j 100
103
    gen (57.1067,34.7828) (57.1067,34.9828) (59.9261,34.9828) (59.9261,34.7828) i 161 167 j
103 105
    gen (57.1067,34.9828) (57.1067,35.1358) (59.9261,35.1358) (59.9261,34.9828) i 161 167 j
105 107
    gen (59.9261,0.0) (59.9261,20.0) (118.6713,20.0) (118.6713,0.0) ratio 1.05,0.93 i 167 217 j 1
31
    gen (59.9261,20.0) (59.9261,33.1572) (118.6713,33.1572) (118.6713,20.0) ratio 1.05,1.0 i
167 217 j 31 87
    gen (59.9261,33.1572) (59.9261,33.3604) (118.6713,33.3604) (118.6713,33.1572) ratio
1.05,1.0 i 167 217 j 87 89
    gen (59.9261,33.3604) (59.9261,34.2748) (118.6713,34.2748) (118.6713,33.3604) ratio
1.05,1.0 i 167 217 j 89 98
    gen (59.9261,34.2748) (59.9261,34.478) (118.6713,34.478) (118.6713,34.2748) ratio
1.05,1.0 i 167 217 j 98 100
    gen (59.9261,34.478) (59.9261,34.7828) (118.6713,34.7828) (118.6713,34.478) ratio
1.05,1.0 i 167 217 j 100 103
    gen (59.9261,34.7828) (59.9261,34.9828) (118.6713,34.9828) (118.6713,34.7828) ratio
1.05,1.0 i 167 217 j 103 105
```

```
gen (59.9261,34.9828) (59.9261,35.1358) (118.6713,35.1358) (118.6713,34.9828) ratio
1.05,1.0 i 167 217 j 105 107
model elastic i=1,216 j=1,106
;delete excessive grids
model null i 1 18 j 105 106
group 'null' i 1 18 j 105 106
group delete 'null'
model null i 19 49 j 105 106
group 'null' i 19 49 j 105 106
group delete 'null'
model null i 50 85 j 105 106
group 'null' i 50 85 j 105 106
group delete 'null'
model null i 86 89 j 105 106
group 'null' i 86 89 j 105 106
group delete 'null'
model null i 91 105 j 105 106
group 'null' i 91 105 j 105 106
group delete 'null'
model null i 107 121 j 105 106
group 'null' i 107 121 j 105 106
group delete 'null'
model null i 122 124 j 105 106
group 'null' i 122 124 j 105 106
group delete 'null'
model null i 126 140 j 105 106
group 'null' i 126 140 j 105 106
group delete 'null'
model null i 142 156 j 105 106
group 'null' i 142 156 j 105 106
group delete 'null'
model null i 157 178 j 105 106
group 'null' i 157 178 j 105 106
group delete 'null'
model null i 179 192 j 105 106
group 'null' i 179 192 j 105 106
group delete 'null'
model null i 193 205 j 105 106
group 'null' i 193 205 j 105 106
group delete 'null'
model null i 207 j 105
group 'null' i 207 j 105
group delete 'null'
model null i 206 215 j 105 106
group 'null' i 206 215 j 105 106
group delete 'null'
model null i 216 j 105 106
group 'null' i 216 j 105 106
group delete 'null'
model null i 73 78 j 103 104
group 'null' i 73 78 j 103 104
```

```
group delete 'null'
model null i 54 72 j 103 104
group 'null' i 54 72 j 103 104
group delete 'null'
model null i 24 53 j 103 104
group 'null' i 24 53 j 103 104
group delete 'null'
model null i 1 23 j 103 104
group 'null' i 1 23 j 103 104
group delete 'null'
model null i 71 78 j 100 102
group 'null' i 71 78 j 100 102
group delete 'null'
model null i 37 70 j 100 102
group 'null' i 37 70 j 100 102
group delete 'null'
model null i 9 36 j 100 102
group 'null' i 9 36 j 100 102
group delete 'null'
model null i 1 8 j 100 102
group 'null' i 1 8 j 100 102
group delete 'null'
model null i 155 160 j 100 104
group 'null' i 155 160 j 100 104
group delete 'null'
model null i 153 154 j 100 104
group 'null' i 153 154 j 100 104
group delete 'null'
model null i 161 166 j 100 104
group 'null' i 161 166 j 100 104
group delete 'null'
model null i 64 j 87 99
group 'null' i 64 j 87 99
group delete 'null'
model null i 65 j 87 99
group 'null' i 65 j 87 99
group delete 'null'
model null i 17 63 j 87 99
group 'null' i 17 63 j 87 99
group delete 'null'
model null i 1 16 j 87 99
group 'null' i 1 16 j 87 99
group delete 'null'
model null i 58 61 j 83 86
group 'null' i 58 61 j 83 86
group delete 'null'
model null i 54 57 j 79 82
group 'null' i 54 57 j 79 82
group delete 'null'
model null i 51 57 j 79 86
group 'null' i 51 57 j 79 86
```

```
group delete 'null'
model null i 51 53 j 75 78
group 'null' i 51 53 j 75 78
group delete 'null'
model null i 35 50 j 75 86
group 'null' i 35 50 j 75 86
group delete 'null'
model null i 44 49 j 71 74
group 'null' i 44 49 j 71 74
group delete 'null'
model null i 36 45 j 67 70
group 'null' i 36 45 j 67 70
group delete 'null'
model null i 34 41 j 63 66
group 'null' i 34 41 j 63 66
group delete 'null'
model null i 30 37 j 59 62
group 'null' i 30 37 j 59 62
group delete 'null'
model null i 26 33 j 55 58
group 'null' i 26 33 j 55 58
group delete 'null'
model null i 25 29 j 51 54
group 'null' i 25 29 j 51 54
group delete 'null'
model null i 35 43 j 71 74
group 'null' i 35 43 j 71 74
group delete 'null'
model null i 25 35 j 63 70
group 'null' i 25 35 j 63 70
group delete 'null'
model null i 19 34 j 60 86
group 'null' i 19 34 j 60 86
group delete 'null'
model null i 19 29 j 51 59
group 'null' i 19 29 j 51 59
group delete 'null'
model null i 22 25 j 47 50
group 'null' i 22 25 j 47 50
group delete 'null'
model null i 18 21 j 43 46
group 'null' i 18 21 j 43 46
group delete 'null'
model null i 18 21 j 47 50
group 'null' i 18 21 j 47 50
group delete 'null'
model null i 13 17 j 39 42
group 'null' i 13 17 j 39 42
group delete 'null'
model null i 6 17 j 43 86
group 'null' i 6 17 j 43 86
```

```
group delete 'null'
model null i 18 j 51 86
group 'null' i 18 j 51 86
group delete 'null'
model null i 9 13 j 35 38
group 'null' i 9 13 j 35 38
group delete 'null'
model null i 7 9 j 31 34
group 'null' i 7 9 j 31 34
group delete 'null'
model null i 6 12 j 35 42
group 'null' i 6 12 j 35 42
group delete 'null'
model null i 6 j 31 34
group 'null' i 6 j 31 34
group delete 'null'
model null i 1 5 j 31 86
group 'null' i 1 5 j 31 86
;alter shape
gen 44.7369,34.478 45.7465,34.9828 46.13695,34.9828 46.13695,34.478 ratio
0.9963045,0.9960688 i 79 86 j 100 105
model null i 66 67 j 87
group 'null' i 66 67 j 87
group delete 'null'
model null i 66 67 j 88
group 'null' i 66 67 j 88
group delete 'null'
model null i 66 68 j 89 90
group 'null' i 66 68 j 89 90
group delete 'null'
model null i 66 69 j 91 92
group 'null' i 66 69 j 91 92
group delete 'null'
model null i 66 70 j 93 94
group 'null' i 66 70 j 93 94
group delete 'null'
model null i 66 71 j 95 96
group 'null' i 66 71 j 95 96
group delete 'null'
model null i 66 72 j 97 98
group 'null' i 66 72 j 97 98
group delete 'null'
model null i 66 73 j 99
group 'null' i 66 73 j 99
group delete 'null'
model null i 62 66 j 86
group 'null' i 62 66 j 86
group delete 'null'
model null i 62 65 j 85
group 'null' i 62 65 j 85
group delete 'null'
```

```
model null i 62 64 j 84
group 'null' i 62 64 j 84
group delete 'null'
model null i 62 63 j 83
group 'null' i 62 63 j 83
group delete 'null'
model null i 58 62 j 82
group 'null' i 58 62 j 82
group delete 'null'
model null i 58 61 j 81
group 'null' i 58 61 j 81
group delete 'null'
model null i 58 60 j 80
group 'null' i 58 60 j 80
group delete 'null'
model null i 58 59 j 79
group 'null' i 58 59 j 79
group delete 'null'
model null i 54 58 j 78
group 'null' i 54 58 j 78
group delete 'null'
model null i 54 57 j 77
group 'null' i 54 57 j 77
group delete 'null'
model null i 54 56 j 76
group 'null' i 54 56 j 76
group delete 'null'
model null i 54 55 j 75
group 'null' i 54 55 j 75
group delete 'null'
model null i 50 54 j 74
group 'null' i 50 54 j 74
group delete 'null'
model null i 50 53 j 73
group 'null' i 50 53 j 73
group delete 'null'
model null i 50 52 j 72
group 'null' i 50 52 j 72
group delete 'null'
model null i 50 51 j 71
group 'null' i 50 51 j 71
group delete 'null'
model null i 46 50 j 70
group 'null' i 46 50 j 70
group delete 'null'
model null i 46 49 j 69
group 'null' i 46 49 j 69
group delete 'null'
model null i 46 48 j 68
group 'null' i 46 48 j 68
group delete 'null'
```

```
model null i 46 47 j 67
group 'null' i 46 47 j 67
group delete 'null'
model null i 42 46 j 66
group 'null' i 42 46 j 66
group delete 'null'
model null i 42 45 j 65
group 'null' i 42 45 j 65
group delete 'null'
model null i 42 44 j 64
group 'null' i 42 44 j 64
group delete 'null'
model null i 42 43 j 63
group 'null' i 42 43 j 63
group delete 'null'
model null i 38 42 j 62
group 'null' i 38 42 j 62
group delete 'null'
model null i 38 41 j 61
group 'null' i 38 41 j 61
group delete 'null'
model null i 40 j 60
group 'null' i 40 j 60
group delete 'null'
model null i 38 39 j 60
group 'null' i 38 39 j 60
group delete 'null'
model null i 38 39 j 59
group 'null' i 38 39 j 59
group delete 'null'
model null i 34 38 j 58
group 'null' i 34 38 j 58
group delete 'null'
model null i 34 37 j 57
group 'null' i 34 37 j 57
group delete 'null'
model null i 34 36 j 56
group 'null' i 34 36 j 56
group delete 'null'
model null i 34 35 j 55
group 'null' i 34 35 j 55
group delete 'null'
model null i 30 34 j 54
group 'null' i 30 34 j 54
group delete 'null'
model null i 30 33 j 53
group 'null' i 30 33 j 53
group delete 'null'
model null i 30 32 j 52
group 'null' i 30 32 j 52
group delete 'null'
```

```
model null i 30 31 j 51
group 'null' i 30 31 j 51
group delete 'null'
model null i 26 30 j 50
group 'null' i 26 30 j 50
group delete 'null'
model null i 26 29 j 49
group 'null' i 26 29 j 49
group delete 'null'
model null i 26 28 j 48
group 'null' i 26 28 j 48
group delete 'null'
model null i 26 27 j 47
group 'null' i 26 27 j 47
group delete 'null'
model null i 22 26 j 46
group 'null' i 22 26 j 46
group delete 'null'
model null i 22 25 j 45
group 'null' i 22 25 j 45
group delete 'null'
model null i 22 24 j 44
group 'null' i 22 24 j 44
group delete 'null'
model null i 22 23 j 43
group 'null' i 22 23 j 43
group delete 'null'
model null i 18 22 j 42
group 'null' i 18 22 j 42
group delete 'null'
model null i 18 21 j 41
group 'null' i 18 21 j 41
group delete 'null'
model null i 10 15 j 31
group 'null' i 10 15 j 31
group delete 'null'
model null i 10 15 j 32 34
group 'null' i 10 15 j 32 34
group delete 'null'
model null i 16 j 33 34
group 'null' i 16 j 33 34
group delete 'null'
model null i 14 17 j 35 36
group 'null' i 14 17 j 35 36
group delete 'null'
model null i 14 18 j 37 38
group 'null' i 14 18 j 37 38
group delete 'null'
model null i 18 19 j 39 40
group 'null' i 18 19 j 39 40
group delete 'null'
```

```
model null i 20 j 40
group 'null' i 20 j 40
group delete 'null'
model null i 20 j 39
group 'null' i 20 j 39
group delete 'null'
model null i 19 j 37 38
group 'null' i 19 j 37 38
group delete 'null'
model null i 18 j 35 36
group 'null' i 18 j 35 36
group delete 'null'
model null i 17 j 34
group 'null' i 17 j 34
group delete 'null'
gen 49.0424,34.478 49.0424,34.9828 49.68045,34.663776 49.68045,34.478 ratio
0.999973,0.9960688 i 113 116 j 100 105
gen 49.68045,34.478 49.68045,34.663776 50.3185,34.9828 50.3185,34.478 ratio
0.9960738,0.99554783 i 116 119 j 100 105
gen 53.22395,34.478 53.22395,34.9828 53.6144,34.9828 54.609123,34.478 ratio
1.0041904,0.9960688 i 146 153 j 100 105
model null i 163 165 j 87
group 'null' i 163 165 j 87
group delete 'null'
model null i 163 165 j 88
group 'null' i 163 165 j 88
group delete 'null'
model null i 162 165 j 89 90
group 'null' i 162 165 j 89 90
group delete 'null'
model null i 161 164 j 91 92
group 'null' i 161 164 j 91 92
group delete 'null'
model null i 160 164 j 93 94
group 'null' i 160 164 j 93 94
group delete 'null'
model null i 159 164 j 95 96
group 'null' i 159 164 j 95 96
group delete 'null'
model null i 158 164 j 97 98
group 'null' i 158 164 j 97 98
group delete 'null'
model null i 157 j 99
group 'null' i 157 j 99
group delete 'null'
model null i 158 166 j 98 99
group 'null' i 158 166 j 98 99
group delete 'null'
model null i 165 166 j 87 97
group 'null' i 165 166 j 87 97
group delete 'null'
```

```
model null i 166 j 84
group 'null' i 166 j 84
group delete 'null'
model null i 165 166 j 85 86
group 'null' i 165 166 j 85 86
group delete 'null'
model null i 164 j 86
group 'null' i 164 j 86
group delete 'null'
; last step to finish grid generation
gen 59.9261,32.45235 66.2378,34.9828 74.26906,34.9828 74.26906,32.45235 ratio
1.05,0.9671929 i 167 193 j 84 105
model null i 211 216 j 31 104
group 'null' i 211 216 j 31 104
group delete 'null'
model null i 194 210 j 99 104
group 'null' i 194 210 j 99 104
group delete 'null'
model null i 195 210 j 92 98
group 'null' i 195 210 j 92 98
group delete 'null'
model null i 197 210 j 86 91
group 'null' i 197 210 j 86 91
group delete 'null'
model null i 198 210 j 83 85
group 'null' i 198 210 j 83 85
group delete 'null'
model null i 199 210 j 79 82
group 'null' i 199 210 j 79 82
group delete 'null'
model null i 200 210 j 76 78
group 'null' i 200 210 j 76 78
group delete 'null'
model null i 201 210 j 73 75
group 'null' i 201 210 j 73 75
group delete 'null'
model null i 202 210 j 68 72
group 'null' i 202 210 j 68 72
group delete 'null'
model null i 203 210 j 64 67
group 'null' i 203 210 j 64 67
group delete 'null'
model null i 204 210 j 61 63
group 'null' i 204 210 j 61 63
group delete 'null'
model null i 205 210 j 58 60
group 'null' i 205 210 j 58 60
group delete 'null'
model null i 206 210 j 54 57
group 'null' i 206 210 j 54 57
group delete 'null'
```

```
model null i 207 210 j 50 53
group 'null' i 207 210 j 50 53
group delete 'null'
model null i 208 210 j 45 49
group 'null' i 208 210 j 45 49
group delete 'null'
model null i 209 210 j 41 44
group 'null' i 209 210 j 41 44
group delete 'null'
model null i 210 j 36 40
group 'null' i 210 j 36 40
group delete 'null'
;assign properties
group 'User:rail' i 90 j 105 106
model elastic group 'User:rail'
prop density=7842.0 bulk=1.75E11 shear=8.07692E10 group 'User:rail'
group 'User:rail' i 106 j 105 106
model elastic group 'User:rail'
prop density=7842.0 bulk=1.75E11 shear=8.07692E10 group 'User:rail'
group 'User:rail' i 125 j 105 106
model elastic group 'User:rail'
prop density=7842.0 bulk=1.75E11 shear=8.07692E10 group 'User:rail'
group 'User:rail' i 141 j 105 106
model elastic group 'User:rail'
prop density=7842.0 bulk=1.75E11 shear=8.07692E10 group 'User:rail'
group 'User:sleeper' i 86 110 j 103 104
model elastic group 'User:sleeper'
prop density=2398.0 bulk=9.6667E9 shear=4.4615E9 group 'User:sleeper'
group 'User:sleeper' i 121 145 j 103 104
model elastic group 'User:sleeper'
prop density=2398.0 bulk=9.6667E9 shear=4.4615E9 group 'User:sleeper'
group 'User:ballast' i 79 115 j 100 102
model elastic group 'User:ballast'
prop density=2002 bulk=1.3750E8 shear=6.3462E7 group 'User:ballast'
group 'User:ballast' i 79 85 j 103 104
model elastic group 'User:ballast'
prop density=2002 bulk=1.3750E8 shear=6.3462E7 group 'User:ballast'
group 'User:ballast' i 111 115 j 103 104
model elastic group 'User:ballast'
prop density=2002 bulk=1.3750E8 shear=6.3462E7 group 'User:ballast'
group 'User:ballast' i 116 120 j 100 104
model elastic group 'User:ballast'
prop density=2002 bulk=1.3750E8 shear=6.3462E7 group 'User:ballast'
group 'User:ballast' i 121 145 j 100 102
model elastic group 'User:ballast'
prop density=2002 bulk=1.3750E8 shear=6.3462E7 group 'User:ballast'
group 'User:ballast' i 146 152 j 100 104
model elastic group 'User:ballast'
prop density=2002 bulk=1.3750E8 shear=6.3462E7 group 'User:ballast'
group 'User:sub-ballast' notnull i 74 157 j 98 99
model elastic notnull group 'User:sub-ballast'
```

```
prop density=2002 bulk=2.16667E9 shear=4.36242E7 notnull group 'User:sub-ballast'
group 'User:sub-ballast' i 73 j 98
model elastic group 'User:sub-ballast'
prop density=2002 bulk=2.16667E9 shear=4.36242E7 group 'User:sub-ballast'
group 'User:Structural Fill' notnull i 69 157 j 89 97
model elastic notnull group 'User:Structural Fill'
prop density=1922.2 bulk=3.33333E8 shear=1.53846E8 notnull group 'User:Structural Fill'
group 'User:Structural Fill' notnull i 158 161 j 89 96
model elastic notnull group 'User:Structural Fill'
prop density=1922.2 bulk=3.33333E8 shear=1.53846E8 notnull group 'User:Structural Fill'
group 'User:Structural Fill' i 68 76 j 87 88
model elastic group 'User:Structural Fill'
prop density=1922.2 bulk=3.33333E8 shear=1.53846E8 group 'User:Structural Fill'
group 'User:Structural Fill' i 155 162 j 87 88
model elastic group 'User:Structural Fill'
prop density=1922.2 bulk=3.33333E8 shear=1.53846E8 group 'User:Structural Fill'
group 'User:Structural Fill' notnull i 163 165 j 84 86
model elastic notnull group 'User:Structural Fill'
prop density=1922.2 bulk=3.33333E8 shear=1.53846E8 notnull group 'User:Structural Fill'
group 'User:Structural Fill' i 163 164 j 83
model elastic group 'User:Structural Fill'
prop density=1922.2 bulk=3.33333E8 shear=1.53846E8 group 'User:Structural Fill'
group 'User:Structural Fill' notnull i 64 69 j 83 86
model elastic notnull group 'User:Structural Fill'
prop density=1922.2 bulk=3.33333E8 shear=1.53846E8 notnull group 'User:Structural Fill'
group 'User:Structural Fill' notnull i 60 65 j 79 82
model elastic notnull group 'User:Structural Fill'
prop density=1922.2 bulk=3.33333E8 shear=1.53846E8 notnull group 'User:Structural Fill'
group 'User:Structural Fill' notnull i 56 61 j 75 78
model elastic notnull group 'User:Structural Fill'
prop density=1922.2 bulk=3.33333E8 shear=1.53846E8 notnull group 'User:Structural Fill'
group 'User:Structural Fill' notnull i 52 57 j 71 74
model elastic notnull group 'User:Structural Fill'
prop density=1922.2 bulk=3.33333E8 shear=1.53846E8 notnull group 'User:Structural Fill'
group 'User:Structural Fill' notnull i 48 53 j 67 70
model elastic notnull group 'User:Structural Fill'
prop density=1922.2 bulk=3.33333E8 shear=1.53846E8 notnull group 'User:Structural Fill'
group 'User:Structural Fill' notnull i 44 49 j 63 66
model elastic notnull group 'User:Structural Fill'
prop density=1922.2 bulk=3.33333E8 shear=1.53846E8 notnull group 'User:Structural Fill'
group 'User:Structural Fill' notnull i 40 45 j 59 62
model elastic notnull group 'User:Structural Fill'
prop density=1922.2 bulk=3.33333E8 shear=1.53846E8 notnull group 'User:Structural Fill'
group 'User:Structural Fill' notnull i 36 41 j 55 58
model elastic notnull group 'User:Structural Fill'
prop density=1922.2 bulk=3.33333E8 shear=1.53846E8 notnull group 'User:Structural Fill'
group 'User:Structural Fill' notnull i 32 37 j 51 54
model elastic notnull group 'User:Structural Fill'
prop density=1922.2 bulk=3.33333E8 shear=1.53846E8 notnull group 'User:Structural Fill'
group 'User:Structural Fill' notnull i 28 33 j 47 50
model elastic notnull group 'User:Structural Fill'
```

```
prop density=1922.2 bulk=3.33333E8 shear=1.53846E8 notnull group 'User:Structural Fill'
group 'User:Structural Fill' notnull i 24 29 j 43 46
model elastic notnull group 'User:Structural Fill'
prop density=1922.2 bulk=3.33333E8 shear=1.53846E8 notnull group 'User:Structural Fill'
group 'User:Structural Fill' notnull i 21 25 j 39 42
model elastic notnull group 'User:Structural Fill'
prop density=1922.2 bulk=3.33333E8 shear=1.53846E8 notnull group 'User:Structural Fill'
group 'User:Structural Fill' notnull i 19 21 j 35 38
model elastic notnull group 'User:Structural Fill'
prop density=1922.2 bulk=3.33333E8 shear=1.53846E8 notnull group 'User:Structural Fill'
group 'User:Structural Fill' notnull i 16 22 j 31 34
model elastic notnull group 'User:Structural Fill'
prop density=1922.2 bulk=3.33333E8 shear=1.53846E8 notnull group 'User:Structural Fill'
group 'User:Foundation soil' i 165 166 j 79 83
model elastic group 'User:Foundation soil'
prop density=1840.0 bulk=2.9E8 shear=6.21429E7 group 'User:Foundation soil'
group 'User:Foundation soil' i 161 166 j 75 78
model elastic group 'User:Foundation soil'
prop density=1840.0 bulk=2.9E8 shear=6.21429E7 group 'User:Foundation soil'
group 'User:Foundation soil' i 157 166 j 71 74
model elastic group 'User:Foundation soil'
prop density=1840.0 bulk=2.9E8 shear=6.21429E7 group 'User:Foundation soil'
group 'User:Foundation soil' i 156 j 71 74
model elastic group 'User:Foundation soil'
prop density=1840.0 bulk=2.9E8 shear=6.21429E7 group 'User:Foundation soil'
group 'User:Foundation soil' i 148 162 j 67 70
model elastic group 'User:Foundation soil'
prop density=1840.0 bulk=2.9E8 shear=6.21429E7 group 'User:Foundation soil'
group 'User:Foundation soil' i 147 j 67 70
model elastic group 'User:Foundation soil'
prop density=1840.0 bulk=2.9E8 shear=6.21429E7 group 'User:Foundation soil'
group 'User:Foundation soil' i 128 164 j 63 66
model elastic group 'User:Foundation soil'
prop density=1840.0 bulk=2.9E8 shear=6.21429E7 group 'User:Foundation soil'
group 'User:Foundation soil' i 116 151 j 59 62
model elastic group 'User:Foundation soil'
prop density=1840.0 bulk=2.9E8 shear=6.21429E7 group 'User:Foundation soil'
group 'User:Foundation soil' i 102 151 j 55 58
model elastic group 'User:Foundation soil'
prop density=1840.0 bulk=2.9E8 shear=6.21429E7 group 'User:Foundation soil'
group 'User:Foundation soil' i 85 118 j 51 54
model elastic group 'User:Foundation soil'
prop density=1840.0 bulk=2.9E8 shear=6.21429E7 group 'User:Foundation soil'
group 'User:Foundation soil' i 74 106 j 47 50
model elastic group 'User:Foundation soil'
prop density=1840.0 bulk=2.9E8 shear=6.21429E7 group 'User:Foundation soil'
group 'User:Foundation soil' i 70 106 j 43 46
model elastic group 'User:Foundation soil'
prop density=1840.0 bulk=2.9E8 shear=6.21429E7 group 'User:Foundation soil'
group 'User:Foundation soil' i 66 73 j 39 42
model elastic group 'User:Foundation soil'
```

```
prop density=1840.0 bulk=2.9E8 shear=6.21429E7 group 'User:Foundation soil'
group 'User:Foundation soil' i 62 73 j 35 38
model elastic group 'User:Foundation soil'
prop density=1840.0 bulk=2.9E8 shear=6.21429E7 group 'User:Foundation soil'
group 'User:Foundation soil' i 58 73 j 31 34
model elastic group 'User:Foundation soil'
prop density=1840.0 bulk=2.9E8 shear=6.21429E7 group 'User:Foundation soil'
group 'User:Foundation soil' i 1 147 j 1 30
model elastic group 'User:Foundation soil'
prop density=1840.0 bulk=2.9E8 shear=6.21429E7 group 'User:Foundation soil'
group 'User:Foundation soil' i 74 160 j 31 42
model elastic group 'User:Foundation soil'
prop density=1840.0 bulk=2.9E8 shear=6.21429E7 group 'User:Foundation soil'
group 'User:Foundation soil' i 107 160 j 43 50
model elastic group 'User:Foundation soil'
prop density=1840.0 bulk=2.9E8 shear=6.21429E7 group 'User:Foundation soil'
group 'User:Foundation soil' i 119 160 j 51 54
model elastic group 'User:Foundation soil'
prop density=1840.0 bulk=2.9E8 shear=6.21429E7 group 'User:Foundation soil'
group 'User:Foundation soil' i 152 160 j 55 62
model elastic group 'User:Foundation soil'
prop density=1840.0 bulk=2.9E8 shear=6.21429E7 group 'User:Foundation soil'
group 'User:Foundation soil' i 148 200 j 1 30
model elastic group 'User:Foundation soil'
prop density=1840.0 bulk=2.9E8 shear=6.21429E7 group 'User:Foundation soil'
group 'User:Foundation soil' i 161 200 j 31 62
model elastic group 'User:Foundation soil'
prop density=1840.0 bulk=2.9E8 shear=6.21429E7 group 'User:Foundation soil'
group 'User:Foundation soil' i 163 200 j 67 70
model elastic group 'User:Foundation soil'
prop density=1840.0 bulk=2.9E8 shear=6.21429E7 group 'User:Foundation soil'
group 'User:Foundation soil' i 165 200 j 63 66
model elastic group 'User:Foundation soil'
prop density=1840.0 bulk=2.9E8 shear=6.21429E7 group 'User:Foundation soil'
group 'User:Foundation soil' i 167 193 j 71 104
model elastic group 'User:Foundation soil'
prop density=1840.0 bulk=2.9E8 shear=6.21429E7 group 'User:Foundation soil'
group 'User:Foundation soil' notnull i 194 201 j 71 98
model elastic notnull group 'User:Foundation soil'
prop density=1840.0 bulk=2.9E8 shear=6.21429E7 notnull group 'User:Foundation soil'
group 'User:Foundation soil' notnull i 201 216 j 1 70
model elastic notnull group 'User:Foundation soil'
prop density=1840.0 bulk=2.9E8 shear=6.21429E7 notnull group 'User:Foundation soil'
group 'User:LDS' i 77 154 j 87 88
model elastic group 'User:LDS'
prop density=2400.0 bulk=1.56E10 shear=1.27E10 group 'User:LDS'
group 'User:EPS39' i 70 162 j 83 86
model elastic group 'User:EPS39'
prop density=38.4 bulk=4.3241E6 shear=4.66908E6 group 'User:EPS39'
group 'User:EPS29' i 66 164 j 79 82
model elastic group 'User:EPS29'
```

```
prop density=28.8 bulk=3.14861E6 shear=3.39982E6 group 'User:EPS29'
group 'User:EPS29' i 62 160 j 75 78
model elastic group 'User:EPS29'
prop density=28.8 bulk=3.14861E6 shear=3.39982E6 group 'User:EPS29'
group 'User:EPS29' i 58 155 j 71 74
model elastic group 'User:EPS29'
prop density=28.8 bulk=3.14861E6 shear=3.39982E6 group 'User:EPS29'
group 'User:EPS29' i 54 146 j 67 70
model elastic group 'User:EPS29'
prop density=28.8 bulk=3.14861E6 shear=3.39982E6 group 'User:EPS29'
group 'User:EPS22' i 50 127 j 63 66
model elastic group 'User:EPS22'
prop density=21.6 bulk=2.09908E6 shear=2.26655E6 group 'User:EPS22'
group 'User:EPS22' i 46 115 j 59 62
model elastic group 'User:EPS22'
prop density=21.6 bulk=2.09908E6 shear=2.26655E6 group 'User:EPS22'
group 'User:EPS22' i 42 101 j 55 58
model elastic group 'User:EPS22'
prop density=21.6 bulk=2.09908E6 shear=2.26655E6 group 'User:EPS22'
group 'User:EPS22' i 38 84 j 51 54
model elastic group 'User:EPS22'
prop density=21.6 bulk=2.09908E6 shear=2.26655E6 group 'User:EPS22'
group 'User:EPS22' i 34 73 j 47 50
model elastic group 'User:EPS22'
prop density=21.6 bulk=2.09908E6 shear=2.26655E6 group 'User:EPS22'
group 'User:EPS22' i 30 69 j 43 46
model elastic group 'User:EPS22'
prop density=21.6 bulk=2.09908E6 shear=2.26655E6 group 'User:EPS22'
group 'User:EPS22' i 26 65 j 39 42
model elastic group 'User:EPS22'
prop density=21.6 bulk=2.09908E6 shear=2.26655E6 group 'User:EPS22'
group 'User:EPS22' i 22 61 j 35 38
model elastic group 'User:EPS22'
prop density=21.6 bulk=2.09908E6 shear=2.26655E6 group 'User:EPS22'
group 'User:EPS22' i 23 57 j 31 34
model elastic group 'User:EPS22'
prop density=21.6 bulk=2.09908E6 shear=2.26655E6 group 'User:EPS22'
model null i 99 j 104
group 'null' i 99 j 104
group delete 'null'
model null i 99 115 j 86 103
group 'null' i 99 115 j 86 103
group delete 'null'
model null i 99 142 j 70 85
group 'null' i 99 142 j 70 85
group delete 'null'
model null i 99 157 j 38 69
group 'null' i 99 157 j 38 69
group delete 'null'
model null i 99 162 j 10 37
group 'null' i 99 162 j 10 37
```

```
group delete 'null'
model null i 99 164 j 1 9
group 'null' i 99 164 j 1 9
group delete 'null'
model null i 165 202 j 1 35
group 'null' i 165 202 j 1 35
group delete 'null'
model null i 163 164 j 10 36
group 'null' i 163 164 j 10 36
group delete 'null'
model null i 100 178 j 70 104
group 'null' i 100 178 j 70 104
group delete 'null'
model null i 106 j 105 106
group 'null' i 106 j 105 106
group delete 'null'
model null i 125 j 105 106
group 'null' i 125 j 105 106
group delete 'null'
model null i 141 j 105 106
group 'null' i 141 j 105 106
group delete 'null'
model null i 158 188 j 36 69
group 'null' i 158 188 j 36 69
group delete 'null'
model null i 179 193 j 70 104
group 'null' i 179 193 j 70 104
group delete 'null'
model null i 189 203 j 36 69
group 'null' i 189 203 j 36 69
group delete 'null'
model null i 194 201 j 70 98
group 'null' i 194 201 j 70 98
group delete 'null'
model null i 204 216 j 1 60
group 'null' i 204 216 j 1 60
group delete 'null'
model null i 203 j 1 35
group 'null' i 203 j 1 35
group delete 'null'
;group 'User:EPS22' i 85 98 j 51 54
;model elastic group 'User:EPS22'
;prop density=21.6 bulk=2.09908E6 shear=2.26655E6 group 'User:EPS22'
;group 'User:EPS22' i 74 98 j 47 50
;model elastic group 'User:EPS22'
;prop density=21.6 bulk=2.09908E6 shear=2.26655E6 group 'User:EPS22'
;group 'User:EPS22' i 70 98 j 43 46
;model elastic group 'User:EPS22'
;prop density=21.6 bulk=2.09908E6 shear=2.26655E6 group 'User:EPS22'
;group 'User:EPS22' i 66 98 j 39 42
;model elastic group 'User:EPS22'
```

```
;prop density=21.6 bulk=2.09908E6 shear=2.26655E6 group 'User:EPS22'
;group 'User:EPS22' i 62 98 j 35 38
;model elastic group 'User:EPS22'
;prop density=21.6 bulk=2.09908E6 shear=2.26655E6 group 'User:EPS22'
;group 'User:EPS22' i 58 98 j 31 34
;model elastic group 'User:EPS22'
;prop density=21.6 bulk=2.09908E6 shear=2.26655E6 group 'User:EPS22'
;group 'User:EPS22' i 22 j 31 34
;model elastic group 'User:EPS22'
;prop density=21.6 bulk=2.09908E6 shear=2.26655E6 group 'User:EPS22'
;boundary conditions
;settlement duing to self weight of the system is already finished
;set gravity=9.81
fix  x y i 1 99 j 1
fix  x y i 1 j 1 31
fix  x i 99 j 1 105
model null i 1 98 j 1 8
group 'null' i 1 98 j 1 8
group delete 'null'
model null i 1 6 j 9 30
group 'null' i 1 6 j 9 30
group delete 'null'
fix  x y i 7 99 j 9
fix  x y i 7 j 9 31
model null i 7 98 j 9 15
group 'null' i 7 98 j 9 15
group delete 'null'
model null i 7 11 j 16 30
group 'null' i 7 11 j 16 30
group delete 'null'
fix  x y i 12 99 j 16
fix  x y i 12 j 16 31
model null i 12 15 j 16 30
group 'null' i 12 15 j 16 30
group delete 'null'
model null j 16 30
group 'null' j 16 30
group delete 'null'
fix  x y i 16 99 j 31
fix  x y i 16 j 31 33
apply yforce -45584 from 90,107 to 90,107
apply yforce -45584 from 91,107 to 91,107
solve
```

F.2 3D Model

The codes presented here are for the model of final iteration.

```
set mechanical ratio 0.5e-5
```

```
gen zone brick size 80 95 80 p0 0 0 0 p1 32.39445 0 0 p2 0 23.75 0 p3 0 0 15.1358 ratio 0.96
1.0 0.96;
model elas
prop bulk 3.33333e8 shear 1.53846e8 range x 0 32.39445 y 0 23.75 z 0 15.1358; fill in
shoulder of slope EPS and under subballast
model null range x 0 31.58645 z 14.9828 15.1358; outside of rail
model null range x 31.66445 32.39445 z 14.9828 15.1358; inside of rail
model null range x 0 31.1365 z 14.9328 14.9828; outside of upper sleeper
model null range y 0.249 0.751 z 14.9328 14.9828 ; gap under rail between sleepers
model null range y 0.999 1.501 z 14.9328 14.9828 ; gap under rail between sleepers
model null range y 1.749 2.251 z 14.9328 14.9828 ; gap under rail between sleepers
model null range y 2.499 3.001 z 14.9328 14.9828 ; gap under rail between sleepers
model null range y 3.249 3.751 z 14.9328 14.9828 ; gap under rail between sleepers
model null range y 3.999 4.501 z 14.9328 14.9828 ; gap under rail between sleepers
model null range y 4.749 5.251 z 14.9328 14.9828 ; gap under rail between sleepers
model null range y 5.499 6.001 z 14.9328 14.9828 ; gap under rail between sleepers
model null range y 6.249 6.751 z 14.9328 14.9828 ; gap under rail between sleepers
model null range y 6.999 7.501 z 14.9328 14.9828 ; gap under rail between sleepers
model null range y 7.749 8.251 z 14.9328 14.9828 ; gap under rail between sleepers
model null range y 8.499 9.001 z 14.9328 14.9828 ; gap under rail between sleepers
model null range y 9.249 9.751 z 14.9328 14.9828 ; gap under rail between sleepers
model null range y 9.999 10.501 z 14.9328 14.9828 ; gap under rail between sleepers
model null range y 10.749 11.251 z 14.9328 14.9828 ; gap under rail between sleepers
model null range y 11.499 12.001 z 14.9328 14.9828 ; gap under rail between sleepers
model null range y 12.249 12.751 z 14.9328 14.9828 ; gap under rail between sleepers
model null range y 12.999 13.501 z 14.9328 14.9828 ; gap under rail between sleepers
model null range y 13.749 14.251 z 14.9328 14.9828 ; gap under rail between sleepers
model null range y 14.499 15.001 z 14.9328 14.9828 ; gap under rail between sleepers
model null range y 15.249 15.751 z 14.9328 14.9828 ; gap under rail between sleepers
model null range y 15.9 16.6 z 14.9328 14.9828 ; gap under rail between sleepers
model null range y 16.7 17.3 z 14.9328 14.9828 ; gap under rail between sleepers
model null range y 17.499 18.001 z 14.9328 14.9828 ; gap under rail between sleepers
model null range y 18.249 18.751 z 14.9328 14.9828 ; gap under rail between sleepers
model null range y 18.999 19.501 z 14.9328 14.9828 ; gap under rail between sleepers
model null range y 19.749 20.251 z 14.9328 14.9828 ; gap under rail between sleepers
model null range y 20.499 21.001 z 14.9328 14.9828 ; gap under rail between sleepers
model null range y 21.249 21.751 z 14.9328 14.9828 ; gap under rail between sleepers
model null range y 21.999 22.501 z 14.9328 14.9828 ; gap under rail between sleepers
model null range y 22.749 23.251 z 14.9328 14.9828 ; gap under rail between sleepers
model null range y 23.499 23.75 z 14.9328 14.9828 ; gap under rail between sleepers
model null range x 0 30.7065 z 14.8987 14.9828 ; outside of ballast 1
model null range x 0 30.5782 z 14.8145 14.8987 ; outside of ballast 2
model null range x 0 30.4100 z 14.7304 14.8145 ; outside of ballast 3
model null range x 0 30.2417 z 14.6463 14.7304 ; outside of ballast 4
model null range x 0 30.0734 z 14.5621 14.6463 ; outside of ballast 5
model null range x 0 29.9052 z 14.4780 14.5621 ; outside of ballast 6

model null range x 0 28.5496 z 14.2748 14.478; outside of subballast
model null range x 0 28.5496 z 14.0518 14.2748; outside of structual fill 1
model null range x 0 28.0077 z 13.8289 14.0518; outside of structual fill 2
model null range x 0 27.4658 z 13.6059 13.8289; outside of structual fill 3
```

model null range x 0 26.9238 z 13.3830 13.6059; outside of structual fill 4
model null range x 0 26.3819 z 13.1600 13.3830; outside of structual fill 5
model null range x 0 25.8400 z 12.9250 13.1600 ; out side of EPS 1
model null range x 0 25.3786 z 12.6900 12.9250 ; out side of EPS 2
model null range x 0 24.9171 z 12.4550 12.6900 ; out side of EPS 3
model null range x 0 24.4557 z 12.2200 12.4550 ; out side of EPS 4
model null range x 0 23.9943 z 11.9850 12.2200 ; out side of EPS 5
model null range x 0 23.5329 z 11.7500 11.9850 ; out side of EPS 6
model null range x 0 23.0714 z 11.5150 11.7500 ; out side of EPS 7
model null range x 0 22.6100 z 11.2800 11.5150 ; out side of EPS 8
model null range x 0 22.1486 z 11.0450 11.2800 ; out side of EPS 9
model null range x 0 21.6871 z 10.8100 11.0450 ; out side of EPS 10
model null range x 0 21.2257 z 10.5750 10.8100 ; out side of EPS 11
model null range x 0 20.7643 z 10.3400 10.5750 ; out side of EPS 12
model null range x 0 20.3029 z 10.1050 10.3400 ; out side of EPS 13
model null range x 0 19.8414 z 9.8700 10.1050 ; out side of EPS 14
model null range x 0 19.3800 z 9.6350 9.8700 ; out side of EPS 15
model null range x 0 18.9186 z 9.4000 9.6350 ; out side of EPS 16
model null range x 0 18.4571 z 9.1650 9.4000 ; out side of EPS 17
model null range x 0 17.9957 z 8.9300 9.1650 ; out side of EPS 18
model null range x 0 17.5343 z 8.6950 8.9300 ; out side of EPS 19
model null range x 0 17.0729 z 8.4600 8.6950 ; out side of EPS 20
model null range x 0 16.6114 z 8.2250 8.4600 ; out side of EPS 21
model null range x 0 16.1500 z 7.9900 8.2250 ; out side of EPS 22
model null range x 0 15.6886 z 7.7550 7.9900 ; out side of EPS 23
model null range x 0 15.2271 z 7.5200 7.7550 ; out side of EPS 24
model null range x 0 14.7657 z 7.2850 7.5200 ; out side of EPS 25
model null range x 0 14.3043 z 7.0500 7.2850 ; out side of EPS 26
model null range x 0 13.8429 z 6.8150 7.0500 ; out side of EPS 27
model null range x 0 13.3814 z 6.5800 6.8150 ; out side of EPS 28
model null range x 0 12.9200 z 6.3450 6.5800 ; out side of EPS 29
model null range x 0 12.4586 z 6.1100 6.3450 ; out side of EPS 30
model null range x 0 11.9971 z 5.8750 6.1100 ; out side of EPS 31
model null range x 0 11.5357 z 5.6400 5.8750 ; out side of EPS 32
model null range x 0 11.0743 z 5.4050 5.6400 ; out side of EPS 33
model null range x 0 10.6129 z 5.1700 5.4050 ; out side of EPS 34
model null range x 0 10.1514 z 4.9350 5.1700 ; out side of EPS 35
model null range x 0 9.6900 z 4.7000 4.9350 ; out side of EPS 36
model null range x 0 9.2286 z 4.4650 4.7000 ; out side of EPS 37
model null range x 0 8.7671 z 4.2300 4.4650 ; out side of EPS 38
model null range x 0 8.3057 z 3.9950 4.2300 ; out side of EPS 39
model null range x 0 7.8443 z 3.7600 3.9950 ; out side of EPS 40
model null range x 0 7.3829 z 3.5250 3.7600 ; out side of EPS 41
model null range x 0 6.9214 z 3.2900 3.5250 ; out side of EPS 42
model null range x 0 6.4600 z 3.0550 3.2900 ; out side of EPS 43
model null range x 0 5.9986 z 2.8200 3.0550 ; out side of EPS 44
model null range x 0 5.5371 z 2.5850 2.8200 ; out side of EPS 45
model null range x 0 5.0757 z 2.3500 2.5850 ; out side of EPS 46
model null range x 0 4.6143 z 2.1150 2.3500 ; out side of EPS 47
model null range x 0 4.1529 z 1.8800 2.1150 ; out side of EPS 48
model null range x 0 3.6914 z 1.6450 1.8800 ; out side of EPS 49

```
    model null range x 0 3.2300 z 1.4100 1.6450 ; out side of EPS 50
    model null range x 0 2.7686 z 1.1750 1.4100 ; out side of EPS 51
    model null range x 0 2.3071 z 0.9400 1.1750 ; out side of EPS 52
    model null range x 0 1.8457 z 0.7050 0.9400 ; out side of EPS 53
    model null range x 0 1.3843 z 0.4700 0.7050 ; out side of EPS 54
    model null range x 0 0.9229 z 0.2350 0.4700 ; out side of EPS 55
    model null range x 0 0.4614 z 0.0000 0.2350 ; out side of EPS 56
    prop bulk 1.75e11 shear 8.07692e10 range z 14.9828 15.1358; rail steel
    prop bulk 1.6361e7 shear 7.5513e6 range z 14.478 14.9328; ballast
    prop bulk 28333e6 shear 13077e6 range x 31.1365 32.39445 y -0.001 0.251 z 14.7828
14.9828 ; sleeper concrete 1
    prop bulk 28333e6 shear 13077e6 range x 31.1365 32.39445 y 0.749 1.001 z 14.7828
14.9828 ; sleeper concrete 2
    prop bulk 28333e6 shear 13077e6 range x 31.1365 32.39445 y 1.499 1.751 z 14.7828
14.9828 ; sleeper concrete 3
    prop bulk 28333e6 shear 13077e6 range x 31.1365 32.39445 y 2.249 2.501 z 14.7828
14.9828 ; sleeper concrete 4
    prop bulk 28333e6 shear 13077e6 range x 31.1365 32.39445 y 2.999 3.251 z 14.7828
14.9828 ; sleeper concrete 5
    prop bulk 28333e6 shear 13077e6 range x 31.1365 32.39445 y 3.749 4.001 z 14.7828
14.9828 ; sleeper concrete 6
    prop bulk 28333e6 shear 13077e6 range x 31.1365 32.39445 y 4.499 4.751 z 14.7828
14.9828 ; sleeper concrete 7
    prop bulk 28333e6 shear 13077e6 range x 31.1365 32.39445 y 5.249 5.501 z 14.7828
14.9828 ; sleeper concrete 8
    prop bulk 28333e6 shear 13077e6 range x 31.1365 32.39445 y 5.999 6.251 z 14.7828
14.9828 ; sleeper concrete 9
    prop bulk 28333e6 shear 13077e6 range x 31.1365 32.39445 y 6.749 7.001 z 14.7828
14.9828 ; sleeper concrete 10
    prop bulk 28333e6 shear 13077e6 range x 31.1365 32.39445 y 7.449 7.751 z 14.7828
14.9828 ; sleeper concrete 11
    prop bulk 28333e6 shear 13077e6 range x 31.1365 32.39445 y 8.249 8.501 z 14.7828
14.9828 ; sleeper concrete 12
    prop bulk 28333e6 shear 13077e6 range x 31.1365 32.39445 y 8.999 9.251 z 14.7828
14.9828 ; sleeper concrete 13
    prop bulk 28333e6 shear 13077e6 range x 31.1365 32.39445 y 9.749 10.001 z 14.7828
14.9828 ; sleeper concrete 14
    prop bulk 28333e6 shear 13077e6 range x 31.1365 32.39445 y 10.499 10.751 z 14.7828
14.9828 ; sleeper concrete 15
    prop bulk 28333e6 shear 13077e6 range x 31.1365 32.39445 y 11.249 11.501 z 14.7828
14.9828 ; sleeper concrete 16
    prop bulk 28333e6 shear 13077e6 range x 31.1365 32.39445 y 11.999 12.251 z 14.7828
14.9828 ; sleeper concrete 17
    prop bulk 28333e6 shear 13077e6 range x 31.1365 32.39445 y 12.749 13.001 z 14.7828
14.9828 ; sleeper concrete 18
    prop bulk 28333e6 shear 13077e6 range x 31.1365 32.39445 y 13.499 13.751 z 14.7828
14.9828 ; sleeper concrete 19
    prop bulk 28333e6 shear 13077e6 range x 31.1365 32.39445 y 14.249 14.501 z 14.7828
14.9828 ; sleeper concrete 20
    prop bulk 28333e6 shear 13077e6 range x 31.1365 32.39445 y 14.999 15.251 z 14.7828
14.9828 ; sleeper concrete 21
```

```
    prop bulk 28333e6 shear 13077e6 range x 31.1365 32.39445 y 15.749 16.001 z 14.7828
14.9828 ; sleeper concrete 22
    prop bulk 28333e6 shear 13077e6 range x 31.1365 32.39445 y 16.4 16.8 z 14.7828 14.9828 ;
sleeper concrete 23
    prop bulk 28333e6 shear 13077e6 range x 31.1365 32.39445 y 17.2 17.6 z 14.7828 14.9828 ;
sleeper concrete 24
    prop bulk 28333e6 shear 13077e6 range x 31.1365 32.39445 y 17.999 18.251 z 14.7828
14.9828 ; sleeper concrete 25
    prop bulk 28333e6 shear 13077e6 range x 31.1365 32.39445 y 18.749 19.001 z 14.7828
14.9828 ; sleeper concrete 26
    prop bulk 28333e6 shear 13077e6 range x 31.1365 32.39445 y 19.499 19.751 z 14.7828
14.9828 ; sleeper concrete 27
    prop bulk 28333e6 shear 13077e6 range x 31.1365 32.39445 y 20.249 20.501 z 14.7828
14.9828 ; sleeper concrete 28
    prop bulk 28333e6 shear 13077e6 range x 31.1365 32.39445 y 20.999 21.251 z 14.7828
14.9828 ; sleeper concrete 29
    prop bulk 28333e6 shear 13077e6 range x 31.1365 32.39445 y 21.749 22.001 z 14.7828
14.9828 ; sleeper concrete 30
    prop bulk 28333e6 shear 13077e6 range x 31.1365 32.39445 y 22.499 22.751 z 14.7828
14.9828 ; sleeper concrete 31
    prop bulk 28333e6 shear 13077e6 range x 31.1365 32.39445 y 23.249 23.501 z 14.7828
14.9828 ; sleeper concrete 32
    prop bulk 2.16667e9 shear 4.36242e7 range z 14.2748 14.478; subballast
    prop bulk 1.56e10 shear 1.27e10 range x 29.4 32.39445 z 13.1572 13.3604; LDS
    prop bulk 4.3241e6 shear 4.66908e6 range x 27.2 32.39445 z 12.2 13.1572; EPS39
    prop bulk 3.14861e6 shear 3.39982e6 range x 25.3 32.39445 z 11.3 12.2; EPS29 1
    prop bulk 3.14861e6 shear 3.39982e6 range x 23.4 32.39445 z 10.3378 11.3; EPS29 2
    prop bulk 3.14861e6 shear 3.39982e6 range x 21.6154 32.39445 z 9.395 10.3378; EPS29 3
    prop bulk 3.14861e6 shear 3.39982e6 range x 19.7358 32.39445 z 8.4582 9.395; EPS29 4
    prop bulk 2.09908e6 shear 2.26655e6 range x 17.8562 32.39445 z 7.5184 8.4582; EPS22 1
    prop bulk 2.09908e6 shear 2.26655e6 range x 15.9766 32.39445 z 6.5786 7.5184; EPS22 2
    prop bulk 2.09908e6 shear 2.26655e6 range x 14.097 32.39445 z 5.6388 6.5786; EPS22 3
    prop bulk 2.09908e6 shear 2.26655e6 range x 12.2174 30.9 z 4.699 5.6388; EPS22 4
    prop bulk 2.09908e6 shear 2.26655e6 range x 10.3378 28.9 z 3.7592 4.699; EPS22 5
    prop bulk 2.09908e6 shear 2.26655e6 range x 8.4582 27.1 z 2.8194 3.7592; EPS22 6
    prop bulk 2.09908e6 shear 2.26655e6 range x 6.5786 25.3 z 1.8796 2.8194; EPS22 7
    prop bulk 2.09908e6 shear 2.26655e6 range x 4.699 23.4 z 0.9398 1.8796; EPS22 8
    prop bulk 2.09908e6 shear 2.26655e6 range x 5.1689 21.6154 z 0 0.9398; EPS22 9
    prop bulk 2.9e8 shear 6.21429e7 range x 30.9 32.39445 z 4.699 5.6388; Foundation soil 1
    prop bulk 2.9e8 shear 6.21429e7 range x 28.9 32.39445 z 3.7592 4.699; Foundation soil 2
    prop bulk 2.9e8 shear 6.21429e7 range x 27.1 32.39445 z 2.8194 3.7592; Foundation soil 3
    prop bulk 2.9e8 shear 6.21429e7 range x 25.3 32.39445 z 1.8796 2.8194; Foundation soil 4
    prop bulk 2.9e8 shear 6.21429e7 range x 23.4 32.39445 z 0.9398 1.8796; Foundation soil 5
    prop bulk 2.9e8 shear 6.21429e7 range x 21.6154 32.39445 z 0 0.9398; Foundation soil 6
    ;
    ;boundary condisions
    fix x y z range z -0.01 0.01; fix base
    fix x y z range x -0.01 0.01; fix left boundary
    fix y range y -0.01 0.01 ; fixes front face in y direction (axis of symmetry)
    fix y range y 23.74 23.76 ; fixes back face in y direction (axis of symmetry)
    fix x range x 32.394 32.395; fixes right boundary in x direction (axis of symmetry)
```

```
;
    apply zforce -83.404e3 range x 31.581 31.583 y 6.74 6.76 z 15.135 15.137 ; axle load 1 left
node
    apply zforce -83.404e3 range x 31.665 31.667 y 6.74 6.76 z 15.135 15.137 ; axle load 1 right
node
    apply zforce -83.404e3 range x 31.581 31.583 y 9.49 9.51 z 15.135 15.137 ; axle load 2 left
node
    apply zforce -83.404e3 range x 31.665 31.667 y 9.49 9.51 z 15.135 15.137 ; axle load 2 right
node
    apply zforce -45.584e3 range x 31.581 31.583 y 13.99 14.01 z 15.135 15.137 ; axle load 3
left node
    apply zforce -45.584e3 range x 31.665 31.667 y 13.99 14.01 z 15.135 15.137 ; axle load 3
right node
    apply zforce -45.584e3 range x 31.581 31.583 y 16.74 16.76 z 15.135 15.137 ; axle load 4
left node
    apply zforce -45.584e3 range x 31.665 31.667 y 16.74 16.76 z 15.135 15.137 ; axle load 4
right node
    hist n = 5
    hist unbal
    hist gp zdisp 31.582 9.5 15.136
    hist gp zdisp 31.666 9.5 15.136
    hist gp zdisp 31.582 6.75 15.136
    hist gp zdisp 31.666 6.75 15.136
    hist gp zdisp 31.582 14.0 15.136
    hist gp zdisp 31.666 14.0 15.136
    hist gp zdisp 31.582 16.75 15.136
    hist gp zdisp 31.666 16.75 15.136
    print hist
    ;step 10000
    Solve
    plot create PROPV ; shows properties in X section
    plot set color On
    plot set caption On
    plot set caption left
    plot set caption size 26
    plot set title On
    plot set title top
    plot set foreground black
    plot set background white
    plot set window position (0.00,0.00) size(1.00,0.89)
    ;plot set plane normal (0.000,1.000,0.000)
    ;plot set plane origin (15.0000e+000,10.00e+000,7.5000e+000)
    plot set mode model
    plot set center (15.0000e+000,10.00e+000,7.5000e+000)
    plot set rotation (0.00, 0.00, 0.00)
    plot set distance 180
    plot set angle 22
    plot set magnification  1.0e+000
    plot add block prop bulk
    plot add contour zdisp
    save 3DUTA-EPS3.sav
```

REFERENCES

Aabøe, R., and Frydenlund, T. E., (2011). "40 years of experience with the use of EPS geofoam blocks in road construction", *EPS 2011*, Lillestrom, Norway.

Alfhein, S., Flaate, K., Refsdal, G., Rygg, N., and Aarhus, K., (2011). "The first EPS geoblock road embankment – 1972", NRRL, Norwegian Public Roads Administration, Road Authority of Akershus County, Norwegian Public Roads Administration.

American Railway Engineering and Maintenance-of-Way Association, (2007). "Economics of railway engineering and operations - construction and maintenance operations", *Manual for Railway Engineering*, Volume 4, Chapter 16, Part 10.11.

Arellano, D., and Bartlett, S. F., (2012). "Evaluation of geofoam for support of freight rail tracks", proposal of National Center for Freight and Infrastructure Research and Education (CFIRE), University of Memphis, Herff College of Engineering.

Arellano, D., Stark, T. D., Horvath, J. S., and Leshchinsky, D., (2011). "Guidelines for geofoam applications in slope stability projects", final report prepared for National Cooperative Highway Research Program (NCHRP24-11), Transportation Research Board of the National Academies.

ASTM D6817/D6817M-13a (2013), Standard specification for rigid cellular polystyrene geofoam, *American Society for Testing and Materials (ASTM) International*, West Conshohocken, PA.

Bartlett, S.F. and Farnsworth, C.B. (2004). "Monitoring and modeling of innovative foundation treatment and embankment construction used on the I-15 reconstruction project, project management plan and instrument installation report," *Utah Department of Transportation (UDOT)* research report No. UT-04.19, University of Utah, Department of Civil and Environmental Engineering, 202.

Bartlett, S. F., Lawton, E. C., Farnsworth, C. B. and Newman, M. P, (2012), "Design and evaluation of expanded polystyrene geofoam embankments for the I-15 reconstruction project, Salt Lake City, Utah", report prepared for *Utah Department of Transportation Research Division.* University of Utah, Department of Civil and Environmental Engineering

Duskov, M., (1997), "EPS as a light-weight sub-base material in pavement structures," Thesis, Delft University of Technology, Delft, Netherlands, 91-95.

European Manufacturers of EPS (EUMEPS) (2011), "EPS white book, EUMEPS background information on standardisation of EPS", Version 31/03/11, Belgium.

Esveld, C., (2001). "Modern railway track," 2nd Ed., MRT-Productions, Zaltbommel, The Netherlands.

Esveld, C., Markine, V. and Duškov, M., (2001). "Feasibility of EPS as a lightweight sub-base material in railway track structures," *Proceedings of the third international conference on EPS Geofoam,* Salt Lake City, Utah, 10-12 December, 1-10.

Farnsworth C. F., Bartlett S. F., Negussey, D. and Stuedlein A. (2008). "Construction and post-construction settlement performance of innovative embankment systems, I-15 reconstruction project, Salt Lake City, Utah," *Journal of Geotechnical and Geoenvironmental Engineering*, 134, 289-301.

Frydenlund, T. E., Myhre, O., Refsdal, G., Aaboe, R., 1987. "Plastic foam in road embankments," Norwegian Road Research Laboratory, Norwegian Edition 61 (in English).

Grabe, P. J., (2002). "Resilient and permanent deformation of railway foundations under principal stress rotation," PhD Dissertation, University of Southampton, UK.

Helwany, S., (2007). "Applied soil mechanics with ABAQUS applications," John Wiley & Sons, Inc., Hoboken, New Jersey.

International Union of Railways (1994). "UCI Code 719R: Earthworks and trackbed layers for railway lines," Paris, France.

Itasca Consulting Group, Inc. (1993-2002). "Fast Lagrangian Analysis of Continua in Three Dimensions, Version 3.00-261." Minneapolis, Minnesota.

Itasca Consulting Group, Inc. (2005). "FLAC: Fast Lagrangian Analysis of Continua: Structural Elements, Version 5." Minneapolis, Minnesota.

Kaynia, A. M., Madshus, C., and Zackrisson, P (2000). "Ground vibration from high-speed trains: prediction and countermeasure," *J. Geotech. Geoenviron. Eng*, 126(6), 531-537.

Miki, G. (1996). "Ten year history of EPS method in Japan and its future challenges," *Proceeding of International Symposium on EPS Construction Method*, Tokyo, 29-30 October, 394-411.

Negussey, D. and Stuedlein, A. (2003). "Geofoam fill performance monitoring." *Utah Department of Transportaion Research Division* Report No. UT-03.17.

O'Riordan, N. and Phear, A. (2001). "Design and construction of ballasted track formation and subgrade for high speed lines," *Proceedings of the International Conference of Hail way Engineering*, London, 30 April-1 May

Powrie, W., Yang, L. A., and Clayton, C. R. I. (2007). "Stress changes in the ground below ballasted railway track during train passage," *Proceedings of the Institution of Mechanical Engineers, Part F, Journal of rail and rapid transit*, March, 221(2), 247-262.

Riad, H. L., Ricci, A. L., Osborn, P. W., D'Angelo, D. A. and Horvath, J. S. (2004). "Design of lightweight fills for road embankments on Boston's central artery/tunnel project," *Proceedings: Fifth international conference on case histories in geotechnical engineering*, New York, NY, 13-17 April.

Snow, R., Webb J., Sander M., (2010). "Light rail on geofoam West Valley UTA TRAX project", *2010 AREMA Conference and Exposition*, Orlando, Florida.

Stark, T. D., Arellano, D., Horvath, J. S., and Leshchinsky, D., (2004). "Geofoam applications in the design and construction of highway embankments", Report prepared for National Cooperative Highway Research Program (NCHRP Web Document 65, Project 24-11), Transportation Research Board of the National Academies.

Stark, T. D., Arellano, D., Horvath, J. S., and Leshchinsky, D., (2004), "Guideline and recommended standard for geofoam applications in highway embankments", Report prepared for National Cooperative Highway Research Program (NCHRP 529), Transportation Research Board of the National Academies.

The Permanent Way Institution (1993). "British railway track-design, construction and maintenance," 6th edition (Ed. G. H. Cope), Echo Press, Loughborough, Leicester, UK.

United States Department of Transportation - Federal Highway Administration (2011), "Expanded Polystyrene (EPS) Geofoam." <http://www.fhwa.dot.gov/research/deployment/geofoam.cfm> (5 April, 2014)

United States Department of Transportation - Federal Highway Administration (2013), "Case in point: the Woodrow Wilson Bridge." <http://www.fhwa.dot.gov/bridge/abc/epscasestudy.cfm> (5 April, 2014)

Zakeri, J. A., and Sadeghi, J. (2007). "Field investigation on load distribution and deflections of railway track sleepers," *Journal of Mechanical Science and Technology*, 21(12), 1948-1956.